Reliability Centered Maintenance (RCM) and Ultrasonic Leakage Detection (ULD) as a maintenance and condition monitoring technique for freight rail airbrakes in cold weather conditions

by

Vivek Poddar

A thesis submitted in partial fulfillment of the requirements for the degree of

Master of Science

in
Engineering Management

Department of Mechanical Engineering
University of Alberta

University of Alberta

ABSTRACT

Freight rail airbrakes need improvement in reliability to reduce failures, which can lead to harm to the environment, loss of human life, and a negative impact on the economy. This research focuses on identifying the failures of airbrakes using a Reliability Centered Maintenance (RCM) framework, which uses Failure Modes and Effects Analysis (FMEA) to identify and rank failures. For the purpose of our research, the FMEA result of railroad operating companies was used to research on condition-monitoring techniques for airbrake leakages. Ultrasound Leakage Detection (ULD) is presented as an alternative to the soap and bubble test, as it is a more effective, proactive method to locate and quantify leakages. Experiments were conducted both in the field and in laboratory with simulated and original components to qualitatively and quantitatively evaluate and verify the implications of ULD in cold weather conditions. Correlations between operating pressure, temperature, leakage orifice size, flow-rate and ultrasound intensity were performed to analyze interdependencies. Principal Component Analysis was applied on the spectral features of dynamic sound signatures to reduce the number of variables and find the correlation between them. The contribution that the frequency ranges made to the factors was estimated to find those having significant impact on spectral feature value for different levels of a particular operating variable. For the sum of contributions from individual spectral features, the frequency range of 2400 – 2500 Hz has the maximum contribution. Frequency range, 1100 – 1200 Hz can be used as a feature for discriminating orifice size, as it has 46% contribution for the Root Mean Square (RMS) value of Power Spectral

Density (PSD). The results of this research compares the contribution values of frequency ranges, but it does not state the value at which the readings become significant. With extensive quantitative research on the contribution of frequency ranges and an operational inspection strategy, ULD will result in an effective detection method for airbrake leakages in rail service that will be useful for assessing leakage location and severity with more accuracy. This will facilitate reliable airbrakes operations at severe weather and topographical conditions.

ACKNOWLEDGMENTS

I would like to thank the Canadian Rail Research Laboratory (CaRRL) for providing me with the opportunity to participate in this research. My deepest gratitude goes to my supervisor, Dr. Michael Lipsett, for his invaluable dedication, guidance and insight during the two years of thorough research. He was always there, whenever I needed help. Huge thanks go to Dr. Michael Hendry and Dr. Derek Martin, who were always ready to provide any kind of financial support for field visits, experimental components and workshops. Without their hard work and help, the experimental setup could not have been accomplished. I also appreciate the support I received from other members of the laboratory in the Mechanical and Civil Engineering Department, namely Roger Marchand and Christine Heygers. I learned a lot from their dedication, technical knowledge and positive attitude. They were so willing to provide assistance every time I asked. Thank you all for making my graduate life fruitful and smooth at the University of Alberta.

I would like also to thank Transport Canada, Canadian Pacific and Canadian National. Special thanks also go to Dale Iverson, Abe Aronian, Mitchelle Jameison and Karen from Canadian National, Canadian Pacific and Wabtech for being always ready with support related to data or field visits. Sandy and Alan from SDT were supportive with instrument knowledge and rental for conducting experiments.

Of course, gratitude is owed to my parents, brothers and friends who have fully supported me throughout my education and my life and stuck with me even on the days when I was not at my best. Lastly, I am thankful to my peers and my senior colleagues Laura Ibarra, Azadeh Shadkar, Chunendra Sahu, Vivek Bhushan, Waqas Aawan and Tamran Lengyel for always uplifting whenever it was required.

STATEMENT OF ORIGINALITY

I hereby certify that all of the work described within this thesis is the original work of the author. Any published (or unpublished) ideas and/or techniques from the work of others are fully acknowledged in accordance with the standard referencing practices.

Vivek Poddar

August 5, 2014

TABLE OF CONTENTS

List Of Tables

LIST OF FIGURES

ACRONYMS

ULD: Ultrasonic Leakage Detection

RCM: Reliability Centered Maintenance

LDS: Leakage Detection System

ABS: Airbrake Solution

CP: Canadian Pacific

CN: Canadian National

FFT: Frequency Fourier Transform

US: Ultrasound

PSD: Power Spectral Density

PCA: Principal Component Analysis

AAR: American Association of Railroads

TC: Transport Canada

SCT: Single Car Test

CHAPTER 1: INTRODUCTION

1.1 BACKGROUND AND MOTIVATION

The motivation for the present work comes from the losses due to improper functioning of freight rail airbrakes in cold weather. Since 2002, there has been an increase in railway accidents and main-track train derailments in Canada, which has had a significant impact on human life, the environment and the economy [32]. Freight rail in 2012 accounted for 69% of 1011 accidents, of which 30% were equipment-related. The major sources of equipment-related failures are airbrakes, wheels, track, axles and engines [41]. Improper functioning of airbrakes can lead not only to a failure of airbrake functionality, but can also affect the function of other components, such as wheels, axles and tracks. Airbrakes are critical components in the reliability of rolling stock. “Current airbrake inspection practices are intended to identify defects prior to failure, but due to the inherent limitations of manual, visual inspection they generally do not enable preventive maintenance capabilities” [39].

On December 11, 2011, as freight train LIM-55 was descending a long steep grade between Bybee and Tika in Newfoundland and Labrador, the locomotive engineer, unable to control the train speed using the dynamic and automatic brakes, applied the emergency brakes to stop his movement. One hour later, the train ran away, descending the grade for a distance of almost 15 miles and reaching a maximum speed of 63 mph. This was a result of a loss of air pressure in the airbrakes due to leakages from cold weather conditions. As hand-brake inspections and single-car tests were not conducted on the vast majority of cars before they were put into service, the braking-system deficiencies were not identified [40]. It was fortunate that the train did not derail; at 63 mph, the impact could have been disastrous.

Methods to detect unreliable airbrakes need to be improved before another incident occurs. Airbrakes have been useful in stopping trains for the last 150 years and have been found safe and reliable in their operation [6], provided that the brakes are appropriately operated and maintained. The 800-foot long, 20-car, 250-ton freight train of the 1870's has grown to 100 to 150 or more cars, from 5,000 to 10,000 feet in length, weighing between 5,000 and 20,000 tons [6]. This has required modifications to the effectiveness and range of airbrake systems. Any loss of pressure in the system due to leakages initiated from cracks can cause the air compressor to consume more energy. It will also take longer to charge the system to an adequate pressure level.

The repair and replacement cost of airbrakes accounts for 20 percent of the maintenance cost for rail operating companies [15]. The impact of weather conditions such as snow, precipitation, wind and temperature on infrastructure and operator performance demands detailed and planned maintenance with minimal human involvement for efficient and effective operations [43]. There are both direct and indirect costs involved in maintenance; therefore it can be useful to follow an approach to target critical areas. Reliability Centered Maintenance (RCM) is described as an optimum mix of reactive time or interval-based, condition-based, and proactive maintenance practices that can target critical areas. RCM focuses on the application of Failure Modes and Effects Analysis (FMEA) and criticality analysis for a technically and economically feasible, simple, precise, easily understood, executed and controlled maintenance strategy [14]. RCM is a well-known strategy used for aerospace, nuclear and transportation sectors. It can be replicated for significant impact on airbrakes as a means to improve the reliability, availability and maintainability of railway system in cold weather operations in Canada.

1.2 Problem Definition

The maintenance strategies currently used by Canadian railroad operating companies for airbrakes are traditional, and require high human involvement [39]. The present inspection techniques, such as the pressure decay test, cannot identify leakage location. It involves measuring the loss of pressure over a particular time duration to obtain an indication of leakage. The soap and bubble test is used in tandem with pressure decay to locate leakage locations. However, this test involves more time and human effort [20]. The real need is to find the location of failure, which is both time-consuming and prone to errors. Improved inspection methods or automatic condition monitoring techniques are required that reduce human effort and are more accurate in identifying failures. The extent of failure, indicating the need for on-condition proactive maintenance, also needs to be evaluated, to correctly schedule inspections (and maintenance activities). Therefore, the problem for the present work is to find an inspection system for leakage detection that is more accurate, efficient, and quantifiable and makes it easy to identify, evaluate and locate leakages.

This chapter outlines the scope of a research project aimed at improving the reliability of railway airbrakes in cold weather conditions. This introduction describes the background, motivation, problem definition, objective and organization of the thesis. It addresses present condition-based maintenance strategies that Canadian rail operating companies use for airbrakes.

1.3 Objective

It is important to divide the present work into a list of short-term objectives that can be addressed one at a time to answer the broad problem. To identify the cause of a problem in a system, it is necessary to understand the current system. RCM was used to conceptualize a typical freight rail airbrake system and find the critical failures associated with the system. Ultrasonic Leakage Detection (ULD) was assessed both on the field and in the laboratory for its implications in freight rail airbrake inspection. The main objectives are listed below:

- Apply an RCM approach to address the problem of reducing airbrake leakages in cold weather.
- Assess alternative inspection and monitoring techniques.
- Assess the feasibility of a candidate inspection method through field tests.
- To collect static measurements for the candidate technique, conduct laboratory experiments at different sensor distances, sensor orientations, operating pressures, room temperatures and leakage orifice sizes.

- Analyze the measurements to extract and rank features that can be useful for discriminating outputs related to faults at different operating conditions, without being sensitive to environmental conditions such as ambient temperature.

1.4 Organization

This thesis is divided into five chapters. Following the introductory first chapter, Chapter 2 reviews the literature relevant to the reliability of airbrakes, including system reliability theory, RCM and its application in freight rail airbrakes, fault mode and effects analysis, cause and effect of leakages, use and importance of compressed air, non-destructive leakage testing techniques, and a detailed description of the current airbrake system. Chapter 2 also describes the most important failure modes for airbrakes and current inspection methods used by the American Association of Railroads (AAR) and Transport Canada (TC). Chapter 3 explains the design of the experiment for evaluating a new monitoring technique for airbrake leakages. Chapter 4 outlines the results by analyzing the data captured from the experiments. Chapter 5 summarizes results, offers conclusions and recommends future work for validating a new inspection method and implementing it in industrial practice.

1.5 Important Definitions

The following definitions give a clear understanding of frequently used terms in the remaining part of the thesis.

Reliability: The ability of an item to perform a required function, under given environmental and operational conditions and for a stated period of time [24].

Quality: The features and characteristics of a product or service that bear on its ability to satisfy stated or implied needs [24].

Availability: The ability of an item (under combined aspects of its reliability, maintainability and maintenance support) to perform its required function at a stated instant of time or over a stated period of time [38].

Maintainability: The ability of an item, under stated conditions of use, to be retained in, or restored to, a state in which it can perform its required functions, when maintenance is performed under stated conditions and using prescribed procedures and resources [38].

Safety: Freedom from those conditions that can cause death, injury, occupational illness, or damage to or loss of equipment or property [47].

Dependability: The collective term used to describe the availability performance and its influencing factors: reliability performance, maintainability performance and maintenance support performance [48].

Reliability Centered Maintenance: The process used to determine what must be done to ensure that any physical asset continues to do what its users want it to do in its present context [14].

CHAPTER 2: LITERATURE REVIEW

Starting with building the concept of reliability, this chapter illustrates some of the recent reliability-enhancing methodologies relevant to airbrakes in cold weather. Finally, a potential solution to one aspect of reliability improvement will be proposed, and then described in the subsequent chapters.

2.1 SYSTEM RELIABILITY THEORY

The importance of system reliability became prevalent after World War II, when reliability theory was used to compare operational safety of aircraft engines [19]. System reliability can be broken down into three components: hardware (technology), software (processes) and human (people). Interactions amongst these elements affect the reliability of the system [19]. In this thesis, the concern is primarily with improving hardware reliability, modeled using either physical principles or actuarial information.

In the physical approach, the interaction between the strength (*S*) of the system and the load (L) on the system defines reliability [19].

$$R = \Pr(S > L)$$

Equation 1

In the actuarial approach we use the probability density function, *f(t),* of the time to failure, *t*, which allows the calculation of failure rates and Mean Time to Failure (MTTF).

Considering non-repairable items, the cumulative density function or unreliability, *F(t),* can be modeled from a probability density function, *f (t)*, which represents the failure behavior of a system over time, *t*.

$$F(t) = \Pr(t \le T) = \int_0^t f(u)du \quad , for\ t \geq 0$$

Equation 2

Some of the standard life distribution models are normal, lognormal, weibull, poisson and gamma distribution. Statisticians, mathematicians and engineers formulated these distributions to mathematically model or represent certain behavior. For example, Walloddi Weibull formulated the Weibull distribution and thus it bears his name. Some distributions tend to better represent life data and are most commonly referred to as lifetime distributions. Failure patterns of most of the electrical, structural and mechanical components follow these distributions. If the distribution of a component's failure data can be modeled into one of these distributions, it is easier to find that component's reliability.

Reliability Function *R(t)* is the probability for the item to function till time t,

$$R(t) = 1 - F(t) = \Pr(T > t), for\ t > 0$$

or equivalently,

$$R(t) = 1 - \int_0^{\infty} f(u)du = \int_t^{\infty} f(u)du$$

Equation 3

Failure Rate Function *z (t)*, The probability that an item will fail in the time interval (t,t+∆ t) when we know that the item is functioning at time t is,

$$\Pr(t < T \leq t + \Delta t \parallel T > t) = \frac{\Pr(t < T \leq t + \Delta t)}{\Pr(T > t)} = \frac{F(t + \Delta t) - F(t)}{R(t)}$$

By dividing this probability by Δt, and limiting it by $\Delta t \longrightarrow 0$, we get *z(t),*

$$z(t) = \lim_{\Delta t \longrightarrow 0} \frac{\Pr(t < T \leq t + \Delta t \parallel T > t)}{\Delta t}$$

$$= \lim_{\Delta t \longrightarrow 0} \frac{F(t + \Delta t) - F(t)}{\Delta t} \frac{1}{R(t)} = \frac{f(t)}{R(t)}$$

Equation 4

The failure rate is often high in the initial period due to infant mortality from undiscovered events. The failure rate eventually stabilizes to a constant rate. The failure rate during the entire life of an item can be divided into three phases called the burn-in period, useful-life period and wear-out period [19].

For non-repairable items, maintenance strategies are designed for proper inspection schedules using the reliability values derived from failure data.

The system reliability theory proves that it is impractical to create a 100% reliable system. Therefore, it is important to compute the reliability of a system based on the equations mentioned above. This will help us compare systems based on their reliability and understand the critical strategies that can lead to better reliability. The next section describes the application of reliability theory in designing maintenance strategies.

2.2 Reliability Centered Maintenance (RCM)

2.2.1 Introduction

RCM is a strategic framework that synthesizes the new developments in maintenance engineering into a coherent pattern, which can be sensibly applied to obtain the most value of an equipment. Maintenance is not only a cost component for a company, but also a positive activity for improving component reliability. The amount of capital tied up in fixed assets, together with a sharp increase in the cost of that capital, has led people to start seeking ways in which they can maximize the life of the assets. RCM equips maintenance with tools and techniques required to transform the outlook of a company towards maintenance [14].

RCM has been applied to different systems by researchers. Most of the time it has proven to be successful. For example, its effectiveness is tested with other RCM-like maintenance concepts for developing an efficient and effective maintenance strategy for complex systems [28]. RCM's role in identifying the critical components and monitoring their failure with the help of e-maintenance through computing network technology, PDAs and RFID is illustrated for fuel cells to achieve better reliability, availability and safety [9]. RCM can be used in risk reduction and cost savings. It reduces maintenance work by 40-70% [14]. RCM's implications on rolling stock and on wheel sets have been previously demonstrated [2], [18].

The seven basic questions that provide the framework for the RCM methodology are [14]:

1. What are the functions of the asset?

2. In what way can the asset fail to fulfill its functions?

3. What causes each functional failure?

4. What happens when each failure occurs?

5. What are the consequences of each failure?

6. What should be done to prevent or predict the failure?

7. What should be done if a suitable proactive task cannot be found?

RCM is now becoming as fundamental to the responsible custodianship of physical assets as double-entry bookkeeping is to financial assets.

Some of the important terms as defined by Moubray are as follows:

Functions and Performance Standards: It takes almost one-third of the entire RCM life to decide what users want an asset to do and if it is performing to specified standards. Primary and secondary functions can be associated with an asset.

Functional Failures: We need to identify what failures can occur before we can apply a suitable blend of failure management tools. Failed states are known as functional failures because they occur when an asset is unable to fulfill a function to a standard of performance which is acceptable to the user.

Failure Modes: The events that are reasonably likely to cause a failed state are called failure modes. Wear, tear, design flaws and human error are examples of failure modes. It is important to identify the cause of each failure in enough detail to ensure that time and effort are not wasted trying to treat symptoms instead of causes. On the other hand, it is equally important to ensure that time is not wasted in the analysis itself by going into too much detail.

Failure Effects: Failure effects describe what happens when each failure mode occurs: in what ways it poses a threat to safety or the environment, in what ways it affects production and operations, what physical damage is caused by the failure and what must be done to repair its effects. The process of identifying functions, functional failures, failure modes and failure effects yields surprising and often very exciting opportunities for improving performance and safety, and also for eliminating waste.

The answers to the above questions and terminologies constitute the RCM framework for any system.

2.2.4 Failure Modes Effect and Criticality Analysis (FMECA)

FMECA is a critical part of the RCM process. Failure modes are the events that lead to a functional failure. They can be caused by the falling capability, increased desired performance and initial incapability of an asset. In-depth analysis into the causes of a functional failure leads to the root cause, but most of the time analysis is done to the level at which failure management strategy can be applied. Critical failure modes have high probability of occurrence. Some functional failures have less probability of occurrence, but due to greater consequences they are considered critical for a maintenance strategy. It is almost impossible to deal with all the thousands of failure modes; therefore a matrix consisting of failure modes effects and consequence probabilities should be formulated. This approach will shortlist critical failure modes that require urgent maintenance. MILSTD-1629 is an excellent data source for implementing a Criticality Analysis. The result of the Criticality Analysis leads to the development of a Criticality Matrix. The failure mode criticality number for each specific failure mode (Cm) is calculated as follows [21]:

$$Cm = \beta . \alpha . \lambda p . t$$

Equation 5

Where, Cm= Failure mode criticality number, β = Condition probability of failure effect, α = Failure mode ratio, λp = Part failure rate: e.g., failures per million hours (fpmh), t = Mission phase duration: e.g., operational 20 hours

Failure analysis has been previously performed on fluid operated systems [5] and pneumatic systems like wind turbines [16]. A FMECA has been performed for railway rolling stock where failure modes have classifications for different levels of maintenance [18]. Levels 1 to 4 are generally undertaken by a train operating company (TOC) and would fall within the description of routine maintenance. The antecedents of these classifications seem arcane and most authors appear to have differing opinions, due to no definitive document. The distinction between heavy and light maintenance does not seem to be based on any engineering rationale and is somewhat arbitrary [18]. Most companies are experimenting with, or are already using RCM, and this should eventually replace or radically change the maintenance classifications. A FMECA was also performed on an air-conditioning unit, where Risk-Priority Numbers (RPN) based on the product of frequency of occurrence and severity of failure mode were formulated to determine the critical failure modes [25].

After deciding on the critical failure modes, the technical feasibility of a task is calculated and verified. A task is technically feasible if it is physically possible for the task to reduce, or enable action to be taken to reduce, the consequences of the associated failure mode to an extent that might be acceptable to the asset's owner.

2.2.5 Failure Consequences

A great strength of RCM is that it recognizes that the consequences of failures are far more important than their technical characteristics [14]. Consequences of a failure can be hidden, safety- and environment-related, operational or non-operational. Failure management techniques are divided into two categories: Proactive tasks (scheduled restoration, scheduled discard and on-condition maintenance) and default tasks (failure-finding, redesign and run-to-failure).

A task is technically feasible if it is physically possible for the task to reduce, or enable action to be taken to reduce, the consequences of the associated failure mode to an extent that might be acceptable to the asset's owner. The consequences that result from the failures are the major reason why we conduct maintenance activities. The failures can be hidden or evident, based on whether they can be observed by the operating crew. The consequences can be classified as environmental or safety, operational or non-operational. A firm belief has developed among employers, employees and customers that injuring or killing people or harming the environment are simply not permitted and those failure modes that place a higher risk on the environment and safety are the ones to be maintained at topmost priority [14]. Operations can be hampered as the failure can affect the total output, product quality, customer service and operational cost with direct cost of repair. If the costs involved in the maintenance activity are less than the operational loss, it is worthwhile to conduct the proactive maintenance. For non-operational consequences, a proactive task is worth doing if, over a period of time, it costs less than the cost of repairing the failures it is meant to prevent. Analyzing the failure consequences provides a comprehensive strategic framework for managing failures. As summarized below, failure consequences:

- Classify failures based on their consequences. They separate hidden failures from evident failures, and then rank the consequences in descending order of importance.
- Provide a basis for deciding whether proactive maintenance is worth doing.
- Suggest what actions to be taken if a suitable proactive task cannot be found.

After prioritizing failure consequences, the proactive actions useful for a given failure mode are identified based on the criteria explained in the next section.

2.2.6 Proactive Actions: Preventive and Predictive Tasks

A task is technically feasible if it is physically possible for the task to reduce, or enable action to be taken to reduce, the consequences of the associated failure to an extent that might be acceptable to the asset's owner or user. Failure patterns can be either age-related or not. The failure rate patterns are the rate at which an asset deteriorates during its lifetime. Figure 1 consists of the six types of distinct failure patterns that any functioning equipment, component or system can experience.

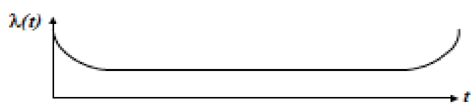	**Pattern A – Bathtub:** Infant mortality, then a constant or increasing failure rate, followed by a distinct wear-out zone *Example*: overhauled reciprocating engine
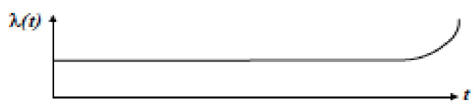	**Pattern B – Traditional Wear-out:** Constant or slowly increasing failure rate followed by a distinct wear-out zone *Example*: reciprocating engine, pump impeller
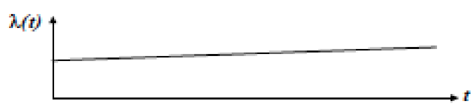	**Pattern C – Gradual Rise with no Distinctive Wear-out Zone:** Gradually increasing failure rate, but no distinct wear-out zone *Example*: gas turbine
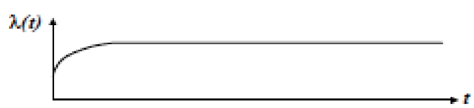	**Pattern D – Initial Increase with a Leveling off:** Low failure rate initially, then a rapid increase to a constant failure probability *Example*: complex equipment under high stress with test runs after manufacture or restoration such as hydraulic systems
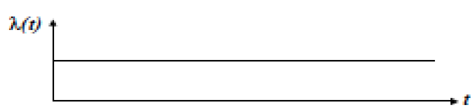	**Pattern E – Random Failure:** Constant failure rate in all operating periods *Example*: roller/ball bearings
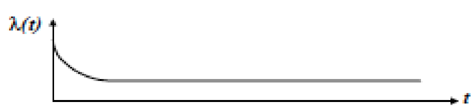	**Pattern F – Infant Mortality:** High infant mortality followed by a constant or slowly rising failure rate *Example*: electronic components

Figure 1: Failure Rate Patterns [14].

Failure patterns A, B and C are age-related whereas D, E and F are not. For age-related failures, preventive tasks, such as scheduled restoration or scheduled discard tasks, can be performed.

Scheduled Restoration: This entails restoring the initial capability of an existing item or component at or before a specified age limit.

Scheduled discard: These tasks entail discarding an item or component on or before a specified age limit, regardless of its condition at that time.

The frequency of scheduled restoration and discard depends on the age at which the asset starts showing a high conditional probability of failure. For non-age-related failures due to variable stress or complexity, there can be no scheduled preventive tasks. This intuitive awareness of the facts has led some people to abandon the idea of preventive maintenance altogether [14]. It can be useful to monitor failures with minor consequences using preventive maintenance, but for failures with serious consequences, predictive maintenance techniques can be used.

Predictive tasks consist of identifying the potential failures and conducting on-condition maintenance tasks for them. Potential failure of an asset is a point at which it starts deteriorating noticeably. The P-F interval is the interval between the occurrence of a potential failure and its decay into a functional failure. Figure 2 shows the point of failure of any item during its lifetime.

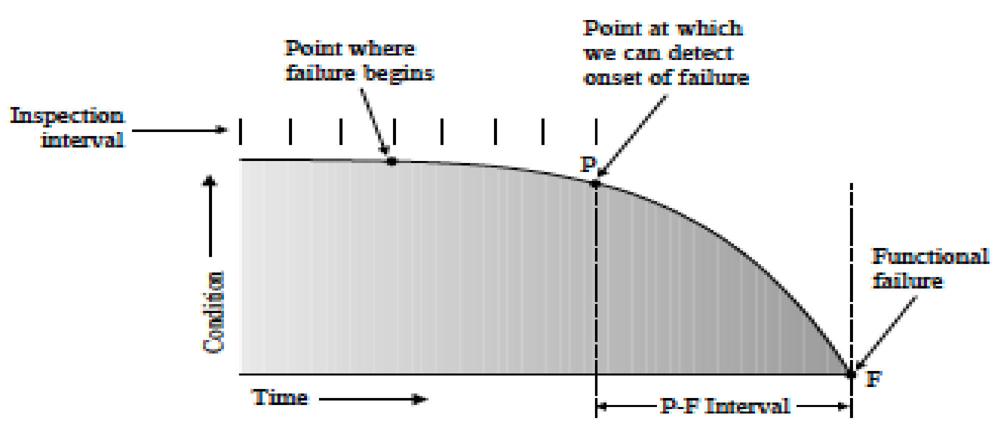

Figure 2: P-F curve [14].

On-condition tasks entail checking for potential failures, so that action can be taken to prevent the functional failure or to avoid the consequences due to the failure. If the P-F interval can be monitored and is consistent, then an on-condition task can be employed if it is feasible to monitor the item at intervals less than the

P-F interval. On-condition monitoring can be classified into four major techniques [14], as follows:

1) Condition monitoring techniques involving the use of specialized equipment to monitor the equipment's condition

2) Techniques based on variation in product quality

3) Primary effects monitoring techniques, which entail the intelligent use of existing gauges and process monitoring equipment

4) Inspection techniques based on human senses

Condition monitoring techniques are used to monitor failure effects due to particle, motion, chemical, physical, temperature and electrical effects. They are highly sensitive versions of human senses but can monitor only one effect at a time. Primary effects monitoring includes effect monitoring by a human using a hand-held device. Based on his experience with the asset, he can use human senses to monitor small failures in a cost effective manner.

2.2.7 Default Actions

If it is not possible to find a proactive task that is both technically feasible and worth doing, then a default action governed by the consequences of the failure can be employed. A failure-finding task must be performed. However, if it is not possible to find a failure-finding task, then the component should be redesigned. For environmental and safety consequences and hidden failure, it is essential to do some kind of maintenance activity. However, with operational and non-operational consequences, when the costs of proactive tasks are higher than the consequences, the default action is no scheduled maintenance [14].

2.2.8 Applying RCM

Moubray has also outlined the important factors for applying RCM in any system. They can be summarized as:

Planning: A successful application of RCM depends on meticulous planning and preparation. The planning process includes deciding the assets to be included, resources required in the analysis, understanding the operating context and proper work allocation.

Review Groups: Maintenance people simply cannot answer the seven basic questions on their own. A member from operations and production is required to form a team. The use of these groups not only enables management to gain access to the knowledge and expertise of each group member on a systematic basis, but the members themselves gain a greatly enhanced understanding of the asset in its operating context.

Facilitators: RCM review groups work under the guidance of RCM experts. The role of the experts is to oversee the system boundaries, maintain the enthusiasm and ensure that the analysis progresses reasonably quickly and is completed on time.

Outcomes of RCM: The RCM analysis has three tangible outcomes: maintenance schedules, revised operating procedures and design changes.

Auditing and Implementation: After the review has been completed, senior managers with overall responsibility for the equipment must satisfy themselves that decisions made by the group are sensible and defensible. The recommendations are implemented by incorporating maintenance schedules into the maintenance planning and control systems.

Results of RCM: The results of RCM can be summarized as greater safety and environmental integrity, improved operating performance, greater maintenance and cost-effectiveness, longer useful life of expensive items and a comprehensive database.

2.3 RCM IN AIRBRAKES

The potential benefits of introducing RCM in railway infrastructure have been analyzed before [11], but there is insufficient practical work done for reliability improvement of airbrakes. This is the first time RCM ideology has been applied to airbrake maintenance. The review group for this application in a freight rail airbrake system consisted of a professor, a mechanical reliability engineer and a student.

2.3.1 Introduction

The first train airbrake system was introduced in the mid-1800's and was known as the "straight airbrake" [6]. This system utilized an air pipe through the length of the train and cylinders in each car. There was had a major limitation, identified by George Westinghouse, the inventor of the straight airbrake: if the train broke in two or if the brake pipe burst or leaked badly, the brakes simply failed to apply. Westinghouse developed "the automatic airbrake," which functioned on the opposite principle: the brake pipe was charged with compressed air to release the train's brakes, and its pressure was reduced to apply them [26]. In the modern world, most airbrakes are automatic, which are used as a fail-safe device to stop or control a train's speed. Similar to car brake system, the train is slowed or stopped when the brake system develops a retarding force at each wheel by means of brake shoes pressing against the wheel treads.

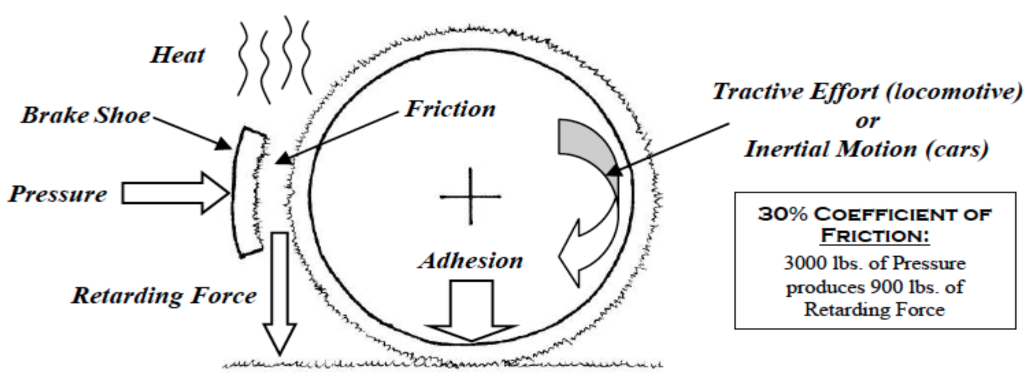

Figure 3: Forces from rail, wheel and brake shoe interaction [26]

The air pressure in the brake cylinder pushing the piston outward and putting force into the brake rigging creates brake shoe force. This force moves against the truck levers and brake beams to press the brake shoes against the wheels. In any event, the retarding force at each wheel tread must not be greater than the adhesive force or grip between the wheel and the rail, or the wheels will slide. Friction is required to both move and stop a locomotive and train. Friction between the wheel and rail is adhesion. A locomotive, through its tractive effort, converts horsepower into pulling power. This tractive effort is limited by adhesion. Likewise, adhesion between a wheel and the rail, combined with friction from a brake shoe, produces a drag force that retards the rotation of the wheels. Inertial motion is stored energy. Any attempt to retard or dissipate this energy through friction produces heat. Therefore, not only must the railroad braking system produce the required retarding force, it must also dissipate the heat generated by the process. Locomotive and car wheels have a very high capacity to absorb and radiate the heat created by braking. However, under extreme conditions, it is possible to overheat both the wheels and the brake components. This can cause a brake failure, or a failure of the wheel and axle assembly, which can result in a derailment. The coefficient of friction is the percentage of the pressure of the brake shoe pressing against the wheel that is converted into the retarding force [26]. This coefficient should be as high as possible to dissipate less heat to the components. Heat can cause any material to expand and contract, which is the major reason that the yield strength of the material will decrease. To prevent this from happening, the coefficient of friction should adhere to regulatory agency specifications.

The pressure developed by the brake cylinder piston works on the principle of equalization. The amount of force exerted by the brake cylinder piston depends upon the pressure in the brake pipe and the distance that the brake cylinder piston has travelled. If a piston travel is adjusted too short, the pressure exerted by the piston will be greater than when the piston is adjusted at a greater distance. If the brake pipe pressure is more than 70 psi, the amount of pressure exerted by the brake cylinder piston will be 2.5 times the reduction in brake pipe pressure [26]. This change in piston travel is controlled by air pressure, which in turn is generated from the flow of compressed air in the airbrake system. Any loss of pressure in the system due to leakages initiated from cracks can cause the air compressor to consume more energy and it delay the amount of time it takes to charge the system to an adequate pressure level.

2.3.2 CRITICAL COMPONENTS

The major components of a typical freight rail airbrake are the air compressor, governor, reservoirs, brake valve, brake pipe, control valve, brake cylinder, and reducing and retaining Valves. These components are arranged as per their functionality in Figure 5.

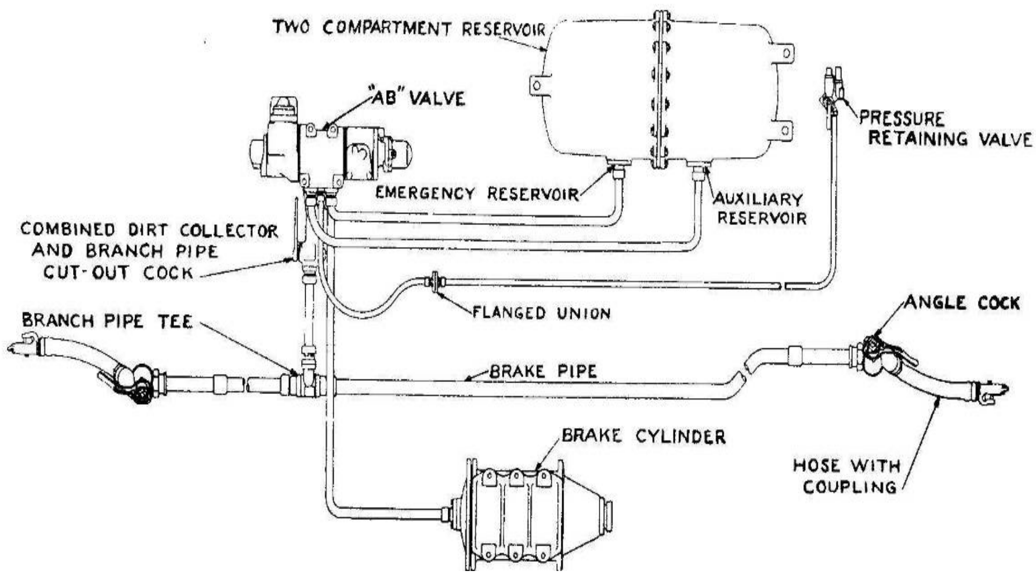

Figure 4: Layout of a truck-mounted airbrake system [26].

The section below describes some of the components critical to the functioning of an airbrake. As per the understanding from the site visit at the Canadian Pacific (CP) yard in Golden, BC. the following section gives a brief description of the functionality of some critical components of airbrakes.

2.3.2.1 Control Valve

The term “triple valve” is used because it has three functions to charge, apply and release the brakes. Most modern freight airbrakes have an AB-type control valve, which consists of a pipe bracket connecting the emergency and service portions. The service portion controls the desired charging of the reservoirs and facilitates the service or manual application of brakes. The emergency portion facilitates the emergency and quick service application. It combines the auxiliary and emergency reservoirs when extra brake pressure is required. Control valves use a system of pistons and/or diaphragms attached to internal valves and porting mechanisms. These pistons and diaphragms use differential air pressure between the brake pipe and the auxiliary reservoirs to open and close the valves and ports, admitting and exhausting air pressure to and from the appropriate chambers in order to apply and release the brakes. The modes of operation for the control valve are as follows:

Release and Charging: When the brake valve in the running position and brake pipe is complete, the air flows from the main reservoir to the air pipe through a feed valve. This air charges the control valve and opens the feed groove to the auxiliary and the main reservoir. As the feed groove valve is very small, the pressure in the air pipe is always higher than it is in the reservoirs in each car. This will continue until the pressure in all the components is same. This process takes from five to seven minutes, depending on the train length.

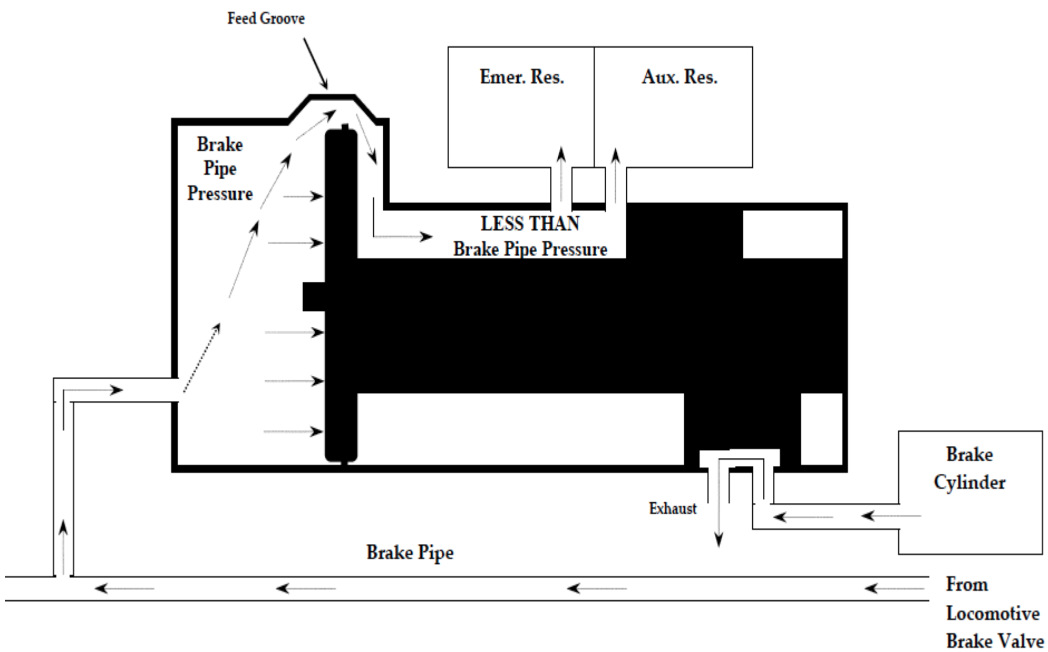

Figure 5: Release and charging [26].

Service Application: When the brake valve is moved from the release position to the service position, air exhausts from the equalizing reservoir. This reduces the pressure in the brake pipe, which then becomes less than the pressure in the auxiliary reservoir. The valve connecting the brake cylinder to the reservoir opens and the cylinder exhaust valve closes.

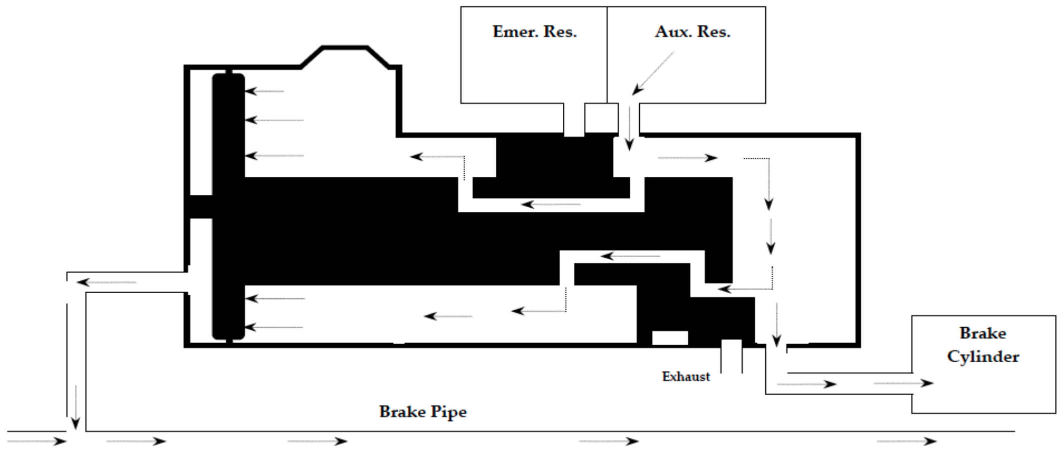

Figure 6: Service application [26].

Lap position: Air flows from the reservoir to the cylinder until the pressure in the reservoir drops to a level just below the brake pipe pressure. Brake pipe pressure now pushes the piston into a lap position, closing off all connections between the pipe, reservoir and cylinder.

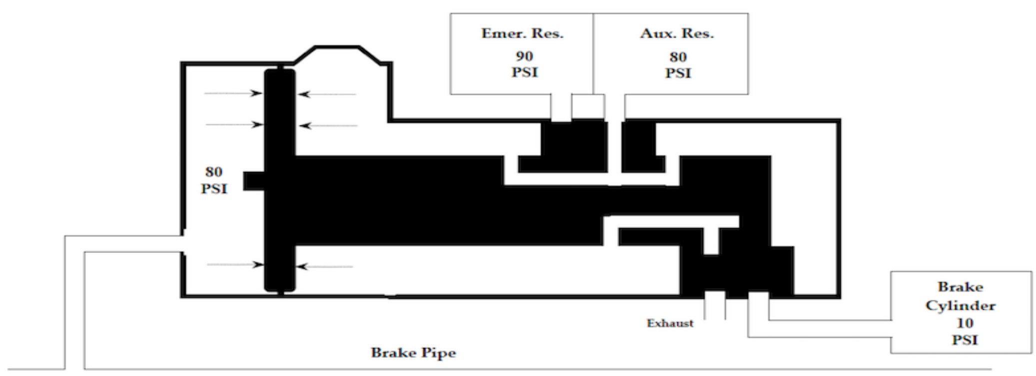

Figure 7: Lap position [26].

Service Release: When the brake valve is placed in the release or running position, a release action occurs. This again charges the brake pipe and allows air to flow from the brake pipe to the reservoirs, thus exhausting the brake cylinder.

Emergency Application: In an emergency-rated car, when the brake valve is placed in the emergency position, the auxiliary and emergency reservoirs connect.

This increases the volume of air available to exert pressure on the piston. Air is also vented from the brake pipe to enable the brakes to be continually applied when air passes from the reservoirs to the cylinder. This results in a 20% increase in brake application.

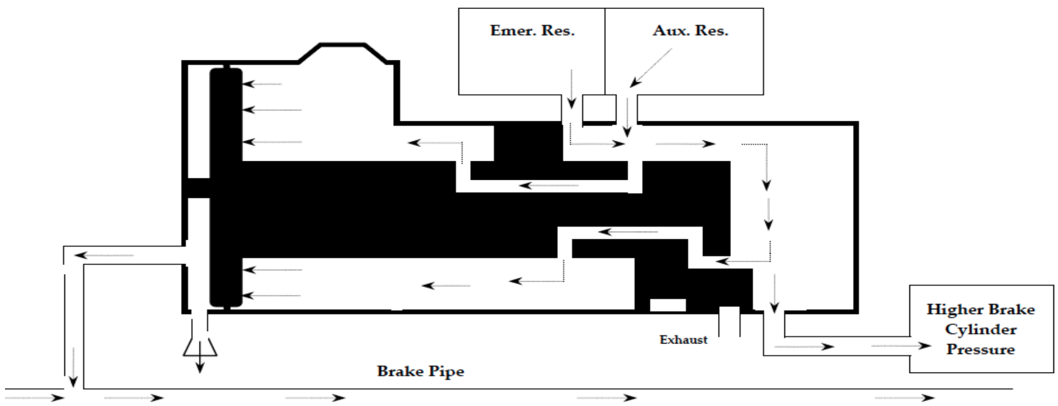

Figure 8: Emergency application of [26].

2.3.2.2 Air Compressor

Air compressors are used to provide the necessary compressed air for brake operation. Most airbrakes in trains use centrifugal-type air compressors, which are continuous duty compressors with rotating impellers that provide the velocity to generate air at a high cubic flow per meter (cfm). Governor is used to control the pressure in the main reservoir and the compressor. Air compressor failures can occur due to sticking valves, ring wear or improper installation, which can lead to excessive leakage [13]. Such leakage can be very costly in terms of loss of compressed air.

2.3.2.3 Brake Valve

The modern brake valve in airbrakes is self-lapping type that provides brake pipe reduction in proportion to the movement of the brake valve handle into an application zone, rather than back-and-forth between the service and lap positions. It also has a pressure-balancing feature that maintains pressure in the brake pipe at any specified level of reduction against minor leakage. Leakage in brake valves can also lead to an excessive loss of compressed air, as the brake valves control the exhaust of air from the whole system.

2.3.3 Functional Failures

The airbrake's primary function is to transmit pressure from the brake valve to the brake shoe. A failure in the airbrake system will be costly because the air compressor will consume extra energy to charge the system and apply the necessary pressure at the brake application point. Some of the functional failures for airbrakes are:

i) Brittle fracture of brake pads, brake shoes and valves due to prolonged exposure to extreme cold weather conditions [38], [44]. This can lead to leakage or a change in the length of a valve, diaphragm or piston.
ii) Freezing of air inside the brake pipe due to extreme cold weather conditions. This can lead to a complete loss of functionality.
iii) Damage to the cylinder seals. This can lead to a loss of pressure required for required brake application.
iv) Leakages in brake pipe, reservoirs or valves. This can cause a loss of air and reduced pressure.
v) Excessive heating of brake rigging components due to improper brake shoe or brake rigging arrangement. This can cause of cracks and loss of structural strength

Almost all of the above failures lead to a loss of air from the airbrake system. The major cause of this loss is leakages, which can be present in the air pipe, brake cylinder, hoses or control valve. The glad hand (coupling joining hoses) between two rail cars is the most critical leaking component [39].

2.3.5 Proactive Actions

Predictive and preventive maintenance techniques are the two types of proactive actions. Predictive maintenance uses the data about the physical characteristics of equipment and applies statistics to find its current state. Preventive maintenance employs regular maintenance strategies based on the P-F curve. These actions can use humans as well as machines. With time, human involvement is decreasing and machines are increasingly used for detecting failures. Some of the proactive condition-monitoring techniques that can be applied to airbrake inspections are as follows:

1. The friction coefficient can be estimated using a kalman filter, which can be used to determine the health of a brake shoe.
2. Digital image correlation can be used to detect cracking failures. High-speed cameras can be used for this purpose.
3. Wayside sensors can be installed onboard to track the wheel profile and locate any ice buildup. These sensors are similar to acoustic sensors that are used to detect the sound of falling bearings. CP currently uses temperature sensing of wheels to detect failed airbrakes.
4. Ultrasonic leakage detectors can be used to detect any leakages in the airbrake components.
5. Vibration detection using ultrasonic detectors can be used to keep the vibrations of components at an optimum range.
6. An on-board monitoring system contains sensors and actuators for tighter monitoring and control. This technique can be better applicable than wayside detectors.
7. Brake pad inspection system. This can be used to monitor the condition of brake rigging components.

After careful consideration about the need and applicability of all the above proactive actions, it was decided to study the implications of ULD. The use of ULD has been growing with the trucking industry. Also, ULD has been the subject of ongoing research in some of the leading universities in North America [30].

2.3.6 Currently Used Leakage Inspection Methods

Currently, there are two main brake tests that Canadian railroad operating companies use to inspect airbrakes: the No.1 brake Test and the No.1A brake test. These tests are very similar, and are primarily performed using either the brake pipe leakage method or the airflow method. The brake tests typically take 60-90 minutes. These brake test checks are based on the pressure decay method and are used to check for brake pipe integrity. The test also ensures that every parameter of the brake is within the specified limits. The operator visually confirms that the brakes actuate and release on every car. During the test, the operator is required to check all the car couplings and make sure that the brake pipe pressure is within 15 psi of the operating pressure as shown in Figure 9 [8].

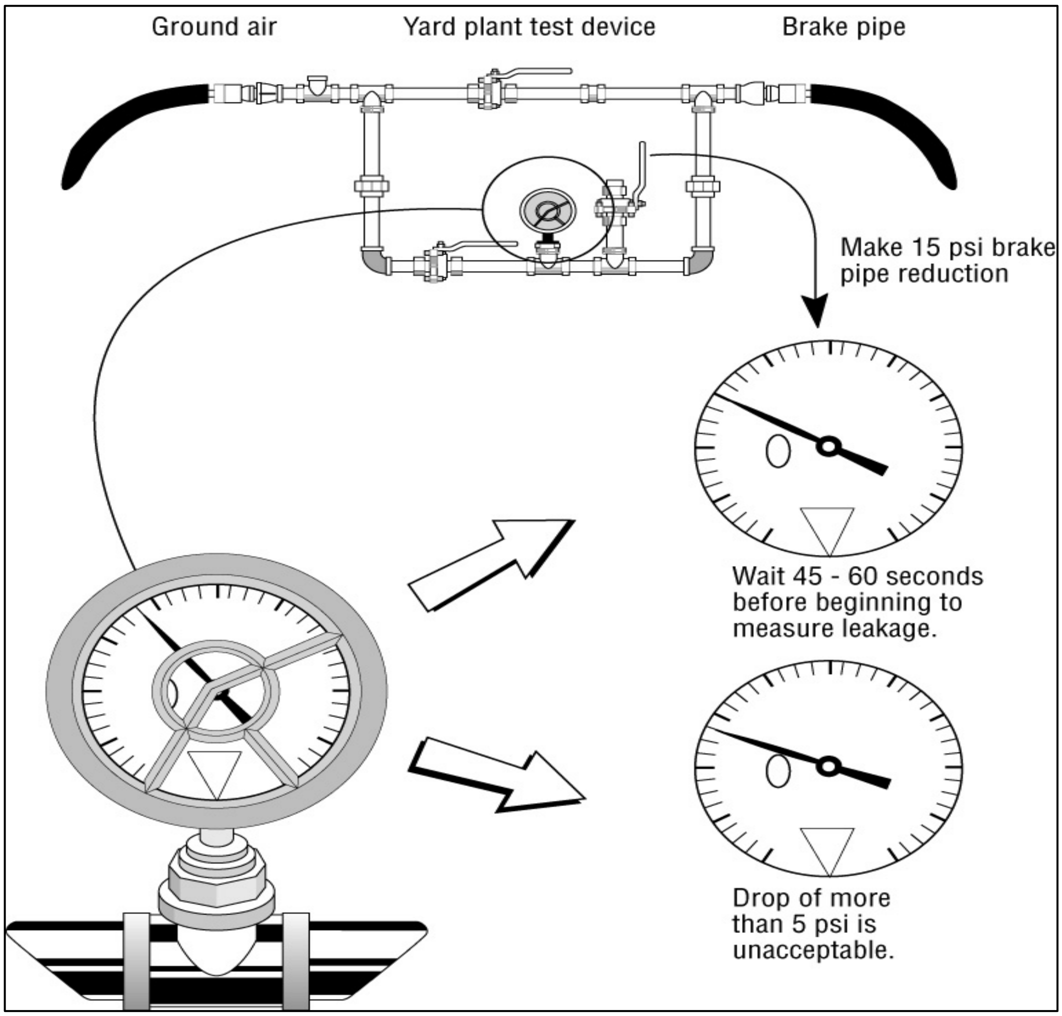

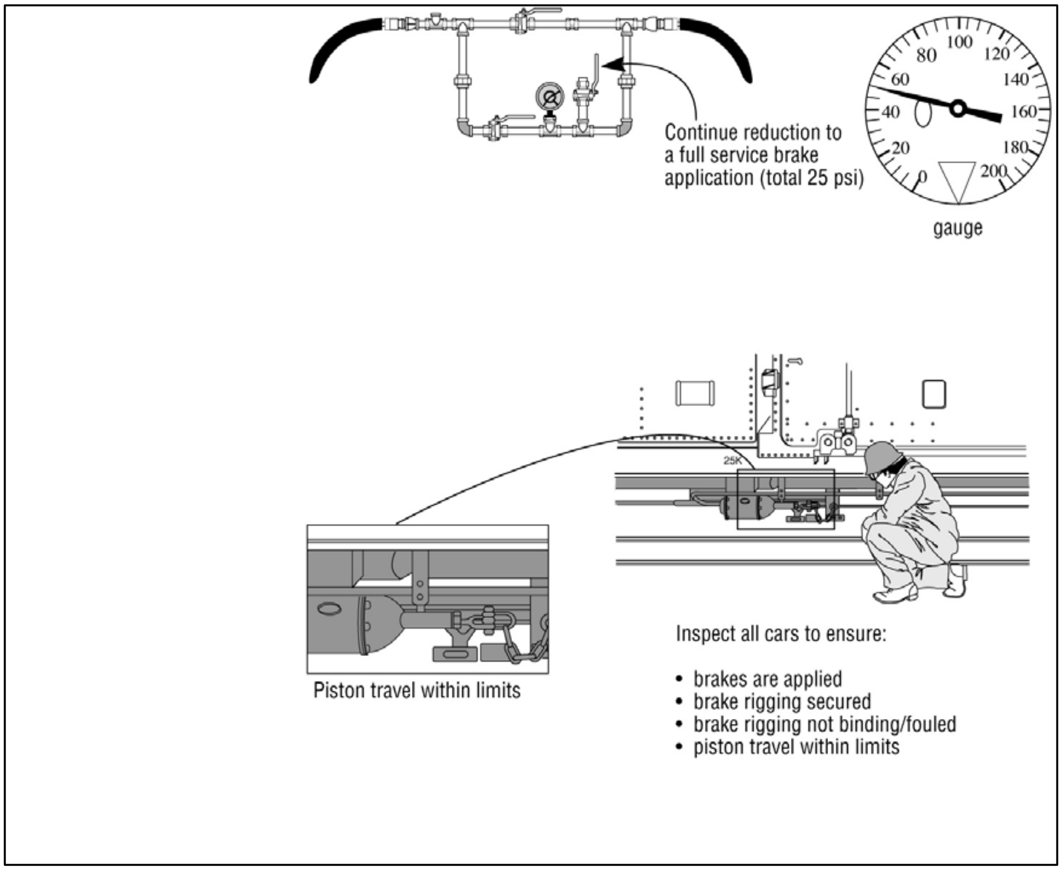

Figure 9: The No. 1 brake test [8].

The current method of inspection involves a lot of manual work, which can encompass all sorts of human errors. Due to an increasing number of complex mechanical parts, the railway industry has to rely more and more on computers and more advanced inspection techniques, with a focus on predictive maintenance as opposed to reactive maintenance. Hot or cold wheel detectors are an example of the type of technology that can be used to inspect airbrakes. Cold wheel detectors can be placed at the stoplights, where trains most likely use brakes. The detectors can see any inconsistencies in the temperature. Low temperatures indicate a malfunctioning brake. This technology allows the railway company to categorize the trains in terms of priority for maintenance. Since wheel detectors are usually far from a station, there is also the benefit of having the brake tested at multiple locations for consistency. A cold wheel is usually designated as having a wheel temperature below 70 F, whereas a hot wheel has a temperature of above 200 F

[15]. In addition to wayside detectors, it would be useful to have an onboard temperature detector near the wheel that could possibly relay the information to the train operators or to the next maintenance station.

The railroad operating companies have been using the “soap and bubble test” in conjunction with pressure decay test to locate leakages. For this test, the complete airbrake line is sprayed with soap to observe the bubbles. Inspectors have to access hard-to-reach locations to see the bubbles. This is both time-consuming and involves considerable human effort. In cold weather conditions the inspections conducted by human inspectors are both incomplete and inefficient because of reduced human senses and the difficult task to reach out to each and every corner [10]. Therefore, ULD can be useful, as it has a flexible sensor to reach hidden locations. The ULD requires inspectors to look at the intensity value displayed in the instrument at hand, which is easy to use and accurate in defining the extent of the leakage.

2.4 MOST CRITICAL FAILURE MODE: LEAKAGE

It is important to know about the types of leakages and their cause and effect. This knowledge will help mitigate the cause and prepare for the consequences. This section will describe the types and cause and effect of, and strategies to avoid, leakages.

A leakage is a crack or hole that allows fluid to escape from a contained surface or joint. On one hand, strict leakage rate standards have to be maintained. On the other hand, the process should be cost effective to mitigate loss due to leakage. A leakage is caused by a pinhole, crack, material porosity, broken seals and valves. Leakage can be measured using the volumetric flow-rate or mass flow-rate. The volumetric flow-rate measures the difference in the volume of fluid on both side of the leakage, whereas the mass flow-rate measures the change in the mass of fluid due to the leakage.

2.4.1 Cause and Effect of Leakage

Many system failures are caused by leakages. Even a pinhole leakage can cause severe failures, leading to accidents. Some of the causes of leakages are:

1. Frequent variation in temperature, pressure and humidity, which can reduce the strength of material due to expansion, contraction and corrosion.
2. Continued stress due to overloading or surface contact.
3. Ice-build up, which can cause leakages due to increased pressure on a surface.
4. Poor assembly of the system, which can cause leakages from loosely fit components.

Some of the effects of leakage are:

1. Water intrusion into critical areas, which can result in corrosion, electrical short-circuiting, component damage, or hydrostatic lockup of moving parts.
2. The escape of lubricating fluids, which can result in overheating, friction-induced damage to mating parts, lockup of moving parts, and damage to parts touched by the escaped fluids.
3. A loss of pressure, which can cause the system to function inefficiently.
4. Stress raisers in boned joints or welded joints, which can provide crack-initiation sites.

In summary, leakages are critical failures that need to be tapped in the early stages of initiation. There can be different types of leakages, which will be explained in the next section.

2.4.2 Types of Leakages.

Leakages can be classified as follows:

Gasket leakages: A gasket is a compressible material squeezed between two mating parts that are usually held together by threaded or other fasteners. It forms a seal between the mating surfaces. Any imperfection on either mating surface, such as a scratch, gouge, or surface finish that is too rough, can cause a leakage.

Inconsistency in the gasket dimension, material or location can lead to leakage. Corroded mating surfaces due to extreme weather conditions may also create a leakage path [17].

O-Ring leakages: These are similar to gasket leakages. The only difference is in the size and geometry of the O-ring. Failure modes are similar to failure modes for gaskets [17].

Bond-Joint leakages: Bond joints can be formed from epoxies, adhesives, or other sealants. Potential failure causes are contamination in epoxies or mating surface, inappropriate adhesive, inaccurate curing time, inappropriate epoxy mixing process or expired epoxies [17].

Weld leakages: Pressurized systems have welded joints to provide a structural connection. Using either the wrong welding technique, welding rod or welding material can cause too much stress, which leads to crack initiation and, finally, leakage [17].

Valve Leakages: Valves are used to seal or control the operating logic of a hydraulic or pneumatic system. The potential causes of leakages are inaccurate operating logic, calibration errors, contaminants, over-tightening of valves, extreme weather conditions leading to dimensional changes, corrosion of internal material, wearing out due to overuse, and drying out of valves due to insufficient lubricant [17].

Structural leakages: Leakages can occur in the walls and external structure of containers, pipes and pressure vessels. Cracks in these structures can create a leakage path, which over time can grow to aggravate the leakage. Cracks can occur as a result of loads outside design limits, excessive vibration or shock, incorrect weld technique, operating the system outside its intended environment, or thermal shock. Corrosion due to foreign contaminants can also cause a leakage path [17].

Gaskets and O-ring leakage can be induced by material, configuration, and mating surface factors. Bond-joint leakage can be induced by epoxy or adhesive process anomalies and mating surface conditions. Weld leakage can be induced by material and weld technique issues. Valve leakages can be induced by any of several causes influencing the valve seating surfaces. Structural failures can be induced by porosity, cracks, foreign object damage, and other factors. All of the aforementioned leakages are susceptible to contaminants, design, material compatibility, and environmental factors [17].

2.4.3 Leakage Detection Methods

Increasing public awareness and concern for the environment have shown that the cost to a company can be alarming due to the downtime and clean-up expenses of a leakage accident. As more stringent statutory regulations are being put into place, cost-effective and reliable Leakage Detection System (LDS) is also in demand [1]. Leakage sensitivity, leakage location identification, operational change, reliability, maintenance requirement and cost-benefit analysis are the attributes used to compare LDS [45]. For example, a false alarm can increase work load, decrease confidence in the detection system and cause WHO to overlook an actual leakage. Therefore, it is essential to design a cost-effective and reliable LDS.

Figure 10 shows leakage detection methods organized into three categories: physical, hardware-based and software-based [12], [45].

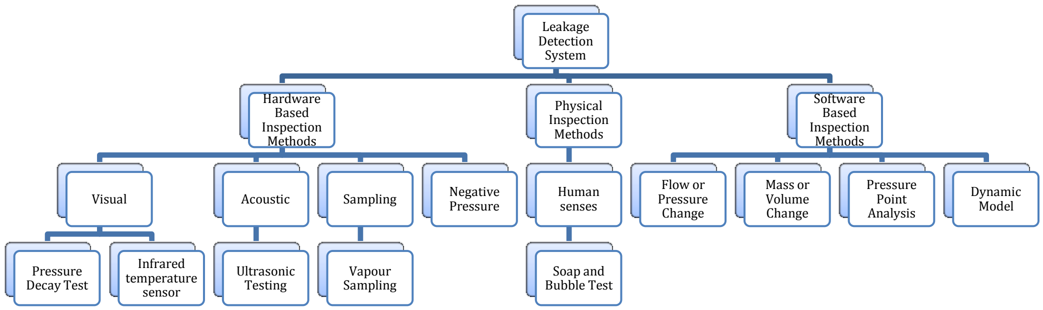

Figure 10: Review of Leakage Detection Methods.

Physical inspection methods: A traditional approach to leakage detection can be deployed using personnel who walk along the system to detect leakages. These inspectors can visually locate a leakage or hear the noise from a leakage. This method is totally human dependent and cannot be used accurately to locate and quantify a leakage consistently amongst all inspection personnel [45].

Hardware-based inspection methods: Fixed or portable devices can be used to monitor the change in temperature, pressure or noise level throughout the system. Any increase or decrease from the tolerable level can raise an alarm, alerting inspectors to a leakage [45].

Software-based inspection methods: Sensors can be deployed to measure the change in pressure, volume, mass or flow due to a leakage. Fluid flow models, a finite element, an equation of state for fluids, conservation of energy, frequency response and spatial discretization can be used to model the dynamic nature of fluid flow. Data is fed into the software to analyze and generate results to accurately simulate a leakage [45]. Operational efficiency, a combination of different LDS techniques and RCM can provide enhanced safety and reliability with decreased cost [45]. Some of the leakage detection methods are:

2.4.3.1 Soap and Bubble Test

The bubble emission requires a gas pressure differential across the pressure boundary. A test liquid is applied at the boundary, which forms bubbles on gas leakage as shown in Figure 12. This method provides immediate indications of the existence and location of large leakages (10^{-2} to 10^{-4} mbar-L/s). Longer inspection times may be needed to detect small leakages (10^{-4} to 10^{-5} mbar-L/s) [12]. The probing medium is the gas that flows through the leakage due to the pressure differential. The test indication is the formation of visible bubbles at the exit point of the leakage. The rate of bubble formation, size of the bubbles formed, and rate of growth in the size of the individual bubbles provide the means to estimate the size of leakage [20]. Bubble tests are often classified according to the test liquid and means of application. In the liquid immersion ("dunking") technique, the pressurized test system is submerged in the test medium. In the liquid film application method, a thin layer of the test medium is flowed over the low-pressure surface of the object. For large leakages, the applied liquid establishes a foam blanket; the rapid escape of gas through this blanket blows through the blanket and reveals the location of the leakage [12].

Figure 11: Soap and bubble test

Bubble testing for leakage location is one of the most widely used non-destructive tests because its simplicity permits its use by workers with minimal training. On an elementary scale, bubble tests can be used to test connections on domestic propane systems or tire inner tubes in a soapy bath. For small vessels, it is appropriate to pressurize the entire vessel, and coat all welds with a detecting medium. For larger vessels, and for welds in piping, it is possible to coat the inspected area with bubble solution and then use a vacuum box to create the pressure differential. Active pressurized piping joints and connections in the vessel can be examined by coating individual or suspect welds when the vessel is operating at a pressure greater than the external pressure. Heavier structures, such as those used in hydropower installations, can be examined using this method. In this case, a vacuum box is needed to create the pressure differential and the welds are examined in short sections, section length being related to the size of the vacuum box [12].

The advantages of bubble leakage testing are its simplicity, rapidity and economy [20]. It is a fairly sensitive leakage detection technique and enables the inspector to very accurately locate the exit points of leakages. Another advantage is that it readily detects very large leakages, yet provides rapid responses for small leakages. It is not necessary to move a probe or sniffer over the surface being inspected.

Conditions that interfere with bubble testing are contamination of the test specimen surfaces; improper temperatures of test specimens; contaminated or foaming test liquids; improper viscosities of test liquids; excessive vacuum over the surface of test liquid; and low surface tension of the test liquid, which can clog the leakages. Prior bubble testing in general can clog leakages or lower the accuracy of subsequent leakage testing by more sensitive methods. For the immersion or dunk testing technique, the handling of the test item is important. Small components can be easily submerged, and very little pressure difference is sufficient. However, this method is not practical for testing larger, heavy objects [12].

In the airbrake system, the soap and bubble test is used in conjunction with the pressure decay test to locate the leakages. Inspection personnel move around the rail cars with a soap spray bottle. Different components have different allowance bubble sizes at particular time durations. Generally, a one-inch bubble size is acceptable for a minimum of 5 sec [3].

2.4.3.2 Pressure Decay Technique

The pressure decay testing method measures the decrease in pressure in an object, as shown in Figure 13. The test object is initially inflated and then a reference pressure is established. After a designated amount of time, the pressure is monitored again, and the initial and final measurements are compared. The change in pressure is used to calculate the leakage rate given the internal volume of the device. A drop in pressure signifies a leakage; the greater the pressure drop, the larger the leakage. This method is convenient in that it is easily automated and dry, and can be used to test small parts at high speeds. As this method tends to detect only big leakages, the pressure drop system is often combined with another leakage detection method such as ammonia sensors or a mass balance system [12], [20].

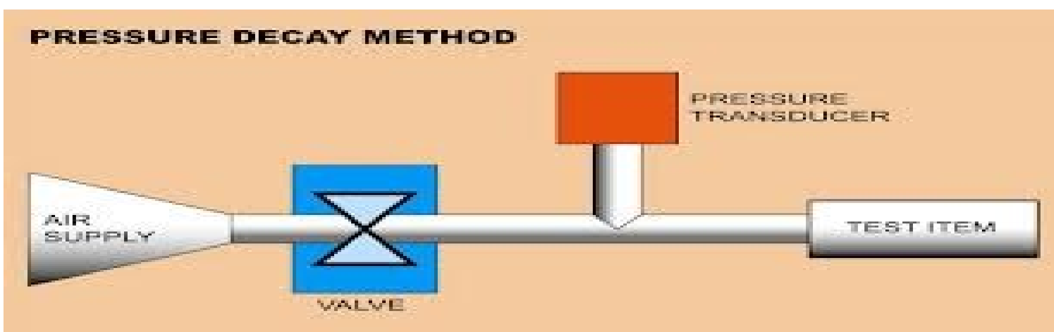

Figure 12: Pressure Decay Test

In the single car test, the brake pipe is charged to 90 psi. The pressure reduction is observed for 1 minute. The reduction should not exceed 1 psi [3].

2.4.3.3 Ultrasonic Leakage Testing

Ultrasonic gas leakage detectors use acoustic sensors to detect changes in the background noise of a machine's environment. Since most gas leakages occur in the ultrasonic range of 25 kHz to 10 MHz, the sensors are able to easily distinguish these frequencies from background noise, which occurs in the audible range of 20

Hz to 20 kHz [27]. The ULD device produces an alarm when there is an ultrasonic deviation from the normal condition of background noise. Although ultrasonic gas leakage detectors do not measure gas concentration, the device is still able to determine the leakage rate of an escaping gas. By measuring the ultrasonic sound level, the detector is able to determine the leakage rate, which depends on the gas pressure and size of the leakage [1]. The bigger the leakage, the larger its ultrasonic sound level will be. Ultrasonic gas detectors are mainly used for outdoor environments where weather conditions can easily dissipate escaping gas before allowing it to reach gas leakage detectors that require contact with the gas in order to detect it and sound an alarm. These detectors are commonly found on offshore and onshore oil or gas platforms, gas compressors and metering stations, gas turbine power plants, and other facilities that house outdoor pipeline [4]. Acoustic ultrasonic leakage detectors are sensitive to airborne sound and inaudible sound waves due to escaping gas. This method can be applied to testing underground supply and distribution pipelines of steel, ductile iron, cast iron, asbestos cement, polyethylene and PVC. The maximum controllable length of plastic pipes such as PVC or (high and low density) polyethylene is about 50 meters when accelerometers are used. Acoustic emission monitoring can be carried out while a system is operating, searching for leakages of the contained fluid, or by imposing an artificial test load in the vessel (pressurizing) [12].

Techniques for leakage testing include visual examination for escaping fluids or bubbles, electronic sensing of the noise emitted by the escaping fluids, or chemical or radiological detection of small quantities of contained fluids or fluids specially introduced as tracers.

NDT equipment has been made as independent of operators as possible. This has led to greater use of computers and automation. Most modern NDT has microprocessors and computers with enhanced capabilities for data acquisition, analysis and image processing. On-line and continuous monitoring of plants and regular equipment inspection is now commonly applied [12]. Therefore, it seems logical to test some latest leakage detection techniques for airbrake systems. ULD involves fewer human senses. The data acquisition procedure for ULD has improved from static intensity readings to dynamic sound signatures, which can be analyzed using several software packages [33]. Human involvement can be completely removed by employing remote monitoring systems on the railway track for data acquisition.

2.4.4 ULD: THEORY

ULD is used to save compressed air by detecting leakages that allow wastage of compressed air, which is the second most used power in the industry, after electric power. Its leakage is a serious problem. The rate of leakage for compressed air can reach up to 10%-30% [22]. As reported in the literature, compressed air accounts for 10% of total industry-energy use for few countries [23]. Compressed air is considered the "phantom utility," because people are unaware of its true cost. In a typical manufacturing operation, the energy costs of running a new compressor will often surpass the initial compressor's purchase price within the first year of operation.

In a typical compressed air system, 25% of consumed energy is wasted due to system inefficiency [29]. Improperly designed and improperly maintained systems reflect this inefficiency through decreased compressor performance, compressed air leakage and distribution system pressure drops. By using adequate maintenance and inspection practices, existing energy costs can be significantly reduced. If the leakage were water rather than air, there would be little doubt that system repair would be given high priority, but because air is difficult to see, smell and, in some cases, hear, it is often blissfully ignored. Leakages do not represent a constant power loss. Leakages will consume energy regardless of whether or not compressed air tools and devices are used. System pressure is the signal that tells the compressor to load or unload. The greater the leakage rate, the more frequently the compressor will run loaded. Valves which require adjustment and seals that wear out are examples of leakages that can only be minimized and not entirely eliminated.

Ultrasonic detection technology in compressed air leakage detection is based on the directionality of ultrasonic propagation. When compressed air leaks out, it generates ultrasonic signal near the leakage point, which can be detected using an ultrasonic leakage detector [1]. A human can hear sound from a large leakage. However, when the leakage is small and the acoustic frequency is lower than 20 kHz, the sounds are imperceptible [42]. Therefore, ULD approach is used widely in leakage detection because of its simple principle, convenient use and online detection. The output voltage signal of the ultrasonic sensor is filtered and amplified by the instrument and an LED displays its amplitude. At this moment, the leakage point can be found in the direction of the ultrasonic sensor. The ultrasonic signal generated by the compressed air leakage has high energy and a considerable difference value with respect to background noise around 40kHz [1]. This system has broad application prospects in the industry because of its small size, good portability, easy operation and high accuracy [34]. The principle of leak hole estimation by detecting the ultrasound generated by the impact of the turbulence is a new technology in current gas leakage detection. The turbulence will produce a certain frequency of sound waves in the vicinity of the leak hole. The intensity of these sound waves is related to the size of the leak hole.

Active, passive and vibro-acoustic are the three specific modes for ULD [7]. The application of these modes ranges from vehicles to aircrafts. The active ultrasound testing method uses one or more emitters and receivers in various contacting or non-contacting configurations. The passive method involves detecting the turbulent response due to passing air through a hole. The ultrasonic signal response can be heterodyned into a lower, audible frequency range where an operator with headphones can listen to the altered signal. The vibro-acoustic method is used in certain pressure vessels that have thin internal membranes covering unused pipe plugholes [7].

The passive ultrasonic detection of acoustic emissions is the latest upcoming leakage detection methodology used for mechanical failures. This technology can be used either in tandem or to replace the existing soap bubble and single car test used for freight and passenger rail airbrake inspection. The ultrasonic frequencies can be heterodyned to human audible ranges using an ultrasonic probe, which can sense the directional, easily detectable and accurate ultrasound frequencies. This instrument can replace the existing time-consuming, tedious, human-dependent and destructive inspection systems used in the industry. To start, the technology can be tested and compared with the existing methods to practically observe its advantages. For further study, experiments can be conducted under controlled temperature environments to record the sound signals.

To develop a relationship between changes in temperature, pressure and leakage size, these sound signatures can be signal processed from artificially introduced leakages. Table 1 shows the comparison of detecting leakages using the soap bubble test, pressure decay and ultrasonic detection. These comparisons are done based on the current literature on NDT techniques and field tests conducted at the CP yard. It can be clearly observed that ULD is the best available leakage detection technique for airborne leakages. The pressure decay and soap and bubble tests are both time-consuming and inaccurate. In spite of having a high initial investment, ULD has high rate of return due to its efficiency and accuracy. From a safety perspective, its ability to detect a leakage at a distance of 20 meters from the leakage source is highly relevant for moving railcars.

Table 1: Comparison among leakage detection methods

	Listening - sonic and ultrasonic emissions	Visual - Soap bubble test	Visual - Pressure decay test
Human involvement	Minimum. Needed only to carry the instrument and record the sound signals	Maximum. Needed to apply soap spray and visually locate the bubbles	Medium. Needed to record the pressure differential
Cold weather effectiveness	Very effective. Cold weather reduces noise and increases directionality of sound	Effective	Effective
Time and Money	Least time-consuming, one-time investment for the instruments and less manpower	Most time-consuming, manpower. Regular use of soap spray	Time-consuming, regular maintenance of single car test equipment
Ease of operation	Simple and fast. Walk along the train with the instrument	Complex. Spray the system, visually see the bubbles and clean the system all along the train	Fewer operations than soap bubble test. Set up the single car test equipment for different airbrake networks.

CHAPTER 3: LEAKAGE ASSESSMENT

Various studies have been conducted for leakage localization and quantification. Understanding the feasibility of ULD in rail airbrakes under cold weather conditions is the prime objective of this research. Field and laboratory tests were conducted to determine the effect of weather and operating conditions on ultrasonic intensity.

3.1 FIELD TESTING: QUALITATIVE ASSESSMENT

The passive ULD technique was tested in the Canadian Pacific (CP) yard in Golden, BC for a freight rail airbrake system. It was useful to conduct our testing in Golden because it has both an internal car repair facility equipped with the latest inspection airbrake methods used by CP, and an external yard for comprehensive inspection of the complete train. A team represented by sales and technical experts from airbrake manufacturing vendor Wabtech, the yard manager, CP's mechanical reliability experts and a team of researchers from the University of Alberta conducted the tests in the car repair facility and the yard to check the feasibility of using the ultrasonic instrument to test for leakages in airbrakes.

Table 2: Data for field tests

Area	Temperature	Type of Sensor	Distance from Leakage	Number of Cars Tested	Duration of Test (min)
Internal Car-Repair Facility	+20 degree Centigrade	Flexible Distance Parabolic Dish	0 2 10	1	3
External Yard Facility	-15 degree Centigrade	Flexible Distance Parabolic Dish	0 2 10	10	20

Table 2 has the data used for testing airbrakes in the field. The testing plan was to use a parabolic dish while seating in a heated vehicle and drive parallel to the train to detect any sort of ultrasonic signal. Once a signal was detected, the sensor was changed to a distance sensor and the inspector walked towards the railcar emanating the signal. The intensity of the signal was observed to be increasing as the sensor was brought close to the leakage source. On reaching a distance of 2 meters from the railcar, the sensor was oriented towards the maximum intensity direction. Then the sensor was again changed to a flexible sensor. This sensor has a flexible head that can be twisted and turned to the direction of maximum intensity. After several twist and turns, the maximum intensity direction can be located. This leakage location was verified using the soap and bubble test.

Based on the above testing, ULD has a certain advantage over pressure decay and the soap and bubble test. The time consumed in checking all the components of airbrakes in a train consisting of 100 railcars is decreased substantially. Instead of checking all the cars, only the leaking cars (approx. 10) have to be checked.

The internal testing in the car repair facility was easy to perform and was used as a platform to validate the external yard testing. The leakages were easily detected with the instrument. The intensity decreased as the sensor was moved away from the leakage. The same leakage would not have been identified if the area had not been lubricated with soap, but the ultrasonic sensors easily captured the ultrasonic signals emanating from the leakages. Leakages could not be detected when the airbrake system was blown down, as the hissing sound from the release valves obstructed the readings. However, this ceases to be a problem as it is only essential to identify leakages during charging and airbrake application. Figure 14 shows the usage of the instrument near a freight airbrake.

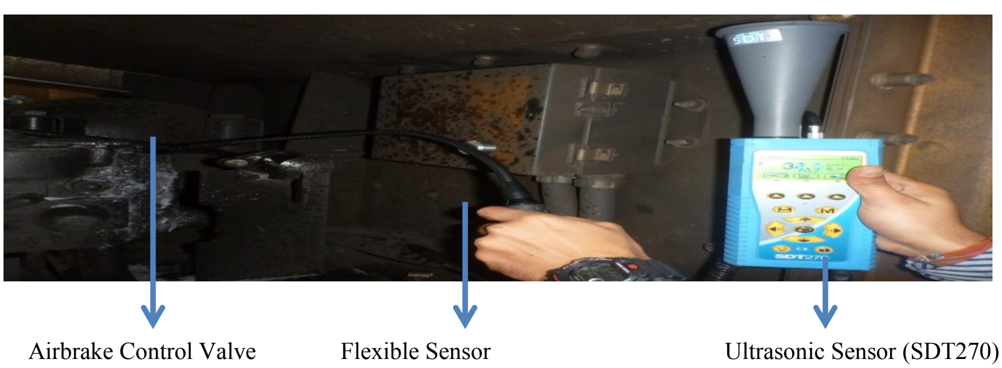

Figure 13: Passive ULD in CP car repair facility

The successful working for the instrument inside the car repair facility validated the use of the instrument in external cold weather conditions of -20C. The instrument was able to detect the leakages even in external conditions. The parabolic dish, the cone and the flexible sensor were all working as per specification. However, there was a problem detecting leakages in hidden places. Although the directional nature of ultrasound attenuates the ultrasound after successive reflections and also decreases the ultrasound intensity, the instrument was able to capture major leakages, even at a distance of 20m from the source. Figure 15 reflects the testing done in the yard.

Figure 14: Passive ULD at CP's yard

The directional nature of ultrasound was clearly observed during the testing. What was also observed was that the ultrasonic intensity increased as the leakage size increased, and the intensity decreased as the sensor was moved further from the leak hole. The above tests gave us a clear indication about the usefulness of the ULD in cold weather conditions. It was an easy and more accurate solution to the problem of leakage detection for rail airbrakes. Considering the positive results of the proposed technique in the field tests, the ULD technique was tested for the effect of variation in operating conditions on ultrasonic sound intensity.

3.2 Laboratory Experiments: Quantitative Assessment

A systematic approach has been used in designing the experiment based on the results of previous studies conducted by some researchers [30]. Before conducting actual experiments, a pre-experiment plan was developed based on the previous studies and field tests conducted in Golden. This plan was useful to understand the problem, determine design factors and get a qualitative idea of the results. Laboratory experiments were then conducted in simulated and actual airbrake components, for which readings were recorded for further analysis.

3.2.1 Design of Experiment

A physical model of a pneumatic airbrake system was developed to conduct experiments under laboratory conditions in order to understand the relationship among design factors and outputs. The strategy of experimentation was to change one factor at one time and observe the effect on the output. The design factors were selected based on results from previous research, experience of ULD experts and field visits to the CP yard.

Problem Statement: A sequential approach is used to conduct a series of experiments to characterize simulated compressed air leakage under different operating conditions. This experiment can lead to the discovery and confirmation of the relationship between design factors and output.

Choice of factors, levels and range: The potential design factors for the experiment were chosen from the Hagen-Poiseuille equation. This equation is used to understand the effect of different parameters on the leakage flow-rate [42].

$$Q = C * \frac{d^4}{L} * \frac{DP}{\mu}$$

Equation 6

where, Q = Volumetric flow-rate , C = Constant, d = Circular diameter, P = Pressure differential across the path, μ = Fluid viscosity, L = Length of fluid flow

This equation clearly shows that the volumetric flow from a leakage depends mainly upon three factors: the pinhole diameter, length of fluid travel and differential pressure across the pipe.

The design factors used for the purpose of experimentation are, compressed air operating pressure, room temperature, distance between leakage and sensor, sensor orientation from leakage and leak hole diameter. As per Bernoulli's equation, an increase in pressure should increase the flow-rate of compressed air. Ultrasound intensity is directly related to the rate of flow of compressed air [30]. The effect of temperature on the flow of compressed air is critical for understanding the use of ULD in cold weather conditions. Distance from the leakage source has an inverse relationship to the ultrasound intensity. The experiment results will determine the magnitude of the effect. The testing at the CP yard indicated the decreasing ultrasonic intensity on decreasing the sensor orientation from perpendicular to zero degrees. Also, the manufacturer of the ULD warns that the sensor orientation will affect the intensity [35]. Therefore, sensor orientation was included in the design factors to understand its effect on ultrasound intensity. The leak hole diameter had the strongest effect on the intensity during field tests; hence, it is one of the most critical design factors.

The ULD instrument gives us the root mean squared value of ultrasound intensity. The airbrake solution measures the flow-rate from the leak hole. This will verify the test results, as the intensity and flow-rate are directly correlated.

Table 3: Factors, Levels and Range of Experiment

Factor	**Type**	**Range**	**Level**
Operating pressure (P)	Design	60 - 90 psi	2
Room temperature (T)	Design	(-)20 - 20 degree C	3
Leakage flow-rate (f)	Output		
Distance between leakage and sensor (d)	Design	0 – 2 m	2
Sensor orientation from leakage (Θ)	Design	0 - 90 degree	2
Orifice size (a)	Design	0.001" - 0.005" (diameter)	5
Ultrasound Intensity (RMS)(Irms)	Output		

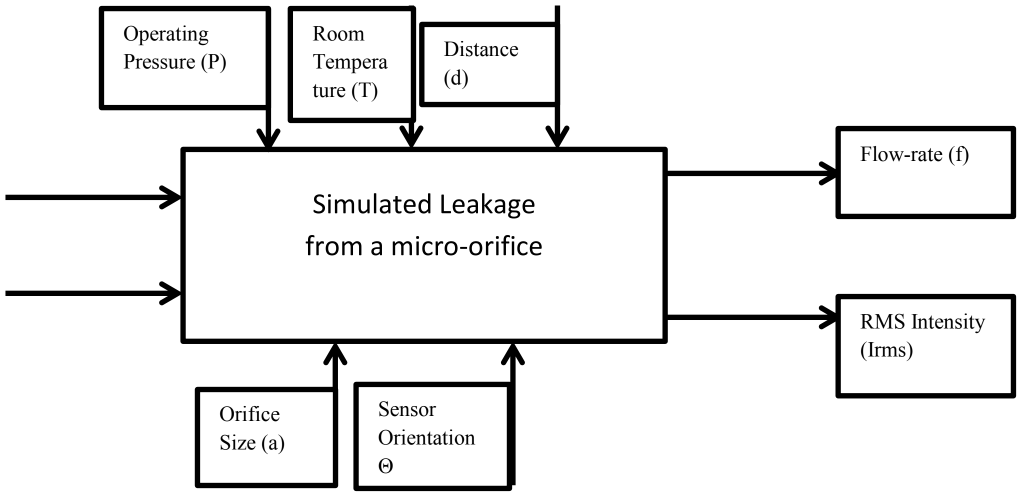

Figure 15: Model for experiment process

Table 3 shows all the design parameters for the experiment, while Figure 16 is a pictorial representation of the experimental process.

3.2.2 Test Rig

The test rig was designed in the Canadian Rail Research Laboratory (CaRRL) at the University of Alberta. Experiments with simulated leakages and actual component leakages were performed in a temperature-controlled chamber. Data acquisition was electronically controlled using a laptop.

All the components of the experiment were purchased or arranged through CaRRL. There was a compressed air line in the laboratory. All software was downloaded from CaRRL's website on a trial basis. The requirement of the experiment was fulfilled with the trial version of Sigview and XLStat software, which saved us additional costs. The Airbrake Solution (ABS) and micro-orifices were purchased from Eutectic Solutions Inc. in Ontario, Canada and O'Keefe Controls Co. in Connecticut, USA respectively.

Figure 21 is the layout of the experiment, which was simple in its design and easy to operate. The only important consideration was to tap any unwanted leakages that can be present in the inlet, ABS or outlet parts of the experimental setup. The compressed air from the laboratory was allowed to enter the airbrake solution at 120 psi. The airbrake solution consists of a pressure regulator, pressure gauges, flow meters and output hose. The inlet pressure was regulated from 100 to 60 psi. This compressed air was allowed to exit the airbrake solution, through a flexible hose, from a simulated leak hole. The leak hole was artificially introduced using micro-orifices. Micro-orifices have a specific diameter (1/8 inch) that could plug into the outlet hose of the airbrake solution. Thread seal tape was wrapped around all joints to block any possible leakage. The ultrasound generated from the leakage was detected using an ULD. Five different sizes of micro-orifices were used to observe the effect of the leak hole diameter. Pressure could be regulated from the regulator in the airbrake solution. Distance and orientation were marked from the leakage source. The instrument was kept on the marking to observe the readings. Figure 22 is the picture taken in the laboratory of the setup used for the experiment.

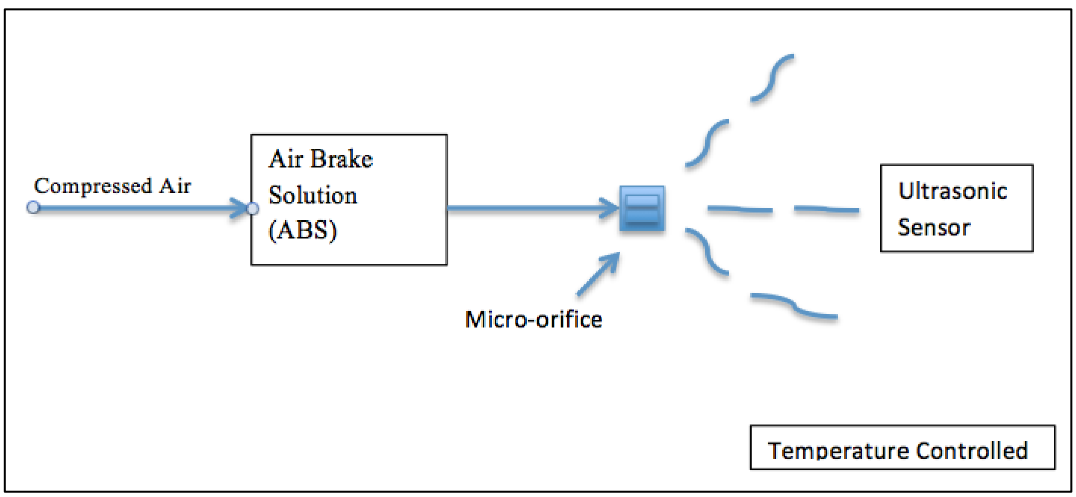

Figure 16: Layout for basic experiment

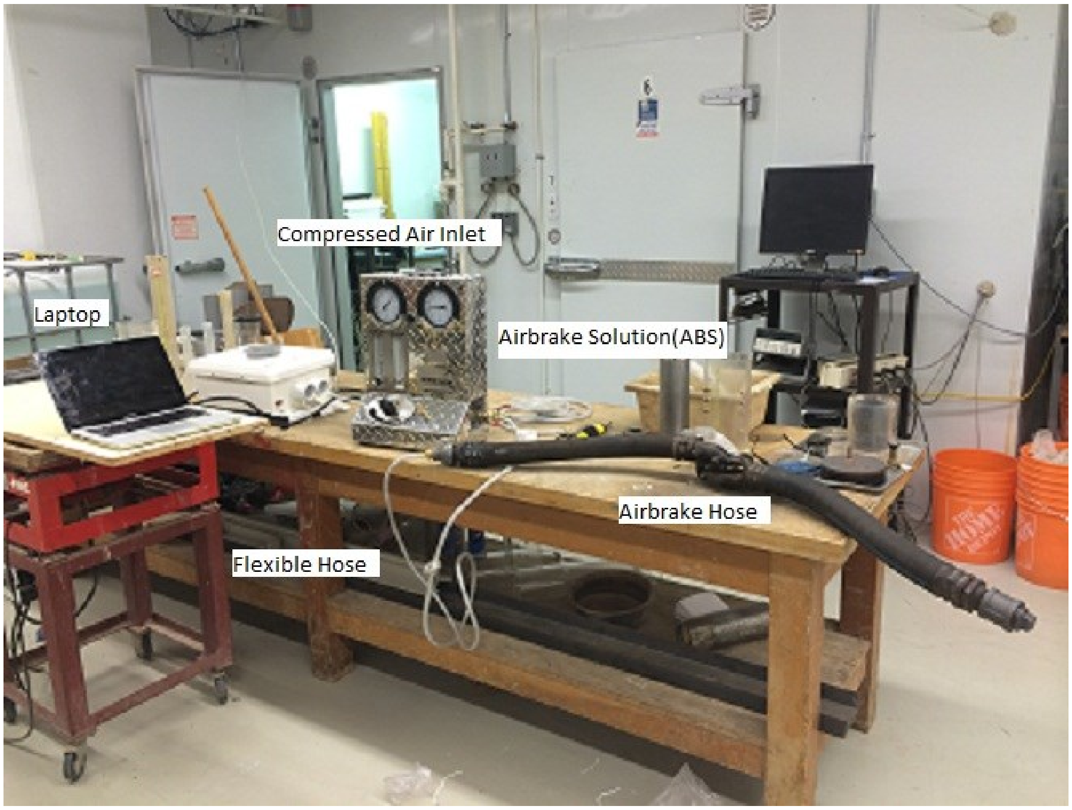

Figure 17: Experiment Setup at CaRRL Laboratory

3.2.2.2 Component and Software Description

Airbrake Solution: The Airbrake Solution, as shown in Figure 19, will provide airflow readings that are within 0.2 LPM of the total leakage from the system. Its purpose is to provide the technician with leakage size information to determine the most appropriate strategy for each leakage, as well as the ability to be certain of the amount of remaining leakage after the repair. It should also be used in a maintenance function to observe the changing integrity of the storage system. It has a control valve that controls the outlet pressure. The outlet hose allows the compressed air to pass through the micro-orifice.

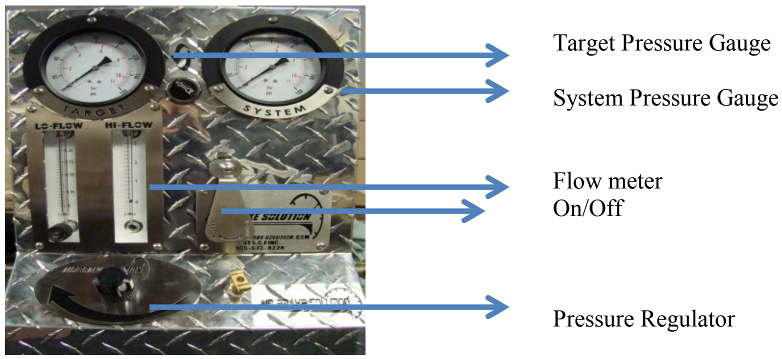

Figure 18: The Airbrake Solution

The ABS takes the place of the vehicle's compressor; it is inserted into the airbrake system directly after the compressor or before the dryer. Shop air is then routed through the instrument at the selected pressure, into the airbrake system. The target and system pressure gauges are observed as the system is being filled. At low-pressure the air flow meters are bypassed.

When the airbrake system pressure rises to approximately 92+psi, airflow is internally diverted through the airflow meters, which will be pinned over maximum for several minutes. As the airbrake system becomes filled close to the selected target pressure, airflow will begin to slow down. When the airflow slows to 3 l/min, the hi-flow meter ball will begin to drop.

As the airflow continues to drop, the high-flow meter ball drops in response. The high-flow meter ball will come to rest several times within the scale for between 15 and 60 seconds (Stable Reading). This is the first indication of the size of the leakage or leakages. Note that in some conditions, the flow meter ball may actually rise for a few moments, especially if the compressor cycles.

Micro-Orifice: The precision micro-orifices, as shown in Figure 20, are constructed of brass or stainless steel with orifice sizes from .0003" to .005" in diameter. The orifices are used to accurately meter very low flow-rates of gases or liquids. Optional stainless steel screens are available to protect the tiny orifices from minute contamination particles. When experiments were conducted with the actual component, an airbrake hose with coupling was used in place of a micro-orifice. The leakage in the hose served the purpose of actual component failure.

Figure 19: Precision Micro-Orifice from O'Keefe Controls Co.

ULD Device, SDT 270: The SDT270 is a portable ultrasound device dedicated to predictive maintenance and energy saving. It covers a wide range of applications and meets the needs of the maintenance departments. The SDT 270 DU model, as shown in Figure 21, was used for laboratory experiments. It has both static and dynamic data recording capabilities.

Figure 20: SDT 270 kit

SDT 270 comes with three types of sensors, as shown in Figure 22. The flexible sensor is useful for proximity leakages that are present in accessible locations or hidden locations. The distance sensor gives an idea of the direction from which the ultrasound is generated. The parabolic sensor gives a wider idea of the location of the origin of sound. The philosophy is to use the parabolic dish to get an idea of the emanating sound direction, and then close in using the distance sensor before finally locating the leakage with the flexible sensor.

Figure 21:Flexible Sensor, Distance Sensor and Parabola Dish

Ultranalysis Suite: This software was used to plan the survey from a computer, upload the survey to the device and analyze the downloaded data [49]. We can download image files of time-domain and frequency-domain signals directly from the computer. This image files can be further analyzed to find discriminating spectral features. Figure 23 is a screen shot of the ultranalysis software. The left pane is the tree structure for a planned survey. The right pane shows the dynamic time and frequency domain ultrasonic signals. Several search strategies can be used to shortlist signals as per requirement.

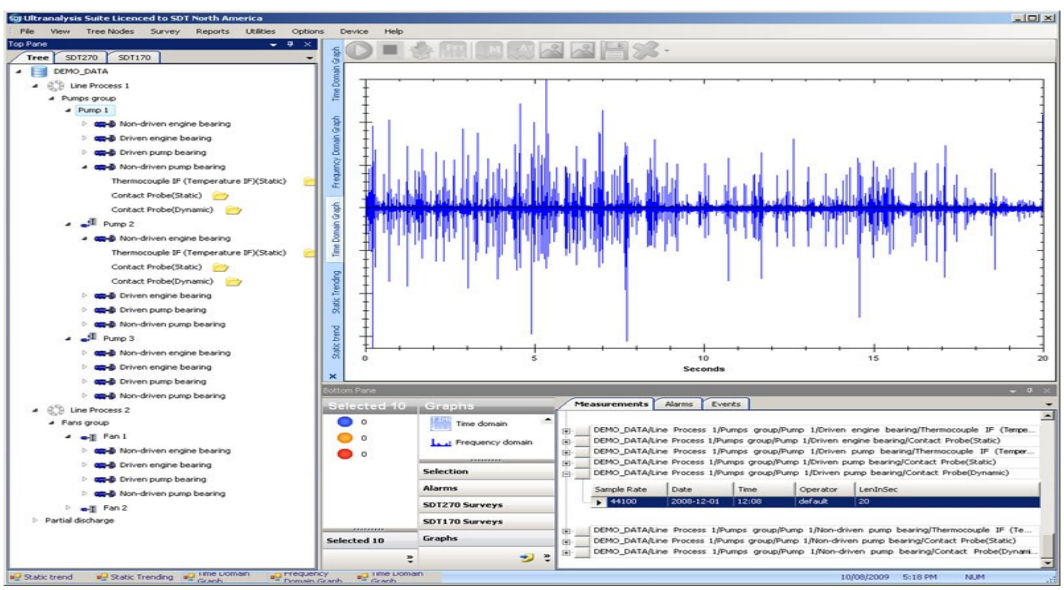

Figure 22: Screen Shot of Ultranalysis software

Sigview: This is a signal processing software, which was used to detect the statistical features of the time-domain and frequency-domain signals [51]. Fast Fourier Transform (FFT) was performed on the time-domain signal to obtain the frequency-domain. A band-pass filter was applied on the FFT to find the frequency range most sensitive to the change in factors.

XLStat: This is statistical software useful to perform most of the statistical operations on a data set [50]. For the purpose of analyzing the data obtained from Sigview, XLStat was used to perform PCA.

3.2.2.3 Experiment Procedure

For the purpose of recording the readings at a pre-defined temperature, the experiment was conducted in a cold chamber. At the particular temperature, the procedure is:

Step 1) Connect the air supply, ABS and a micro-orifice 0.005" in diameter.

Step 2) Pressurize the system to 100 psi with the help of the air regulator in the ABS.

Step 3) Record the flow rates and sound intensities at 0 and 2 meter sensor distances and 0 and 45 degree sensor orientations from the orifice.

Step 4) Decrease the pressure by 20 psi and record the readings with variations of sensor distance and orientation.

Step 5) Change the micro-orifice diameter by 0.001" and repeat steps 2 through 4, until all the orifice sizes from 0.005" to 0.001" are tested.

There should be no leakage in the setup other than the designated artificial leakage. It is essential to be careful when tightening the inlet and outlet valves. The system and target pressure should be same and the indicators in the pressure gauge should be stationary when the readings are recorded.

A set of repeat experiments is conducted to prove that the result values commensurate when they are recorded according to the same experimental conditions. A two-tailed t-test was performed on the difference of the readings from repeat experiments. The null hypothesis that the means of both replicate readings are same is true, as the probability for error is within acceptable limits.

3.2.3 Data Collection and Retrieval

A planned survey for 360 data points was uploaded in the ultrasonic device. Static and dynamic readings for ultrasound intensity were recorded using SDT270. This data was downloaded using a mini USB-to-USB cable connected to the Ultranalysis software for further analysis. The average of the two readings for each observation was performed to obtain a more realistic value of the intensity. Hence, there were 180 observations for 5 orifice sizes, 3 pressure settings, 3 temperature settings, 2 sensor distance variations and 2 sensor orientation variations. The dynamic ultrasonic signal was band-passed into 25 parts of 100 Hz each. For each of these 25 signals, spectral features such as the crest factor, kurtosis, mean frequency, maximum Power Spectral Density (PSD), sum of PSD and Root Mean Square (RMS) value of PSD were recorded.

The Crest Factor is the ratio of the peak value to the average value in a waveform. Kurtosis is also a measure of peaks, but it differs from the crest factor in that it measures the extreme peaks rather than the moderate ones. PSD is a more meaningful spectral feature. It is the distribution of the power of a signal over the different frequency ranges.

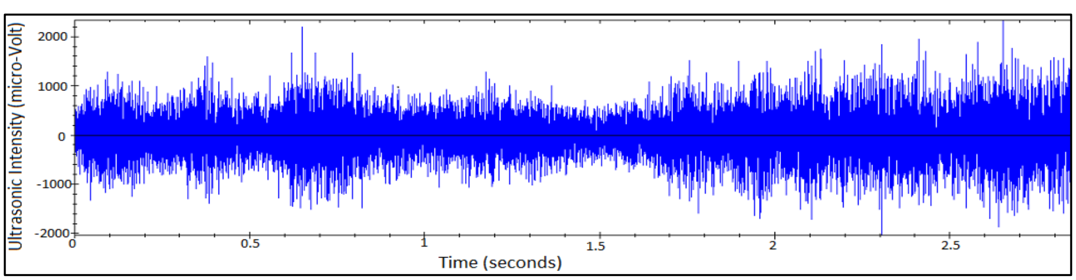

Figure 23: Sample of Time-Domain Ultrasonic Signal

The signal represented by Figure 24 was band-passed for frequency 0-100 Hz, 100-200 Hz ….. 2400-2500 Hz. An FFT was performed on each band-passed signal for observation numbers 5, 17, 29, 31, 37, 38, 41, 45, 53, 105, 107 and 165. The choice of observations was made such that variations in all five variables were accounted for. Five spectral features were recorded, using Sigview for each of the 25 FFT signals of the 12 observations. Therefore, 1500 observations were recorded for further analysis using XLStat. The data for 180 static and 1500 dynamic spectral features can be found in Appendix A and Appendix B.

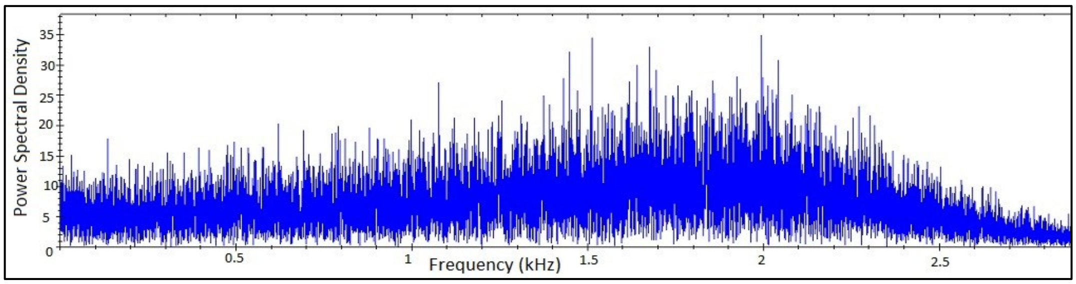

Figure 24: Sample of Frequency-Domain Ultrasonic Signal

Figure 25 is a sample of the frequency domain ultrasonic signal. This signal is divided into 25 equal parts for recording the spectral features to be used for PCA. Signal discriminating features can be distributed among several spectral features, for example maximum value, minimum value, standard deviation, mean, skewness, and crest factor. But, only five features were selected based on previous research and random selection.

The literature counts a number of methods used to identify suitable prognostic features, including engineering judgments, PCA and optimization methods. Feature selection is usually done through engineering judgments and visual assessment. Engineering judgments may lead to satisfactory results. But, it can be tedious and time consuming when there are many features to consider, and also the optimal feature may be ignored in favor of a suitable one. With the help of formulating desirable metrics, it is possible to apply a programmed method to the key features, which results in identifying a suitable single prognostic combined feature [31]. The definition of selected spectral features kurtosis, sum of PSD, Max PSD, RMS PSD and frequency at Max PSD is mentioned in Table 4. After recording the static and dynamic data with spectral features, 27 Microsoft Excel sheets were formatted for PCA application as listed in Table 5.

Table 4: Definition of Spectral Features

Feature	Definition	Equation	Reason
Kurtosis	The measure of sharpness of peaks in a signal	$\frac{1}{N}\sum_{i=1}^{N}(\frac{xi-\mu}{\sigma})^4$, where N= number of points, μ = mean , σ=standard deviation	Its relevance in previous research on vibration monitoring
Power	Total power of a signal	$\sum_{i=1}^{N}(PSD)i$, where N= number of points, (PSD)I = power spectral density at point i	Distribution of power in a signal is an important feature
Maximum power spectral density	The maximum power of a frequency range	$Max\ (PSD)i$	The sum, maximum and rms values of power for a signal can be important features
Root mean square value of power spectral density	Root mean square is a more accurate value to be used for averaging a signal	$\sqrt{\frac{1}{N}\sum_{i=1}^{N}(xi)^2}$	The sum, maximum and rms values of power for a signal can be important features
Frequency at maximum power spectral density	The frequency at which the maximum power occurs for a frequency range	$Frequency\ (\ Max\ (PSD)i)$	The frequency at which maximum power occurs can be a useful discriminating factor.

Table 5: Excel Sheets for PCA in XLStat

S.N.	**Analysis Sheet**	**S.N.**	**Analysis Sheet**
1	Static data for basic experiment	15	Temperature variation for RMS value of PSD
2	Static data for Airbrake Hose experiment	16	Temperature variation for maximum value of PSD
3	Distance variation for Kurtosis	17	Temperature variation for maximum frequency value at maximum PSD
4	Distance variation for sum of PSD	18	Pressure variation for Kurtosis
5	Distance variation for RMS value of PSD	19	Pressure variation for sum of PSD
6	Distance variation for maximum value of PSD	20	Pressure variation for RMS value of PSD
7	Distance variation for maximum frequency value at maximum PSD	21	Pressure variation for maximum value of PSD
8	Orifice variation for Kurtosis	22	Pressure variation for maximum frequency value at maximum PSD
9	Orifice variation for sum of PSD	23	Sensor orientation variation for Kurtosis
10	Orifice variation for RMS value of PSD	24	Sensor orientation variation for Sum of PSD
11	Orifice variation for maximum value of PSD	25	Sensor orientation variation for RMS value of PSD
12	Orifice variation for maximum frequency value at maximum PSD	26	Sensor orientation variation for maximum value of PSD
13	Temperature variation for Kurtosis	27	Sensor orientation variation for maximum frequency value at maximum PSD
14	Temperature variation for sum of PSD		

3.2.4 Validation Testing

The idealized testing with micro-orifices was performed to understand the effect of variations in operating variables on contribution of frequency ranges of frequency-domain ultrasound signal. The results of idealized testing are validated with actual airbrake components.

3.2.4.1 Components

Airbrake consists of valves, pipes and reservoirs. The major source of leakage is different types of valves like reducing valve, glad hands and ball valve. Experiments were performed for new and leaking versions of these components to record the dynamic ultrasound intensity.

		
a) Airbrake Hose	b) Ball Valve	c) Reducing Valve

Figure 25: Airbrake components for validation

The experimental procedure followed is same as the idealized test.

CHAPTER 4: DATA ANALYSIS AND INTERPRETATION

The data was formatted in 26 Excel sheets. The scope of this chapter is to summarize the information gathered from those sheets. It was broken down into four parts: trend analysis of static data from the basic experiment, trend analysis of static data from the airbrake hose, PCA1 or static data, and PCA2 for spectral features.

The evaluation of leak factors previously has been performed by researchers on directionality, distance from the leak, length effect and orifice shape [52]. The level of ultrasound should be measured close to the leakage, due to combined effect of sound divergence, attenuation, reflection and refraction. The ultrasound intensity follows an inverse distance law as follows:

$$L2 = L1 - 20log\frac{r2}{r1}$$

Equation 7: Inverse distance law

where L1 and L2 are the sound levels at the respective r1 and r2 distances from the leakage source.

It has been previously proved through experiments that at closer distances the variation in direction has more effect on intensity. Also, for symmetrical orifice the ultrasound profile is also symmetric [52]. The work done here is a validation for previous research. Also, a new ultrasonic instrument SDT270 is used for our experimental purposes. The result of this analysis will show if there is any effect of change in ultrasound detection instrument on the spectral features. Other variables like operating pressure, temperature, leakage type and size are also considered for analysis.

4.1 TREND ANALYSIS

Static readings for 180 different scenarios were recorded and the data was exported into Microsoft Excel. The variation of ultrasonic intensity with change in orifice size, pressure, temperature, sensor distance and orientation was plotted to observe the increasing or decreasing trend. For each scenario two readings were recorded and the average of both the readings was considered for our analysis. Trend analysis was also performed on data from actual failures of airbrake hoses.

4.1.1 Basic Experiment

The experiment conducted with simulated leakage resulted in some interesting results. These results were plotted, in Figure 25, for different observations to capture any observable trend. These trends will be used as a reference to verify the results from actual component testing. The trends for each variable will be further elaborated using correlation and PCA in the subsequent sections.

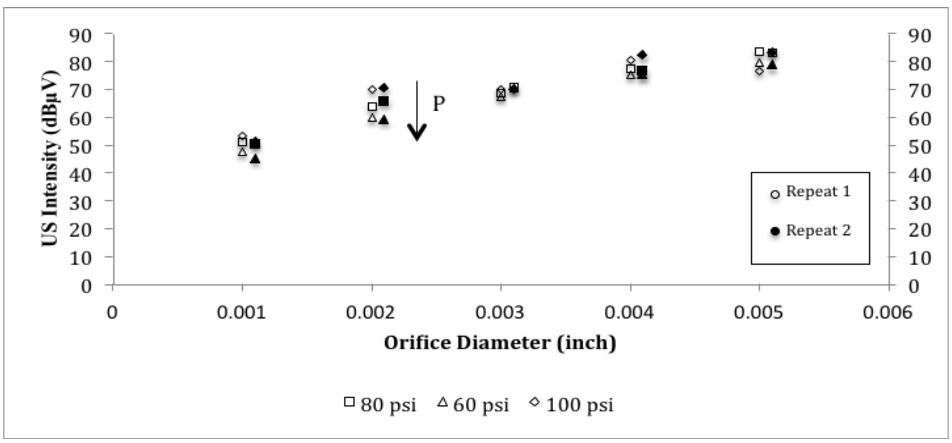

a) Effect of orifice size (a) and pressure (P), at T=22 degree C, A=0 degree, and d=0 m

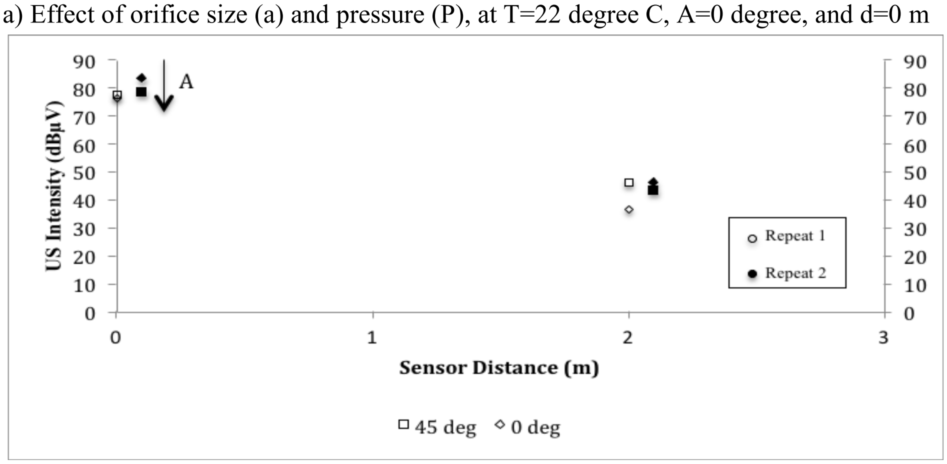

b) Effect of sensor distance (d) and orientation (A), At T=22 degree C, a=0.005”, P=100 psi

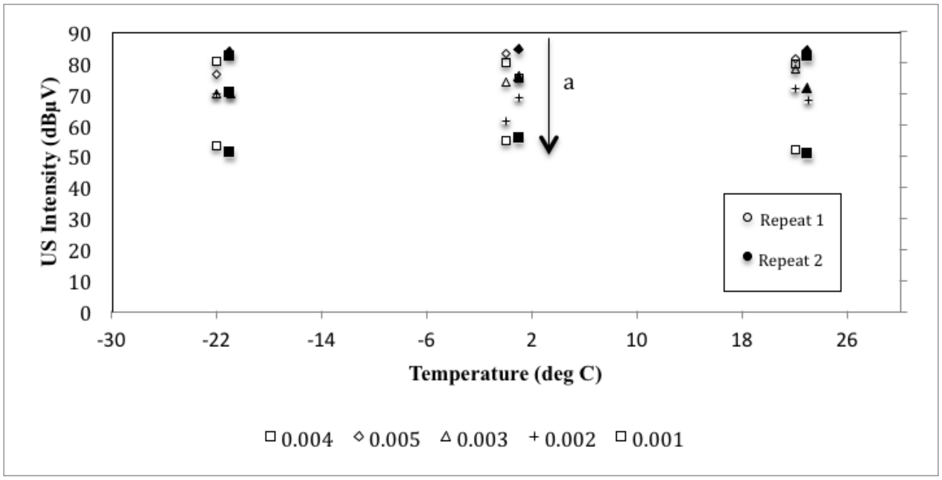

c) Effect of temperature (T), at A=0 degree, d=0 m, and P=100 psi

Figure 26: Effect of operating variables on ultrasonic intensity

When the pressure of the compressed air inside the hose is decreased from 100 to 80 psi and 80 to 60 psi, there is a decrease in ultrasonic intensity as observed by the ULD. The decrease in intensity is less than about 10%. There is no clear trend of increasing or decreasing intensity with a change in temperature. This indicates that ultrasound is not sensitive to ambient temperature, which is a good result for a method that has to be used over a wide range of temperatures. It can be observed that intensity increases with increasing orifice size, which makes sense according to theory. Also, distance has a considerable effect on ultrasonic intensity. With an increase in distance, intensity is reduced. At close distance, a trend of decreasing intensity can be observed. As the distance is increased, a change in orientation shows no particular trend for intensity.

4.1.2 Trend Analysis on Airbrake Hoses

It is essential to verify the basic experiment with a simulated leakage through experiment with actual leakage from airbrake components. Therefore, some used components were brought from the Canadian Pacific yard in Edmonton. An airbrake hose was used for the purpose of the experiment, as the hoses are the most critical leaking components in an airbrake system.

The experiment was similar to the one with simulated leakage. The outlet of the ABS needed to be connected to the airbrake hose. Steel fittings were bought at

Canadian Tire (a general goods and automotive parts store) to ensure that compressed air would pass through the hose without any unwanted leakage. The end of the hose was closed to maintain an operating pressure in the system. As temperature has an insignificant effect on intensity, only the pressure was varied to validate the results from the basic experiment. Repeats were conducted for each case and the average was used for analysis purposes.

Table 6: Intensity data for airbrake hose

Location	US RMS intensity	Pressure	Flow
A1	51.45	100	0.07
A1	51.95	80	0.06
A1	48.9	60	0.05
A2	22.85	100	0.01
A2	24.75	80	0.01
A2	14.8	60	0.01
A3	20	100	0.01
A3	15.5	80	0.01
A3	8.4	60	0.01

The leakage at location A1 can be compared to the results from the basic experiment. Under the same conditions, a simulated leakage size of 0.001 inch is similar to that in hose leakage location A1. As the flow-rate for both cases is the same, it can be confirmed that the leakage size for A1 is 0.001 inch. It can also be confirmed that the orifice sizes for leakages A1 and A2 are small compared to A1. Figure 26 clearly shows that with a decrease in pressure, the ultrasonic intensity decreases as per expectation. Figures 27 and 28 are laboratory pictures of the airbrake hose experiment.

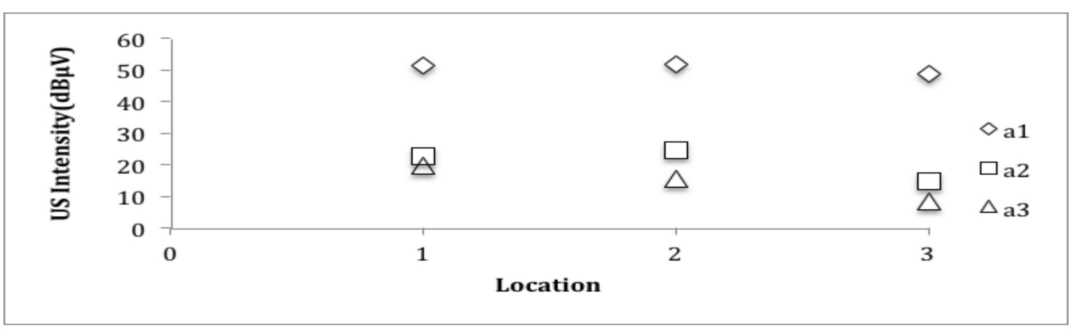

Figure 27: Effect of Pressure on US intensity

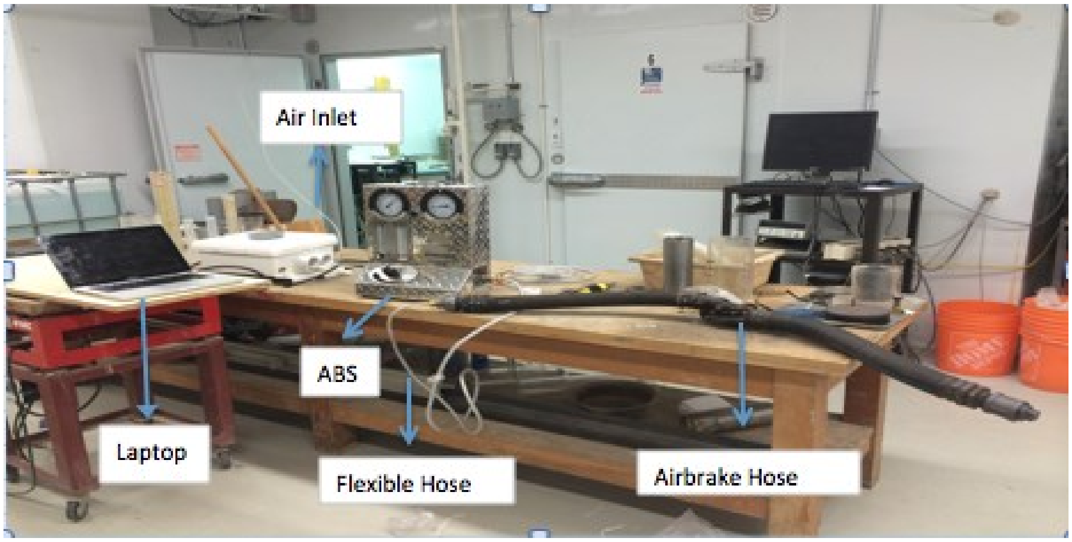

Figure 28: Experiment Setup for Airbrake Hose

		
A1) Inlet	A2) Glad Hands	A3) Closed End

Figure 29: Leakage in an airbrake hose

4.2 PRINCIPAL COMPONENT ANALYSIS

PCA is useful when there are many observed variables and we wish to develop a small group of variables (principal components) that account for maximum variation. The principal components may be used as critical variables in subsequent analysis. It is used to reduce the redundancy in the variables by introducing artificial variables [46].

PCA starts with a Pearson Correlation matrix to find the correlation coefficient between each variable. Bartlett's Sphericity test and Kaiser-Meyer-Olkin (KMO) measure of sampling adequacy are used to find the eligibility for conducting PCA for a dataset. The Bartlett's test compares the observed correlation matrix to the identity matrix. In other words, it checks if there is a certain redundancy between the variables that can be summarized with a few factors. The KMO index has the same goal. It checks to see if the original variables can be factorized efficiently. Once a dataset is eligible, PCA is performed in the following sequence [46]:

Step 1: Extraction of Components

The number of components extracted is equal to the number of variables analyzed. Each component accounts for a certain amount of variance that is represented by an eigenvalue. Generally, the first component accounts for a large amount of variance, while the later components are relatively smaller.

Step 2: Determination of Meaningful Components

The first few components account for meaningful variance. The scree test is used to plot the eigenvalues and look for a break between the components with relatively large eigenvalues and those with small eigenvalues. The components that appear before the break are considered meaningful and retained for rotation. Those appearing after the break are assumed to be unimportant and are not retained.

Step 3: Analyzing Factor Loadings and Factor Scores

Factor loading is the contribution of each factor to the components. The factor scores are the contribution of each observation to the factors. Properly observing the values of factor scores will give the importance of observations on a particular component. The variable that accounts for most of the variation can be shortlisted for subsequent analysis.

4.2.1 PCA1: STATIC RESULT

A pearson correlation was performed on 180 observations of 10 variables: RMS intensity, flow, crest factor, temperature, pressure, distance, orientation and orifice.

Correlation Matrix

The Pearson product-moment correlation coefficient is a measure of the linear correlation (dependence) between two variables, X and Y, giving a value between +1 and −1 inclusive, where 1 is the total positive correlation, 0 is no correlation, and −1 is the total negative correlation. It is widely used in the sciences as a measure of the degree of linear dependence between two variables [46].

Table 7: Correlation Matrix for Static Data of Basic Experiment

Variables	RMS Peak	Peak	Crest Factor	Temp	Orifice	Pressure	Distance	Orientation	Flow
RMS	**0.999**	**0.999**	**0.470**	-0.016	**0.510**	0.109	**-0.827**	-0.063	**0.439**
RMS Peak		**1.000**	**0.493**	-0.019	**0.498**	0.106	**-0.839**	-0.049	**0.428**
Peak			**0.504**	-0.021	**0.498**	0.106	**-0.839**	-0.050	**0.428**
Crest Factor				-0.126	0.007	-0.035	**-0.619**	**0.231**	-0.028
Temp					0.000	0.000	0.000	0.000	-0.099
Orifice						0.000	0.000	0.000	**0.870**
Pressure							0.000	0.000	**0.327**
Distance								0.000	0.000
Orientation									0.000

From Table 7, it can be observed that distance and orifice correlate highly with ultrasonic intensity, while temperature and orientation correlate insignificantly with all of the variables. Table 8 shows the correlation in decreasing order of magnitude.

Table 8: Decreasing Order of Correlation

S.N.	Variable	Correlation
1	Orifice-Flow	+ 0.870
2	Distance-Intensity	- 0.839
3	Distance-Crest Factor	- 0.619
4	Orifice-Intensity	+ 0.498
5	Flow-Intensity	+ 0.439
6	Pressure-Flow	+ 0.327
7	Orientation-Crest Factor	+ 0.231

Eligibility tests

The Kaiser-Meyer-Olkin measure of sampling adequacy tests whether the partial correlations among items are small. Bartlett's test of sphericity tests whether the correlation matrix is an identity matrix, which would indicate that the factor model is inappropriate.

Table 9: Bartlett's Sphericity test and KMO measure of Sampling Adequacy

Bartlett's sphericity test	
Chi-square (Observed value)	3900.150
Chi-square (Critical value)	61.656
DF	45
p-value	< 0.0001
alpha	0.05

Kaiser-Meyer-Olkin (KMO) measure of sampling adequacy	
US RMS	0.797
US intensity RMS peak(dBμV)	0.819
US intensity peak (dBμV)	0.725
US Crest Factor	0.480
Temperature	0.035
Orifice	0.370
Pressure	0.062
Distance	0.556
Orientation	0.195
Flow	0.397
KMO	**0.547**

A KMO value of 0.547 is considered mediocre but eligible for PCA. An alpha value of less than 0.5 indicates there is some meaningful correlation between the variables. Both the tests are positive indications for PCA analysis.

Scree Test

According to the scree plot shown in Figure 29, the first five components are meaningful for PCA. But, for our analysis, only the first two components are used as they represent 63 percent of variability in the data.

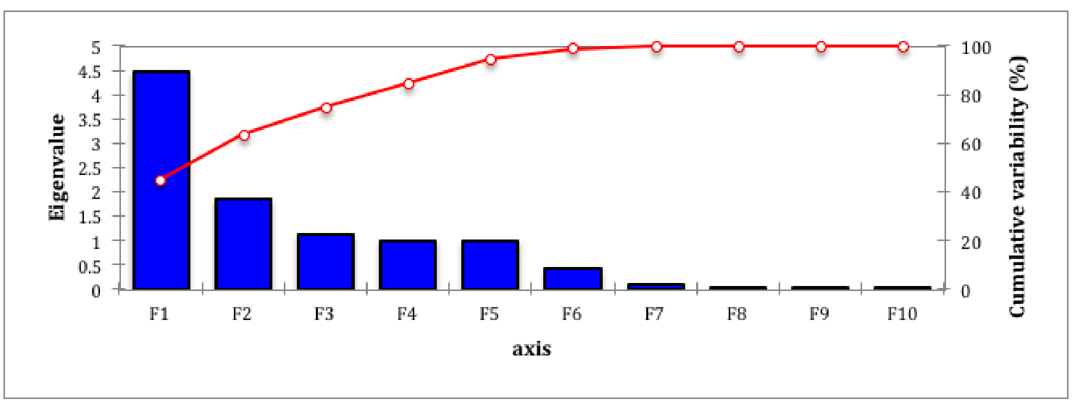

Figure 30: Scree Plot for Static PCA

Bi-plot

Bi-plot display is a visualization technique for investigating the inter-relationships between the observations and variables in multivariate data.

The bi-plot for Factor 1 and Factor 2 accounts for 63.4 percent of variability in data and is plotted in Figure 35. It represents the trend, magnitude and difference in the relationship between variables.

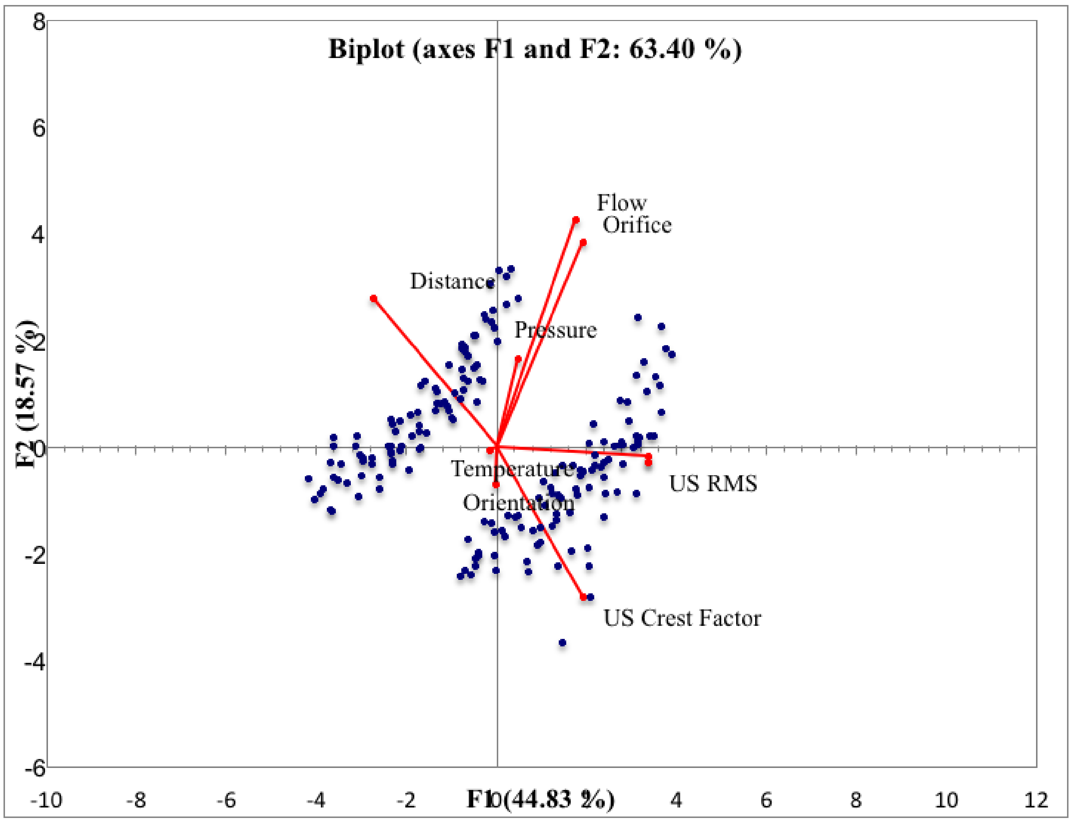

Figure 31: Bi-plot for Static PCA

Figure 30 shows the factor loadings and factor scores for variables and observations in Factor 1 and Factor 2, which together account for a 63.4% variance. The bi-plot clearly shows that flow, orifice and pressure align in the same direction, because they are directly related to each other. The length of the red lines indicates the extent of the relationship between variables. The insignificant effect of temperature is also apparent.

4.2.2 PCA2: DYNAMIC RESULT

To understand the behavior of the time-domain dynamic ultrasonic signal with the change in variables, sound signals in Table 9 are shown as they were analyzed in Sigview. The observations were selected such that the effect of variation in variables is analyzed. The effect of change in one variable is recorded, while keeping other variables constant. Each signal is band-passed into 25 parts: 0-100Hz, 100-200Hz, 200-300 Hz and so on. These band-passed signals are transformed into their frequency-domain counterparts with PSD in the y-axis and frequency in the x-axis. The comparison of spectral features relevant to each signal will highlight some signal-discriminating features.

Table 10: Shortlisted signals for PCA2

Observation Number	**Temperature ©**	**Orifice (inch)**	**Pressure (psi)**	**Distance (m)**	**Orientation (degree)**
37	22.00	0.002	100.00	0.00	0.00
38	22.00	0.002	100.00	0.00	45.00
45	22.00	0.002	60.00	0.00	0.00
105	0.00	0.002	60.00	0.00	0.00
165	-22.00	0.002	60.00	0.00	0.00
41	22.00	0.002	80.00	0.00	0.00
107	0.00	0.002	60.00	2.00	0.00
5	22.00	0.005	80.00	0.00	0.00
17	22.00	0.004	80.00	0.00	0.00
29	22.00	0.003	80.00	0.00	0.00
53	22.00	0.001	80.00	0.00	0.00

PCA is useful when eligibility tests are conducted on the data and the results are eligible for further analysis. Table 11 shows the compilation of eligibility test results for 25 cases.

Eligibility Tests

Eligibility tests were performed on all 25 cases to determine those to which PCA can be applied successfully. Table 11 is the list of Kaiser-Meyer-Olkin **(**KMO) and sphericity test values for each case. For PCA eligibility, a KMO > 0.6 and sphericity p-value < 0.05 are necessary. Nine cases were selected for further analysis. For sum, PSD (RMS), PSD (Max) and frequency at PSD (Max) are eligible for PCA at different orifice size and pressure. The results of PCA will be useful for finding the frequency range (observation) containing the highest number of signal-discriminating characteristics. The observation that makes the greatest contribution to the dominating factors will be most correlated to the change in manipulated variables. The nine cases eligible for PCA are shown in Table 12.

Table 11: Eligibility Results for PCA2

Spectral Feature	Variable	Sphericity Test	KMO Test
Kurtosis	Distance	0.467	0.5
	Angle	0.906	0.5
	Orifice	0.752	0.515
	Temperature	0.807	0.466
	Pressure	0.989	0.493
Sum	Distance	0.0001	0.5
	Angle	0.0001	0.5
	Orifice	**0.0001**	**0.885**
	Temperature	0.0001	0.512
	Pressure	**0.0001**	**0.622**
RMS PSD	Distance	0.0001	0.5
	Angle	0.0001	0.5
	Orifice	**0.0001**	**0.833**
	Temperature	0.0001	0.531
	Pressure	**0.0001**	**0.694**
Max PSD	Distance	0.0001	0.5
	Angle	0.0001	0.5
	Orifice	**0.0001**	**0.782**
	Temperature	0.0001	0.515
	Pressure	**0.0001**	**0.69**
Frequency (at PSD (Max))	Distance	0.0001	0.5
	Angle	0.0001	0.5
	Orifice	**0.0001**	**0.878**
	Temperature	**0.0001**	**0.792**
	Pressure	**0.0001**	**0.788**

Table 12: Shortlisted cases for PCA2

Case	Definition
SO	Effect of Orifice Size on the Sum of PSD
SP	Effect of Pressure on the Sum of PSD
RO	Effect of Orifice Size on PSD (RMS)
RP	Effect of Pressure on PSD (RMS)
MO	Effect of Orifice Size on PSD (Max)

MP	Effect of Pressure on PSD (Max)
FO	Effect of Orifice Size on Frequency at PSD (Max)
FT	Effect of Temperature on Frequency at PSD (Max)
FP	Effect of Pressure on Frequency at PSD (Max)

After the scree test and after the first two factors for all nine cases were shortlisted, the combined contribution of all the observations in Factor 1 and Factor 2 were listed. This gave an idea about the observation that has maximum contribution in total and the observation that stands out for a particular case. The top three contributors for all the cases combined are listed in Table 13.

Table 13: Top 3 contributors (all 9 cases combined)

Obs No.	SO	SP	RO	RP	MO	MP	FO	FT	FP	Total
25	25.03	25.75	23.36	24.91	20.12	18.47	17.57	12.47	11.22	178.9
19	9.74	24.87	8.45	34.76	26.11	14.78	2.99	9.5	6.11	137.31
24	23.65	16.1	11.95	16.58	15.07	14.92	9.42	10.96	12.1	130.75

The contribution of Observation 25 or frequency range 2400-2500 Hz is maximum for all the 9 cases combined. The top three contributors for each case are mentioned in Table 14.

Table 14: Top 3 contributors in each case

SO	SP	RO	RP	MO	MP	FO	FT	FP
25	25	12	19	17	17	2	16	18
24	19	25	25	19	25	25	7	15
18	20	24	20	25	10	11	13	13

Observations 25, 12, 19, 17, 2, 16 and 18 have the highest contributions for individual cases. Observation 12 for RMS value at different Orifice size (case RO) has a 46% contribution; therefore RMS values for PSD for frequency range 1100-1220 Hz can be a discriminating feature for change in the orifice size.

4.2.3 PCA3: Validation Testing

Principal component analysis was performed for the spectral features maximum, root mean square and sum of power spectral density of the frequency domain signals. The analysis for three components with new and leaking conditions was performed for sensor distance, temperature and pressure variations. The terminology used for naming different PCA's is mentioned in Table 15 and Table 16.

Table 15: Component terminology definition

Component No.	Component Type
1	New Airbrake Hose
2	Old Airbrake Hose
3	New Reducing Valve
4	Old Reducing Valve
5	New Ball Valve
6	Old Ball Valve

Table 16: Design Factors and Spectral features terminology definition

Design Factors	Definition	Spectral Feature	Definition
d	sensor distance	s	sum of PSD
p	pressure	r	rms value of PSD
t	temperature	m	maximum value of PSD

The 54 PCA's performed as listed in Table 17.

Table 17: List of PCA3s

PCA-1ds	PCA-3ds	PCA-5ds
PCA-1dr	PCA-3dr	PCA-5dr
PCA-1dm	PCA-3dm	PCA-5dt
PCA-1ps	PCA-3ps	PCA-5ps
PCA-1pr	PCA-3pr	PCA-5pr
PCA-1pm	PCA-3pm	PCA-5pm
PCA-1ts	PCA-3ts	PCA-5ts
PCA-1tr	PCA-3tr	PCA-5tr
PCA-1tm	PCA-3tm	PCA-5tm
PCA-2ds	PCA-4ds	PCA-6ds
PCA-2dr	PCA-4dr	PCA-6dr
PCA-2dm	PCA-4dm	PCA-6dm
PCA-2ps	PCA-4ps	PCA-6ps
PCA-2pr	PCA-4pr	PCA-6pr
PCA-2pm	PCA-4pm	PCA-6pm
PCA-2ts	PCA-4ts	PCA-6ts
PCA-2tr	PCA-4tr	PCA-6tr
PCA-2tm	PCA-4tm	PCA-6tm

1ds stands for component 1, change in sensor distance and sum of PSD. Likewise, 6tm stands for component 6, temperature variations and maximum PSD.

Component 1 and 2 are new and old hoses, 3 and 4 are new and old reducing valves and 5 and 6 are new and old ball valves. The cumulative top contributors for each frequency range are shown in Figure 32 and listed in Table 18.

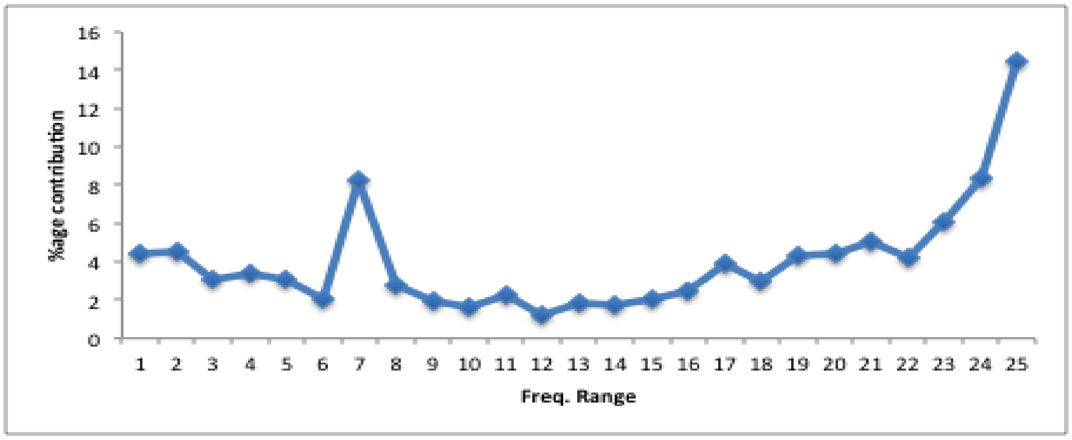

Figure 32: Cumulative contribution of frequency ranges

It can be clearly observed that frequency ranges 600-700 Hz, 2300-2400 Hz and 2400-2500 Hz are the top contributors to the factors.

Table 18: Top cumulative frequency range

Frequency range	%age contribution	Freq. range	%age contribution
25	14.4	**3**	3.0
24	8.3	**18**	3.0
7	8.2	**8**	2.8
23	6.0	**16**	2.5
21	5.0	**11**	2.2
2	4.5	**6**	2.0
1	4.4	**15**	2.0
20	4.4	**9**	2.0
19	4.3	**13**	1.8
22	4.3	**14**	1.7
17	3.9	**10**	1.6
4	3.4	**12**	1.2
5	3.1		

The comparison of leakage behavior from new and leaking components is performed in Table 19. Higher frequency ranges have a high weightage in contribution for reducing valve and old airbrake hose. Whereas, lower frequency ranges have more weightage in contribution for ball valve and new airbrake hose.

Table 19: Top contributors for each frequency range

New Component			Old Component		
Analysis No.	Freq. range	%age contribution	Analysis No.	Freq. range	%age contribution
PCA-1ds	1	41.9	PCA-2ds	25	51.0
PCA-1dr	21	47.6	PCA-2dr	25	49.5
PCA-1dm	1	41.9	PCA-2dm	25	47.3
PCA-1ps	20	31.0	PCA-2ps	25	48.6
PCA-1pr	8	24.9	PCA-2pr	25	46.6
PCA-1pm	8	41.0	PCA-2pm	5	42.2
PCA-1ts	7	57.1	PCA-2ts	25	46.9
PCA-1tr	7	67.7	PCA-2tr	25	46.1
PCA-1tm	7	60.5	PCA-2tm	7	80.5
PCA-3ds	25	43.5	PCA-4ds	25	53.7
PCA-3dr	25	42.6	PCA-4dr	25	49.7
PCA-3dm	5	54.1	PCA-4dm	25	34.6
PCA-3ps	25	51.6	PCA-4ps	23	35.7
PCA-3pr	25	51.3	PCA-4pr	23	35.4
PCA-3pm	25	45.4	PCA-4pm	23	31.6
PCA-3ts	25	50.3	PCA-4ts	25	53.3
PCA-3tr	25	49.1	PCA-4tr	25	53.6
PCA-3tm	7	75.1	PCA-4tm	25	29.9
PCA-5ds	15	31.2	PCA-6ds	17	25.4
PCA-5dr	15	34.1	PCA-6dr	3	23.7
PCA-5dt	2	43.0	PCA-6dm	2	38.6
PCA-5ps	17	19.6	PCA-6ps	4	15.7
PCA-5pr	17	19.7	PCA-6pr	4	18.8
PCA-5pm	2	35.3	PCA-6pm	16	41.3
PCA-5ts	25	40.6	PCA-6ts	7	46.9
PCA-5tr	25	34.9	PCA-6tr	7	61.7
PCA-5tm	7	87.5	PCA-6tm	7	86.6

4.2.3.1 Major Contributors for Components

As shown in Table 20, the frequency range 600-800 Hz is most sensitive for good glad hands and the frequency range 2400-2500 Hz is most sensitive for bad glad hands.

Table 20: Major contributors for Glad Hands (Airbrake Hose)

			Good		Bad	
Component	**Variable**	**Spectral Feature (PSD)**	**Most Sensitive**	**Least Sensitive**	**Most Sensitive**	**Least Sensitive**
Glad Hands	Distance	Sum	1	9	25	10
		RMS	21	15	25	10
		Max	1	9	25	14
		Max/RMS	7	23	12	24
	Pressure	Sum	20	12	25	6
		RMS	8	18	25	6
		Max	8	14	5	16
		Max/RMS	7	3	7	24
	Temperature	Sum	7	4	25	6
		RMS	7	4	25	6
		Max	7	11	7	16
		Max/RMS	7	24	7	3

As shown in Table 21, the lower frequency ranges 0-800 Hz is most sensitive for good reducing valve and the frequency range 600-700 Hz and 2400-2500 Hz is most sensitive for bad reducing valve.

Table 21: Major contributors for reducing valve

			Good		Bad	
Component	**Variable**	**Spectral Feature (PSD)**	**Most Sensitive**	**Least Sensitive**	**Most Sensitive**	**Least Sensitive**
Reducing Valve	Distance	Sum	1	9	25	10
		RMS	21	15	25	10
		Max	1	9	25	14
		Max/RMS	6	1	7	10
	Pressure	Sum	20	12	25	6
		RMS	8	18	25	6
		Max	8	14	5	16
		Max/RMS	5	7	7	14
	Temperature	Sum	7	4	25	6
		RMS	7	4	25	6
		Max	7	11	7	16
		Max/RMS	7	17	7	20

As shown in Table 22, lower frequency ranges 0-800 Hz is most sensitive for good ball valve and frequency range 0-100 Hz and 2400-2500 Hz is most sensitive for bad ball valve.

Table 22: Major contributors for Ball Valve

			Good		Bad	
Component	Variable	Spectral Feature (PSD)	Most Sensitive	Least Sensitive	Most Sensitive	Least Sensitive
Ball Valve	Distance	Sum	1	9	25	10
		RMS	21	15	25	10
		Max	1	9	25	14
		Max/RMS	2	4	2	16
	Pressure	Sum	20	12	25	6
		RMS	8	18	25	6
		Max	8	14	5	16
		Max/RMS	2	10	2	12
	Temperature	Sum	7	4	25	6
		RMS	7	4	25	6
		Max	7	11	7	16
		Max/RMS	2	14	2	12

4.2.3.2 Major contributors for Spectral Features

The contribution of frequency ranges for spectral features are separately analyzed to understand any specific trend of most and least sensitive frequency range.

Table 23: Major Contributors for Sum (PSD)

Sum (PSD)		Good		Bad	
Component	Variable	Most Sensitive	Least Sensitive	Most Sensitive	Least Sensitive
Glad Hands	Distance	1	9	25	10
	Pressure	20	12	25	6
	Temperature	7	4	25	6
Reducing Valve	Distance	1	9	25	10
	Pressure	20	12	25	6
	Temperature	7	4	25	6
Ball Valve	Distance	1	9	25	10
	Pressure	20	12	25	6
	Temperature	7	4	25	6

For Good Component:

- For pressure variations, 1900-2000 Hz is most sensitive 1100-1200 is least sensitive.
- For distance variations, 0-100 Hz is most sensitive and 800-900 Hz is least.
- For temperature variations, 600-700 Hz is most and 300-400 Hz is least

For Bad Component: The frequency range 2400-2500 Hz is most sensitive for all variations, while 900-1000 Hz is least sensitive for distance variations and 500-600 Hz is least sensitive for pressure and temperature variations.

Table 24: Major contributors for RMS (PSD)

RMS (PSD)		Good		Bad	
Component	Variable	Most Sensitive	Least Sensitive	Most Sensitive	Least Sensitive
Glad Hands	Distance	21	15	25	10
	Pressure	8	18	25	6
	Temperature	7	4	25	6
Reducing Valve	Distance	21	15	25	10
	Pressure	8	18	25	6
	Temperature	7	4	25	6
Ball Valve	Distance	21	15	25	10
	Pressure	8	18	25	6
	Temperature	7	4	25	6

For Good Component:

- For pressure variations, 700-800 Hz is most sensitive and 1700-1800 Hz is least sensitive.
- For distance variations, 2000-2100 Hz is most sensitive and 1400-1500 Hz is least.
- For temperature variations, 600-700 Hz is most and 300-400 Hz is least

For Bad Component: The frequency range 2400-2500 Hz is most sensitive for all variations; while 900-1000 Hz is least sensitive for distance variations and 500-600 Hz is least sensitive for pressure and temperature.

Table 25: Major contributors for Max (PSD)

Max(PSD)		Good		Bad	
Component	Variable	Most Sensitive	Least Sensitive	Most Sensitive	Least Sensitive
Glad Hands	Distance	1	9	25	14
	Pressure	8	14	5	16
	Temperature	7	11	7	16
Reducing Valve	Distance	1	9	25	14
	Pressure	8	14	5	16
	Temperature	7	11	7	16
Ball Valve	Distance	1	9	25	14
	Pressure	8	14	5	16
	Temperature	7	11	7	16

For Good Component:

- For pressure variations, 700-800Hz is most sensitive 1300-1400 is least sensitive.
- For distance variations, 0-100 Hz is most sensitive and 800-900 Hz is least.
- For temperature variations, 600-700 Hz is most and 1000-1100 Hz is least

For Bad Component:

- For pressure variations, 400-500 Hz is most sensitive 1500-1600 is least sensitive.
- For distance variations, 2400-2500 Hz is most sensitive and 1300-1400 Hz is least.
- For temperature variations, 600-700 Hz is most and 1500-1600 Hz is least

Table 26: Major contributors for Max/RMS (PSD)

Max/RMS (PSD)		Good		Bad	
Component	Variable	Most Sensitive	Least Sensitive	Most Sensitive	Least Sensitive
Glad Hands	Distance	7	23	12	24
	Pressure	7	3	7	24
	Temperature	7	24	7	3
Reducing Valve	Distance	6	1	7	10
	Pressure	5	7	7	14
	Temperature	7	17	7	20
Ball Valve	Distance	2	4	2	16
	Pressure	2	10	2	12
	Temperature	2	14	2	12

For Good Component:

- For pressure variations, 600-800 Hz is most sensitive
- For glad hands, 600-700 Hz is most sensitive and for ball valve 0-100 Hz is most sensitive

For Bad Component:

- For glad hands and reducing valve 600-700 Hz is most sensitive
- For ball valve, 0-100 Hz is most sensitive

4.2.3.3 Reproducibility

Reproducibility is the ability of an entire experiment or study to be reproduced, either by the researcher or by someone else working independently. Three trials were conducted for each scenario and graphs were plotted in Table 27-32 for the spectral feature values of all six components to observe any considerable difference in repeat readings.

Table 27: Component 1: Airbrake Hose (New)

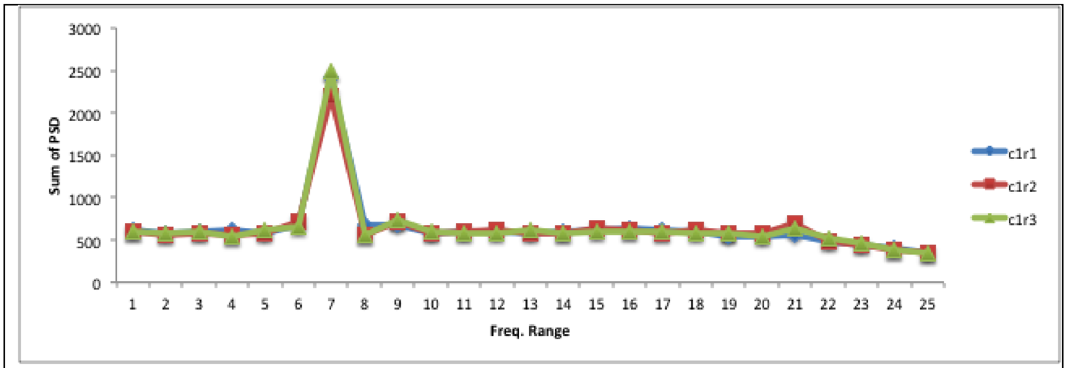

a) Reproducibility check for sum of PSD repeat values for component 1

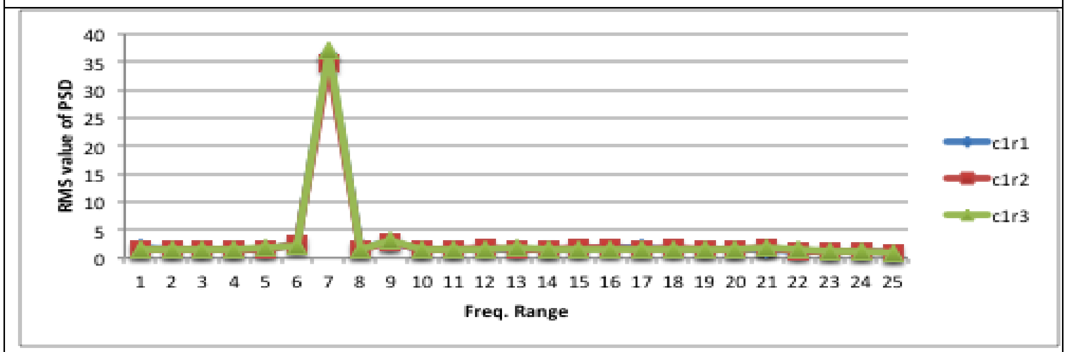

b) Reproducibility check for RMS repeat value of PSD for component 1

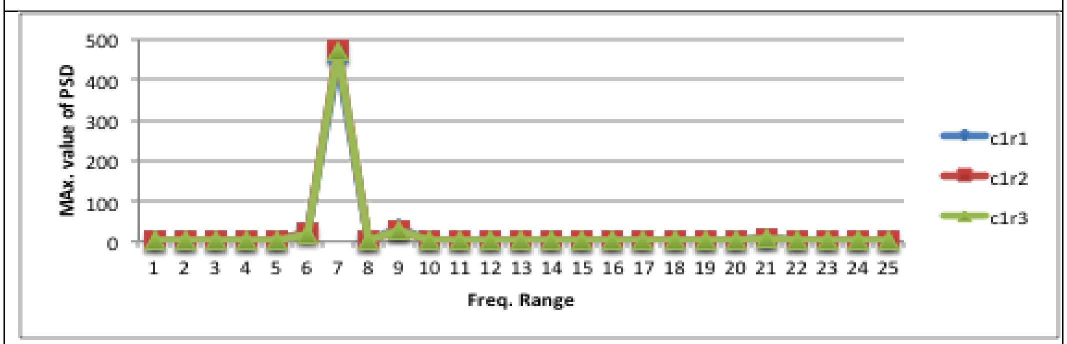

c) Reproducibility check for max. repeat values of PSD for component 1

All three spectral features can be clearly observed as reproducible for component 1.

Table 28: Component 2: Airbrake Hose (Old)

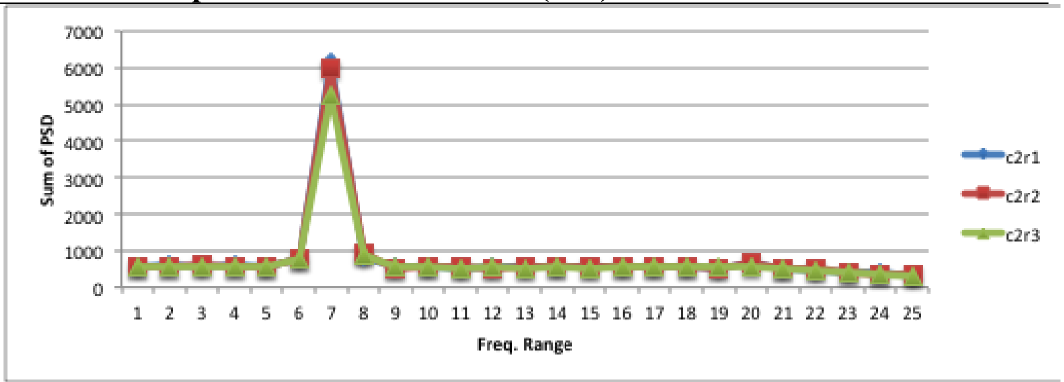

a) Reproducibility check for sum of PSD repeat values for component 2

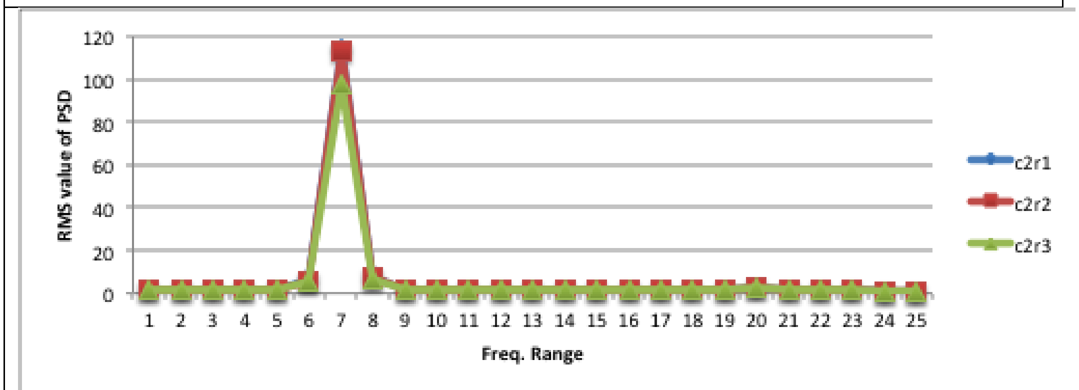

b) Reproducibility check for RMS repeat value of PSD for component 2

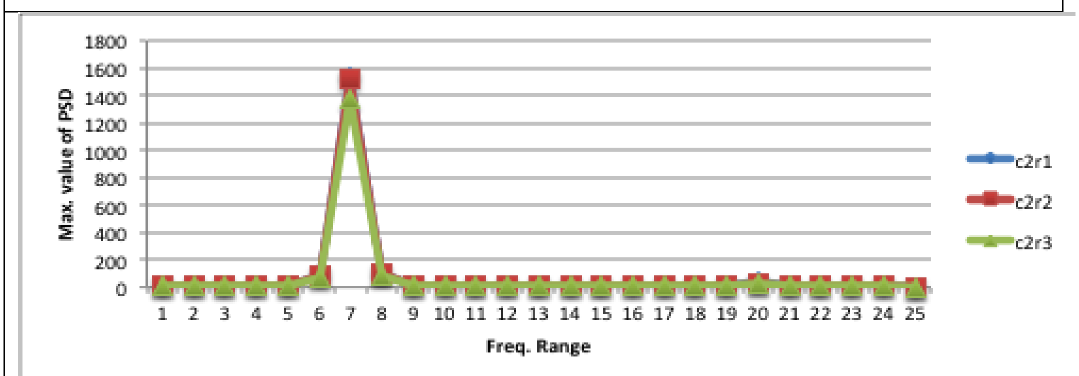

c) Reproducibility check for max. repeat values of PSD for component 2

All three spectral features can be clearly observed as reproducible for component 2.

Table 29: Component 3: Reducing Valve (New)

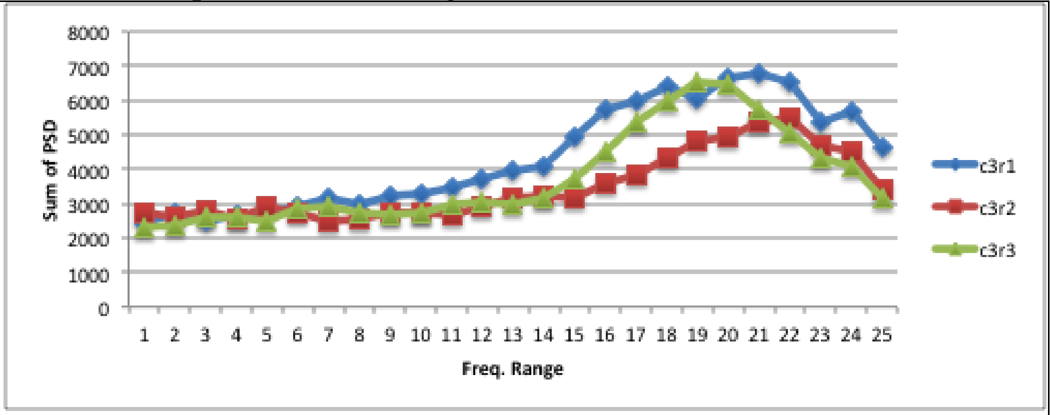

a) Reproducibility check for sum of PSD repeat values for component 3

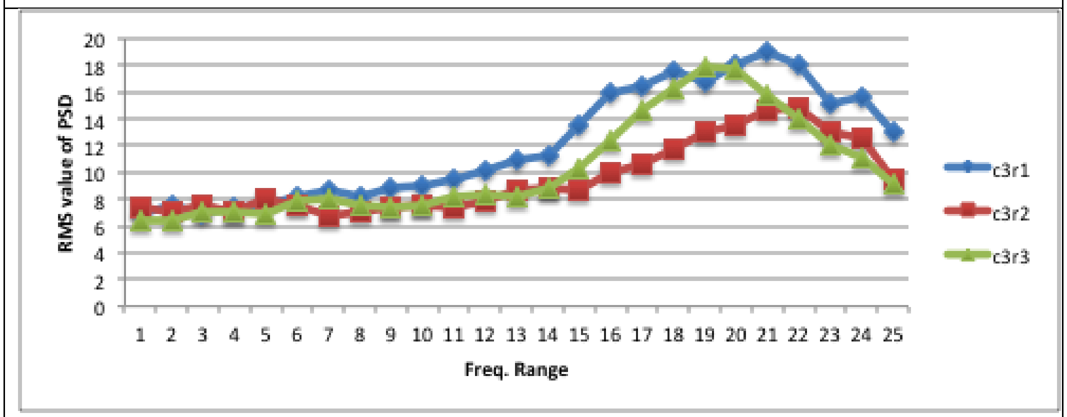

b) Reproducibility check for RMS repeat value of PSD for component 3

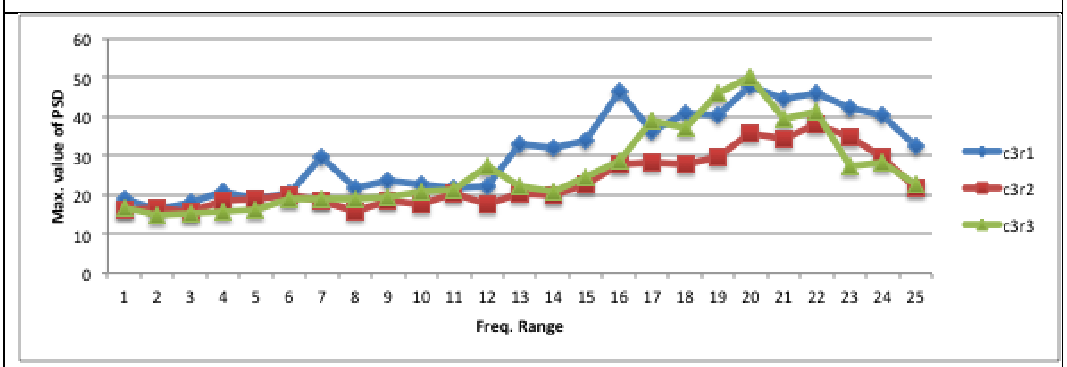

c) Reproducibility check for max. repeat values of PSD for component 3

There is some difference in between the repeat readings, but the difference will have minimal effect on reproducibility for component 3.

Table 30: Component 4: Reducing Valve (Old)

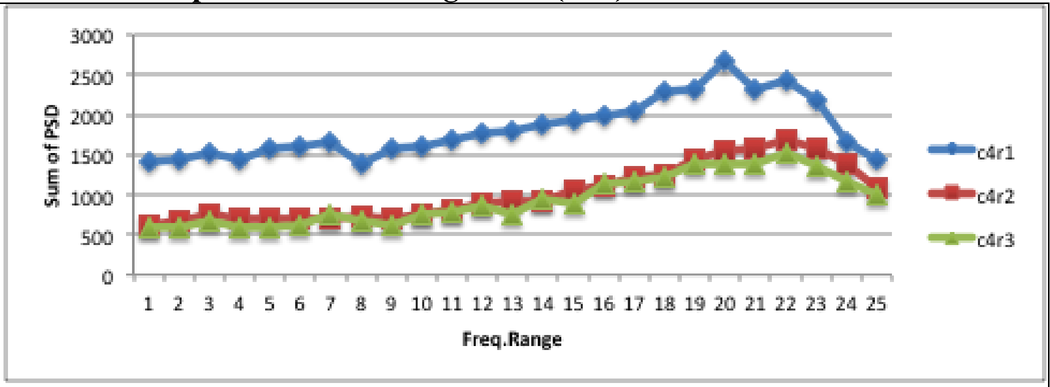

a) Reproducibility check for sum of PSD repeat values for component 4

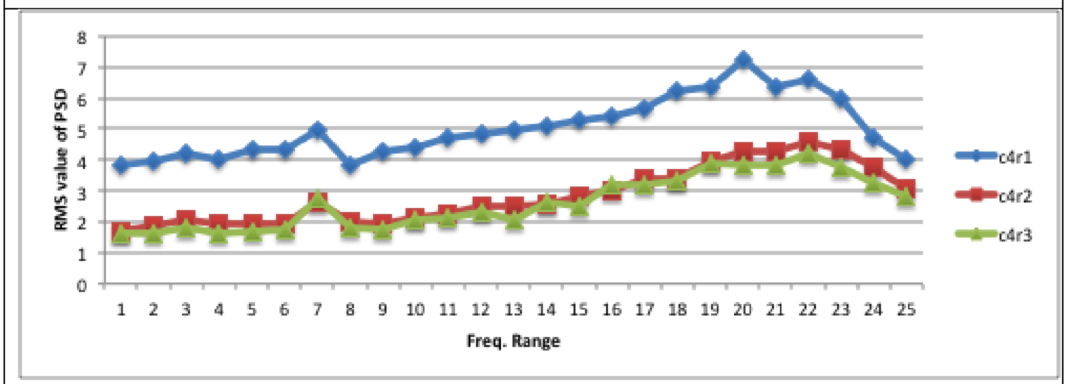

b) Reproducibility check for RMS repeat value of PSD for component 4

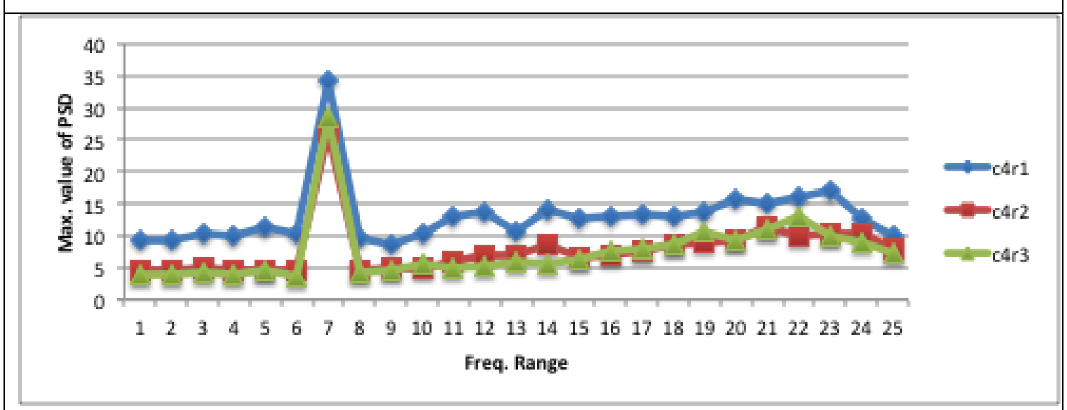

c) Reproducibility check for max. repeat values of PSD for component 4

The repeat 1 reading has considerable difference in value with reading 2 and reading 3. The average valve will be inclined towards reading 2 and 3, therefore there will be minimal effect on reproducibility.

Table 31: Component 5: Ball Valve (New)

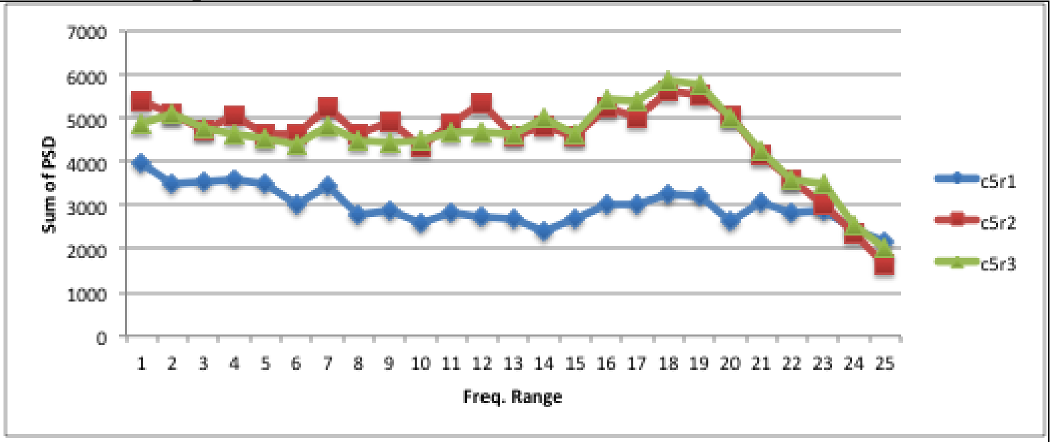

a) Reproducibility check for sum of PSD repeat values for component 5

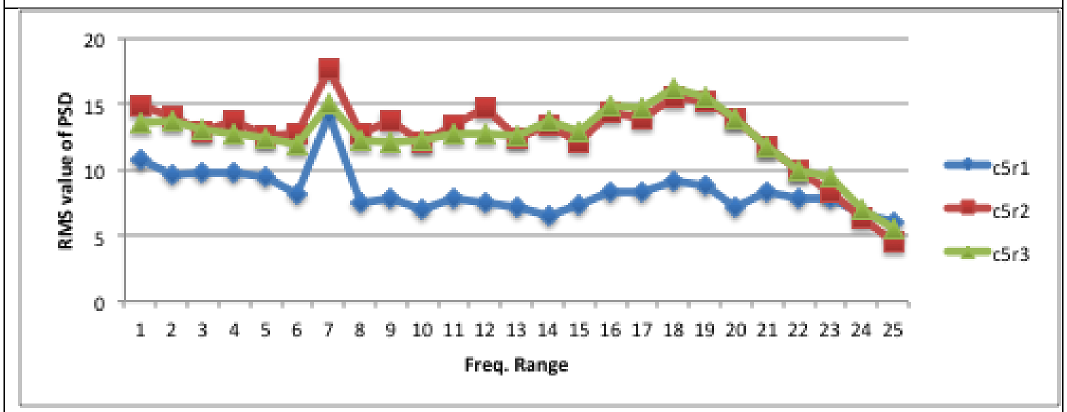

b) Reproducibility check for RMS repeat value of PSD for component 5

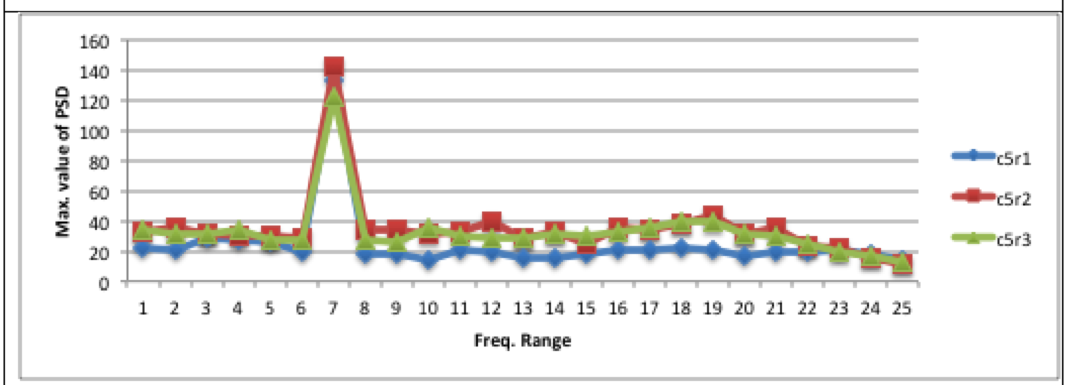

c) Reproducibility check for max. repeat values of PSD for component 5

The repeat 1 reading has considerable difference in value with reading 2 and reading 3. The average valve will be inclined towards reading 2 and 3, therefore there will be minimal effect on reproducibility for component 5.

Table 32: Component 6: Ball Valve (Old)

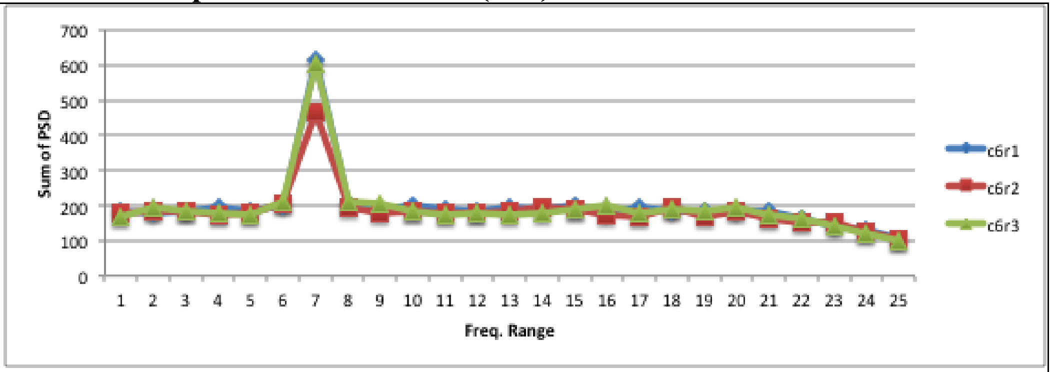

a) Reproducibility check for sum of PSD repeat values for component 6

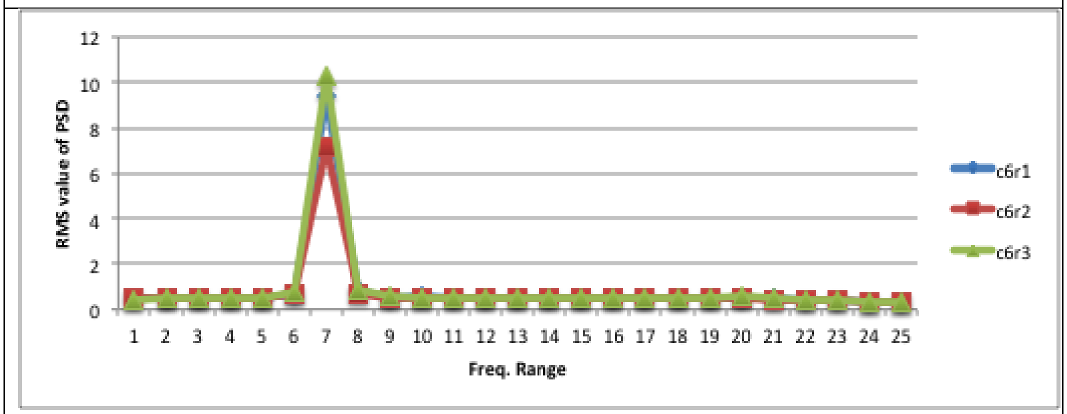

b) Reproducibility check for RMS repeat values of PSD for component 6

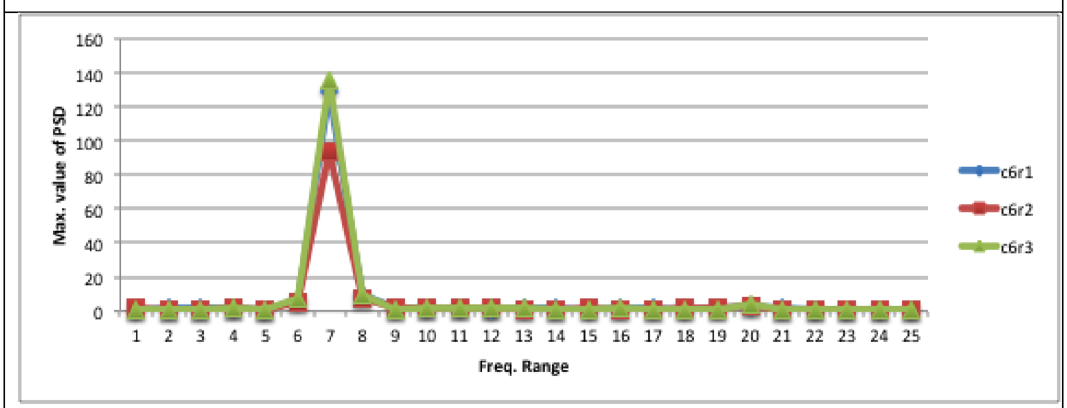

c) Reproducibility check for max. repeat values of PSD for component 6

All three spectral features can be clearly observed as reproducible for component 6.

4.3 ERROR ANALYSIS

Our ability to observe the real world is not perfect. The observations we make are never exactly representative of the process we think we are observing. This is conceptualized as:

Measured value = true value +- error

Equation 8: Measure value v/s true value

The error is a combined measure of the inherent variation in the phenomenon we are observing and the numerous factors that interfere with the measurement. The underlying error in this experiment is truly random, therefore we can gain useful information by making multiple observations or replicated and calculating the average. Here two replicate readings are taken from each observation. The purpose of a t-test is to examine whether the differences between the observed test averages, x_a and x_b, is large relative to the uncertainty in the averages. The null hypothesis is that the difference between n_a and n_b, mean values of the observation variable x, is zero. We assume that the errors in the measurements for the repeats are independently and identically distributed and follow a normal distribution. Once can consider the difference $x_a – x_b$ to be a random variable. The error in this difference has a scaled t-distribution:

$$(x_a - x_b) - (n_a - n_b) \approx t_v \, s_{(xa - xb)}$$

Equation 9: t-distribution for replicate error

The variance of a difference between two variances is the sum of the variances of the variables:

$$\sigma_{(xa - xb)}^{2} = \sigma_{xa}^{2} + \sigma_{xb}^{2}$$

Equation 10: Variance of error distribution

So the standard error in the difference is:

$$s_{(xa - xb)} = \mathrm{sqrt}\,(s_a^2 / n_a + s_b^2 / n_b)$$

Equation 11: Standard error in the difference of replicates

Where sa2 and sb2 are the sample variances for the two experimental conditions. If the magnitude of the errors in the measurements of the x_a and xb are approximately equal, then the degrees of freedom associated with this standard error is the sum of the degrees of freedom for the standard errors in each of xa and xb, i.e. v = na + nb – 2, where na and nb are the number of values in the samples observations for replicates a and b, respectively. The common variance is estimated as:

$$s^2 = \frac{(na-1)sa^2 + (nb-1)sb^2}{na+nb-2}$$

Equation 12: Common variance of replicate distributions

The standard error in the difference of the averages can be written as:

$$s(xa - xb) = s\sqrt{\frac{1}{na} + \frac{1}{nb}}$$

Equation 13: Standard error

To test the null hypothesis that both replicate means are the same, we estimate the probability associated with one of the following possible alternate hypotheses: $n_a \neq n_b$, $n_a < n_b$, or $n_a > n_b$. A two-sided t-test is used to test the alternate hypothesis that the true means are different from each other. The probability associated with this is:

$$Pr\left\{-\left|\frac{xa-xb}{s(xa-xb)}\right| \leq t \leq \left|\frac{xa-xb}{s(xa-xb)}\right|\right\} = 1 - \alpha$$

Equation 14: Two tailed t-test for difference in replicate readings

If the observed difference is large, the probability 1-α will be large.

The above-mentioned t-test is performed for the replicates, with the following result in Table 15.

Table 33: Results for error analysis using t-test

	Test A	Test B	Error (A – B)
Mean	51.245	51.682	-0.437
Standard Deviation	21.301	21.281	2.244
$Pr(-0.19481 \leq tv \leq 0.19481) = 1 - \alpha = 0.1521$			

Therefore the null hypothesis that the means of both replicate readings are same is true, as the probability for error is within acceptable limits.

4.4 Results And Discussion

The qualitative and quantitative assessment of ULD technology for airbrake leakages proved that ULD is a useful method to locate and quantify leakages. The soap and bubble test should be replaced with ULD with immediate effect. The results for our analysis can be summarized as follows:

4.4.1 Qualitative Assessment Results:

1. The variables to be used for the experiment design were identified.
2. ULD proved to be successful in detecting leakages in both external and internal conditions. Cold weather conditions are beneficial for the transmission of sound. As a result, better reception of the sound signal is observed at the sensor.
3. A team of experts from a railroad operating company, an airbrake manufacturer and the yard manager approved the use of ULD.

4.4.2 Trend Analysis Results:

1. When the distance between the sensor and leakage location is increased, the effect of change in orientation on intensity decreases.
2. There is a significant decrease in intensity at increased distance.
3. The rate of change in intensity increases as orifice size is increased.
4. Temperature has no consistent effect on ultrasound intensity.
5. Pressure has a small but consistent effect on intensity. Increasing pressure increases the intensity.

4.4.2.1 PCA1 Results

1. Distance and orifice size have a maximum correlation with ultrasonic intensity.
2. Temperature has an insignificant correlation with all other variables.
3. Orientation has a small correlation with only the crest factor.

4.4.2.2 PCA2 Results

1. The contribution of Observation 25 or frequency range 2400-2500 Hz is highest for all 9 cases combined. The FFTs for all signals have peaks in this frequency range.
2. Observations 25, 12, 19, 17, 2, 16 and 18 have the highest contributions for individual cases. If the spectral feature under consideration is total power, then frequency range 2400-2500 Hz will reflect the maximum effect of change in orifice size and pressure. If the spectral feature under consideration is the RMS value of PSD, then frequency range 1100-1200 Hz will reflect the maximum effect of change in orifice size, and frequency range 1800-1900 Hz will reflect the maximum effect of change in pressure. For a maximum value of PSD, frequency range 1600-1700 Hz is most critical to detect changes in orifice size and pressure. The effect of temperature on ultrasound will be reflected mostly in the frequency at a maximum value of PSD for a range of 1500-1600 Hz. For a change in the orifice, frequency range 100-200 Hz is the most discriminating. For a change in pressure, frequency range 1700-1800 Hz is the most discriminating.
3. Observation 12 for RO has a 46% contribution among all frequency ranges. Therefore, RMS values of PSD at frequency range 1100-1220 Hz can be a strong discriminating feature for change in the orifice size.

4.4.2.3 PCA3: Validation Testing

1. Validation testing proved that frequency range 2400-2500 Hz, 2300-2400 Hz and 600-700 Hz have most signal discriminating characteristics

2. Component 2,3 and 4 tend to be more weighted towards higher frequency ranges like 2200-2300 Hz, 2300-2400 Hz and 2400-2500 Hz
3. Component 1, 5 and 6 tend to be more weighted towards lower frequency ranges like 0-100 Hz, 500-600 Hz and 600-700 Hz.
4. The contribution of frequency ranges is different for different leakage type. For example, RMS valves of PSD at frequency range 1100-1200 Hz is a strong discriminator for circular leakage, but is considerably weaker discriminator for leakage types in ball valve, reducing valve and airbrake hose.

4.4.2.4 Major contributors for components and spectral features

- Frequency range 600-800 Hz is most sensitive for good glad hands.
- Frequency range 2400-2500 Hz is most sensitive for bad glad hands.
- Lower frequency ranges 0-800 Hz is most sensitive for good reducing valve.
- Frequency range 600-700 Hz and 2400-2500 Hz is most sensitive for bad reducing valve.
- Lower frequency ranges 0-800 Hz is most sensitive for good ball valve.
- Frequency range 0-100 Hz and 2400-2500 Hz is most sensitive for bad gall valve.

For Sum (PSD),

- Good Component:
    - For pressure variations, 1900-2000 Hz is most sensitive 1100-1200 is least sensitive.
    - For distance variations, 0-100 Hz is most sensitive and 800-900 Hz is least.

        - For temperature variations, 600-700 Hz is most and 300-400 Hz is least.

- Bad Component: 2400-2500 Hz is most sensitive for all variations, while 900-1000 Hz is least sensitive for distance variations and 500-600 Hz is least sensitive for pressure and temperature.

For RMS (PSD),

- Good Component:
    - For pressure variations, 700-800 Hz is most sensitive and 1700-1800 Hz is least sensitive.
    - For distance variations, 2000-2100 Hz is most sensitive and 1400-1500 Hz is least.
    - For temperature variations, 600-700 Hz is most and 300-400 Hz is least.
- Bad Component: 2400-2500 Hz is most sensitive for all variations, while 900-1000 Hz is least sensitive for distance variations and 500-600 Hz is least sensitive for pressure and temperature.

For Max (PSD),

- Good Component:
    - For pressure variations, 700-800Hz is most sensitive 1300-1400 is least sensitive.
    - For distance variations, 0-100 Hz is most sensitive and 800-900 Hz is least.
    - For temperature variations, 600-700 Hz is most and 1000-1100 Hz is least.

- Bad Component:

  - For pressure variations, 400-500 Hz is most sensitive 1500-1600 is least sensitive.

  - For distance variations, 2400-2500 Hz is most sensitive and 1300-1400 Hz is least.

  - For temperature variations, 600-700 Hz is most and 1500-1600 Hz is least.

For Max/RMS (PSD)

- Good Component:

  - For pressure variations, 600-800 Hz is most sensitive.

  - For glad hands, 600-700 Hz is most sensitive and for ball valve 0-100 Hz is most sensitive

- Bad Component:

  - For glad hands and reducing valve 600-700 Hz is most sensitive.

  - For ball valve, 0-100 Hz is most sensitive.

CHAPTER 5: CONCLUSION AND FUTURE WORK

The aim of applying reliability-centered maintenance to railway airbrakes in Canadian weather conditions helped to understand the functions and failure modes of airbrakes. The most critical failure mode was identified, and condition-monitoring techniques were analyzed. Ultrasound leakage detection (ULD) emerged as the latest and most accurate technology to detect leakages. An examination of ULD as a replacement for the soap and bubble test was performed in field tests and laboratory experiments. A visit to a railway yard was useful in helping us to understand the applicability of the technology to rail airbrakes. The presence of executives from all spheres of rail operation certified the advantages of ULD on the airbrake inspection system. On further experimental analysis, significant characteristics from the ultrasound spectrum were identified that can distinguish different types of leakages in different weather and operating conditions. The effect of pressure, temperature, orifice size, sensor distance and sensor orientation was substantiated to the greatest possible extent. Validation testing was useful in validating the importance of frequency range 2300-2500 Hz as a strong discriminator for varying operating variables.

ULD is a feasible option for detecting leakages, which are one of the most critical failure modes for rail airbrakes. If the leakages are located and quantified correctly and quickly, it will be easier to rectify them before they become a complete failure. The inefficiency of inspectors in using the soap and bubble test in extreme cold weather conditions because of uncomfortable ergonomics leads to neglecting some potential leakages. Leakages lead to a loss of air pressure, which is not present when required. Hence, if the extent of leakage identification increases by using a better LDS it will surely increase the reliability or the available time for airbrakes to function in their normal condition.

The scope of this research was limited to understanding the effect of operating parameters on ULD performance. On further research all parameters affecting ultrasound should be identified and an equation relating them should be modeled. An economic analysis should be performed to determine whether ULD could be a replacement for existing leakage detection techniques. This will help to clarify the payback period of initial investment and cost savings through lesser accidents and lesser human involvement. This study can be further elaborated to accurately estimate the leakage size, flow-rate and, finally, the cost impact of a leakage on the railroad business. This will be useful to point out when and where a leakage in the airbrake system needs to be rectified. A device can be manufactured that uses the input operating parameters to display the exact extent of a leakage from a reliability and cost standpoint. The frequency ranges identified as signal discriminating can be further analyzed with other spectral features to find better results.

The basic experiment was conducted for circular leak holes and specific ranges of variables. Future work can include testing the instrument for different leakage types and geometries. As per manufacturers of ULD instruments, there is a variation in intensity readings for different versions of sensors. A comprehensive test plan including various types of ULD sensors will be a good contribution for understanding the variation among sensors. Pressure and temperature ranges can be varied and tests can be conducted at different levels and ranges to observe peculiar behaviors, if they arise.

Another helpful contribution would be an inspection procedure for incorporating ULD. A decision as to when and where to use the instrument is critical for getting the most out of the instrument. Either hand-held devices or remote monitoring at specific stations can be deployed for data acquisition of ultrasonic intensity readings. Analysis for other dynamic signal discriminating spectral features can lead to results that can discriminate readings at different operating conditions.

REFERENCES

[1] A. Mostafapour, S. Davoudi. "Analysis of leakage in high pressure pipe using acoustic emission method." *Applied Acoustics* (Elsevier) 74 (2013): 335-342.

[2] ADEPA. "Reliability Centered Maintenance(RCM): Approach for Infrastructure and Logistics of Railway Operations." The Rail Consortium, Europe: The Rail Consortium, 2002.

[3] Association of American Railroads. "Section E, Brakes and Brake Equipments." In *Manual of Standards and Recommended Practices*, by Association of American Railroads. Washington, D.C.: The Association of American Railroads, 2010.

[4] Ault, David McMillan and Graham W. "Quantification of Condition Monitoring Benefit for Offshore Wind Turbines." *Wind Engineering* 31, no. 4 (2007): 267-285.

[5] Azevedo, Cesar R.F. "Failure analysis of a crude oil pipeline." *Engineering Failure Analysis* (Elsevier) 14 (2007): 978-994.

[6] Blaine, David G. "Modern Freight Car Airbrakes." Omaha, Nebraska: Simmons-Boardman Publishing Corporation, 1979.

[7] C. Moon, W. C. Brown, S. Mellen, E. Frenz, D. J. Pickering. "Ultrasound Techniques for Leakage Detection." 2009.

[8] Canadian National. "Participant Manual." In *City 9 - (Canada) Airbrake Test*, by Canadian National. CANAN INC, 2010.

[9] D, Baglee, and Knowles M J. "Developing RCM Strategy for Hydrogen Fuel Cells Utilizing On Line E-Condition Monitoring." *Journal of Physics* (IOP Publishing) 364 (2012).

[10] H. Virokannas, H. Anttonen, J. Niskanen. "Health risk assessment of noise, hand-arm vibration and cold in railway track maintenance." *International Journal of Industrial Ergonomics* (Elsevier) 13 (Dec 1993): 247-252.

[11] Hans Svee, Hans Jorgen Sæbo & Jorn Vatn. "Estimating the potential benefit of introducing reliability centred maintenance on railway infrastructure." *Safety and Reliability*, SINTEF Industrial Management, Norway: Lyderson, Hansen and Sandtorv, 1998.

[12] International Atomic Energy Agency. "Training guidelines in non-destructive Testing Techniques: Leakage Testing at Level 2." *Training Guidelines*,

International Atomic Energy Agency, Vienna: IAEA Publishing Section, 2012, 1-171.

[13] Bendix Commerical Vehicle Systems. “Air Brake System Troubleshooting.” Bendix.2013.http://www.bendixvrc.com/itemDisplay.asp?documentID=6240 (accessed 2013).

[14] J, Moubray. *Reliability-Centered Maintenance.* Vol. 2. New York: Industrial Press Inc., 1997.

[15] Jamieson M, Aronian A. "Automated Train Airbrake Effectiveness Test Process at Canadian Pacific." *Joint Rail Conference.* Philadelphia: ASME, 2012. 173-181.

[16] Katharina Fischer, Francois Besnard, Lina Bertling. "Reliability-Centered Maintenance for Wind Turbines Based on Statistical Analysis and Practical Experience." *IEEE Transactions of Energy Conservation* (IEEE) 27, no. 1 (March 2012).

[17] “Leakages: Systems Failure Analysis.” ASM International, 2009.

[18] M, Rezvanizaniani S, Valibeigloo M, Asghari M, Barabady J, and Kumar U. "Reliability Centered Maintenance for Rolling Stock: A Case Study in Coaches' Wheel sets of Passenger Trains of Iranian Railway." *IEEM.* Singapore: IEEE, 2008.

[19] Marvin Rausand, Arnljot Hsyland. *SYSTEM RELIABILITY THEORY: Models, Statistical Methods, and Applications.* New Jersey: JOHN WILEY & SONS, INC., PUBLICATION, 2004.

[20] Miran Mozetic, Andrej Pregelj. "Leakage Detection Methods and Defining the sizes of Leakages." *Application of Contemporary Nondestructive Testing in Engineering.* Ljubljana, Slovenia: 4th International Conference of Slovenian Society for Nondestructive Testing, 1997.

[21] MTain Inc. *Failure Mode Effects and Criticality Analysis (FMECA).* MTain, 2011.

[22] National Productivity Council, India. *Energy Efficiency Guide for Industry in Asia.* Project, Greenhouse Gas Emission Reduction from Industry in Asia and the Pacific, National Productivity Council, India., India: United Nations Environment Programme, 2006.

[23] P Eret, C Harris, G O’Donnell, and C Meskell. "A practical approach to investigating energy consumption of industrial compressed air systems." *the*

Institution of Mechanical Engineers, Part A: Journal of Power and Energy (Sage Publications), Nov 2011.

[24] International Organization for Standardization. *Quality management and quality assurance.* ISO8402:1994

[25] Parkinson, H. J.,Thompson, G.,Iwnicki, S. "The development of an FMEA methodology for rolling stock remanufacture and refurbishment." *IMECHE SEMINAR PUBLICATION.* Professional Engineering Publishing, 1998. 55-66.

[26] Penn, Wayne M. *Airbrake & Train Handling Manual.* 1. Vol. 1. Jamestown, California: Railtown 1897, 2009.

[27] Pingping LIAO, Maolin CAI. "Study on Compressed Air Leakage Detection Using Ultrasonic Detection Technology and Instrument." *6th IEEE Conference on Industrial Electronics and Applications.* Beijing: IEEE, 2011.

[28] Pintelon, L, N Nagarur, and F Van Puyvelde. "Case study: RCM - yes, no or maybe." *Journal of Quality in Maintenance Engineering* (MCB University Press) 5 (1999): 182-191.

[29] R. Saidur, N.A. Rahim, M. Hasanuzzaman. "A review on compressed-air energy use and energy savings." *Renewable and Sustainable Energy Reviews* (Elsevier) 14 (Nov 2009): 1135-1153.

[30] Ramarathnam, Srivatsan. *A Mathematical Model for Airbrake Systems in the presence of Leakages.* MSc Thesis, Mechanical Engineering, Texas A&M University, texas: Office of Graduate Studies, 2008.

[31] Rezaei, Aida. *Multi-Sensor Based Framework For Gear Condition MonitoringI.* Phd Thesis, Mechanical Engineering, Queen's University, Kingston, Ontario, Canada, 2012.

[32] Research and Traffic Group. *Railway Safety Technologies.* Railway Safety Act, Review Sereteriat, 2007.

[33] Rienstra, Allan. *Sustainability Through Ultrasonic Energy Conservation.* 2009. http://reliabilityweb.com/index.php/ (accessed 2012).

[34] Robert C. Youngquist, Steven Moerk. ULTRASONIC LEAKAGE DETECTION SYSTEM. USA Patent 5710377. jan 20, 1998.

[35] SDT International. "Guide for ultrasonic leakage detection in compressed air systems in an industrial enviroment." SDT. 2007. www.sdt.be (accessed 2012).

[36] Shur, E. A. "Rails for Operation at Low Temperatures." JSC "Railway Research Institute", Moscow.

[37] Slobodan Dudic, Ivana Ignjatovic, Dragan Šešlija, Vladislav Blagojevic, Miodrag Stojiljkovic. "Leakage quantification of compressed air using ultrasound and infrared thermography." *Measurement* (elsevier) 45 (April 2012): 1689-1694.

[38] British Standards Institution. *Quality vocabulary. Availability, reliability and maintainability terms. Guide to concepts and related definitions.* BS4778:1991

[39] Abe Aronian (Mechanical Relaibility Head, CP), in discussion with the author, December 2013.

[40] Transport Safety Board of Canada. *Railway Investigation Report: Runaway Train, R11Q0056.* Quebec North Shore and Labrador Railway, Transport Safety Board of Canada, Quebec: Transport Safety Board of Canada, 2011.

[41] Transport Safety Board of Canada. "Statistical Summary, Railway Occurrences 2012." Canada, 2013.

[42] XIAO Huiheng, WANG Tao and FAN Wei. "Study on Leakageing Detecting by Ultrasonic Testing System with Leak Hole Estimation." *Applied Mechanics and Materials* (Trans Tech Publications) 235 (Non 2012): 204-209.

[43] Yuanni Xia, Jos N. Van Ommeren, Piet Rietveld, Willem Verhagen. "Railway infrastructure disturbances and train operator performance: The role of weather." *Transportation Research Part D* (Elsevier) 18 (2013): 97-102.

[44] Zakharov, S. M. " The Influence of Seasonal Climatic Variation on Wheel/Rail Performance: Experience, Causes and Study." JSC "The Railway Research Institute", Moscow.

[45] Zhang, Dr Jun. "Designing a Cost Effective and Reliable Pipeline Leakage Detection System." *Pipeline Reliability Conference.* Houston, USA, 1996.

[46] Jolliffe I.T. *Principal Component Analysis: Second Edition.* New York: Springer Science and Publication Media, 2002.

[47] Department of Defence. *Standard Practice for System Safety.* MIL-STD-882D:2000

[48] International Electro-technical Commission. *Dependability Management.* IEC60300:2003

[49] SDT International (2010) Getting started with UAS tutorial series. SDT. http://www.sdthearmore.com/learning-centre/uas (accessed 2012).

[50] XLStat (2012) XLStat learning center. XLStat. http://www.xlstat.com/en/learning-center.html (accessed 2012).

[51] Sigview (2012) Sigview v2.6 user manual. Sigview. http://www.sigview.com/SigviewUserManual.pdf (accessed 2012).

[52] Wolstencroft, H. and Neale, J. "Characterization of compressed air leaks using airborne ultrasound." *Acoustics 2008*. Victoria, Australia, 2008.

APPENDIX A: STATIC DATA

Observation Number	US RMS Intensity (R1)	US RMS Intensity (R2)	US intensity RMS (dBµV) (average)	US intensity RMS peak(dBµV)	US intensity peak (dBµV)	US Crest Factor	Temperature (degree C)	Orifice (inch)	Pressure (psi)	Distance (m)	Orientation (degree)	Flow (LPM)
1	76.6	83.25	79.93	86.43	97.55	3.52	22.00	0.005	100.00	0.00	0.00	0.25
2	77.6	78.6	78.10	80.33	91.55	4.74	22.00	0.005	100.00	0.00	45.00	0.25
3	36.75	46.1	41.43	42.00	53.70	4.13	22.00	0.005	100.00	2.00	0.00	0.25
4	46.45	43.35	44.90	46.83	57.68	4.46	22.00	0.005	100.00	2.00	45.00	0.25
5	83.85	83.2	83.53	85.45	97.00	4.73	22.00	0.005	80.00	0.00	0.00	0.20
6	75.15	72.7	73.93	76.10	87.40	4.78	22.00	0.005	80.00	0.00	45.00	0.20
7	44.95	44.9	44.93	46.40	56.50	3.98	22.00	0.005	80.00	2.00	0.00	0.20
8	45.55	47.2	46.38	47.38	59.15	4.39	22.00	0.005	80.00	2.00	45.00	0.20
9	79.7	78.55	79.13	82.03	93.78	5.43	22.00	0.005	60.00	0.00	0.00	0.16
10	74.65	67.2	70.93	72.85	83.75	4.41	22.00	0.005	60.00	0.00	45.00	0.16
11	40.9	41.75	41.33	41.68	53.63	4.13	22.00	0.005	60.00	2.00	0.00	0.16
12	42.3	44.05	43.18	44.80	55.50	4.16	22.00	0.005	60.00	2.00	45.00	0.16
13	80.5	82.3	81.40	84.15	94.75	4.77	22.00	0.004	100.00	0.00	0.00	0.15
14	76.6	75.9	76.25	78.80	90.43	5.18	22.00	0.004	100.00	0.00	45.00	0.15
15	41.8	41.85	41.83	42.13	53.58	3.89	22.00	0.004	100.00	2.00	0.00	0.15
16	44.1	45.65	44.88	46.00	57.38	4.23	22.00	0.004	100.00	2.00	45.00	0.15
17	77.4	76.55	76.98	80.55	91.60	5.45	22.00	0.004	80.00	0.00	0.00	0.13
18	73.8	71.6	72.70	74.20	85.53	4.39	22.00	0.004	80.00	0.00	45.00	0.13
19	40.4	40.45	40.43	40.80	51.95	3.77	22.00	0.004	80.00	2.00	0.00	0.13
20	40.85	43.85	42.35	44.03	54.80	4.24	22.00	0.004	80.00	2.00	45.00	0.13
21	75.4	75.05	75.23	76.98	88.95	4.88	22.00	0.004	60.00	0.00	0.00	0.12
22	69.4	67.45	68.43	71.13	82.70	5.30	22.00	0.004	60.00	0.00	45.00	0.12
23	36.65	36.6	36.63	36.88	48.70	4.02	22.00	0.004	60.00	2.00	0.00	0.12
24	34.4	41.5	37.95	39.75	51.18	4.62	22.00	0.004	60.00	2.00	45.00	0.12
25	70.1	70.1	70.10	74.48	85.60	6.01	22.00	0.003	100.00	0.00	0.00	0.11
26	66.6	69.5	68.05	70.30	81.40	4.68	22.00	0.003	100.00	0.00	45.00	0.11
27	34.7	34.25	34.48	34.83	46.23	3.87	22.00	0.003	100.00	2.00	0.00	0.11
28	34.35	40.8	37.58	38.58	50.13	4.25	22.00	0.003	100.00	2.00	45.00	0.11
29	68.7	71.15	69.93	72.50	83.93	5.03	22.00	0.003	80.00	0.00	0.00	0.08
30	64.85	66.05	65.45	69.05	79.90	5.33	22.00	0.003	80.00	0.00	45.00	0.08
31	30.75	30.9	30.83	31.25	43.03	4.09	22.00	0.003	80.00	2.00	0.00	0.08
32	34.4	36.6	35.50	36.65	48.05	4.26	22.00	0.003	80.00	2.00	45.00	0.08
33	67.45	70.7	69.08	70.13	81.28	4.11	22.00	0.003	60.00	0.00	0.00	0.07
34	66.7	66.45	66.58	69.35	79.85	4.73	22.00	0.003	60.00	0.00	45.00	0.07
35	28.3	28.2	28.25	28.55	40.18	3.96	22.00	0.003	60.00	2.00	0.00	0.07
36	28.75	26.3	27.53	29.15	40.08	4.29	22.00	0.003	60.00	2.00	45.00	0.07
37	70.2	70.45	70.33	71.18	82.55	4.12	22.00	0.002	100.00	0.00	0.00	0.08
38	65.75	66.65	66.20	67.53	78.40	4.09	22.00	0.002	100.00	0.00	45.00	0.08
39	26.05	25.8	25.93	26.25	38.08	4.07	22.00	0.002	100.00	2.00	0.00	0.08
40	27.3	29.45	28.38	28.90	40.03	3.83	22.00	0.002	100.00	2.00	45.00	0.08
41	64	65.8	64.90	66.23	77.60	4.32	22.00	0.002	80.00	0.00	0.00	0.07
42	60.6	60.65	60.63	63.98	74.55	5.02	22.00	0.002	80.00	0.00	45.00	0.07
43	24.9	24.95	24.93	25.30	37.65	4.34	22.00	0.002	80.00	2.00	0.00	0.07
44	22.15	26.95	24.55	26.30	37.78	4.61	22.00	0.002	80.00	2.00	45.00	0.07
45	60	59.2	59.60	61.75	72.70	4.58	22.00	0.002	60.00	0.00	0.00	0.05
46	49.45	59.3	54.38	57.65	69.15	5.78	22.00	0.002	60.00	0.00	45.00	0.05
47	20.8	20.35	20.58	20.90	32.73	4.06	22.00	0.002	60.00	2.00	0.00	0.05
48	19.8	18.65	19.23	20.18	31.65	4.19	22.00	0.002	60.00	2.00	45.00	0.05
49	53.45	51.05	52.25	54.73	66.03	4.90	22.00	0.001	100.00	0.00	0.00	0.07
50	38.3	37.8	38.05	41.40	54.13	6.56	22.00	0.001	100.00	0.00	45.00	0.07
51	10.65	10.05	10.35	10.73	22.28	3.97	22.00	0.001	100.00	2.00	0.00	0.07
52	12.3	8.75	10.53	11.10	22.40	3.93	22.00	0.001	100.00	2.00	45.00	0.07
53	51.4	50.35	50.88	52.48	63.40	4.24	22.00	0.001	80.00	0.00	0.00	0.05
54	39.55	39.4	39.48	42.45	54.15	5.52	22.00	0.001	80.00	0.00	45.00	0.05
55	9.25	8.85	9.05	9.45	22.13	4.52	22.00	0.001	80.00	2.00	0.00	0.05
56	13	12.45	12.73	13.50	25.18	4.21	22.00	0.001	80.00	2.00	45.00	0.05
57	47.85	45.15	46.50	48.35	59.05	4.25	22.00	0.001	60.00	0.00	0.00	0.04
58	37.55	38	37.78	40.48	52.03	5.25	22.00	0.001	60.00	0.00	45.00	0.04
59	6.15	5.7	5.93	6.23	17.80	3.93	22.00	0.001	60.00	2.00	0.00	0.04

60	5.3	6.05	5.68	7.18	18.28	4.28	22.00	0.001	60.00	2.00	45.00	0.04
61	83.2	84.25	83.73	86.68	97.73	5.13	0.00	0.005	100.00	0.00	0.00	0.27
62	70.95	77.25	74.10	78.08	89.60	5.97	0.00	0.005	100.00	0.00	45.00	0.27
63	44.75	44.8	44.78	45.60	57.20	4.19	0.00	0.005	100.00	2.00	0.00	0.27
64	47.1	46.25	46.68	47.85	59.88	4.58	0.00	0.005	100.00	2.00	45.00	0.27
65	76.85	84.75	80.80	83.18	93.60	4.39	0.00	0.005	80.00	0.00	0.00	0.21
66	75.2	72.65	73.93	77.58	89.63	6.21	0.00	0.005	80.00	0.00	45.00	0.21
67	43.75	42.85	43.30	44.58	56.00	4.32	0.00	0.005	80.00	2.00	0.00	0.21
68	45.35	46.15	45.75	46.85	58.05	4.13	0.00	0.005	80.00	2.00	45.00	0.21
69	79.95	82	80.98	83.48	94.95	5.18	0.00	0.005	60.00	0.00	0.00	0.16
70	76.25	73.15	74.70	77.68	88.70	5.13	0.00	0.005	60.00	0.00	45.00	0.16
71	40.35	40.85	40.60	41.88	52.93	4.14	0.00	0.005	60.00	2.00	0.00	0.16
72	41.55	42.3	41.93	43.30	55.05	4.60	0.00	0.005	60.00	2.00	45.00	0.16
73	80.3	75.3	77.80	80.95	92.45	5.59	0.00	0.004	100.00	0.00	0.00	0.14
74	73.15	68.95	71.05	75.48	87.63	6.87	0.00	0.004	100.00	0.00	45.00	0.14
75	41.4	42.7	42.05	43.03	54.08	4.01	0.00	0.004	100.00	2.00	0.00	0.14
76	44	44.45	44.23	45.73	57.38	4.64	0.00	0.004	100.00	2.00	45.00	0.14
77	77.6	75.7	76.65	78.05	90.53	5.01	0.00	0.004	80.00	0.00	0.00	0.14
78	69.4	70	69.70	72.58	83.60	5.02	0.00	0.004	80.00	0.00	45.00	0.14
79	40.6	40.15	40.38	41.10	53.20	4.39	0.00	0.004	80.00	2.00	0.00	0.14
80	42.75	40.95	41.85	43.60	55.53	4.87	0.00	0.004	80.00	2.00	45.00	0.14
81	74.9	78.55	76.73	79.53	91.13	5.58	0.00	0.004	60.00	0.00	0.00	0.11
82	72.4	69.4	70.90	73.08	83.80	4.50	0.00	0.004	60.00	0.00	45.00	0.11
83	37.5	37.6	37.55	38.33	50.13	4.26	0.00	0.004	60.00	2.00	0.00	0.11
84	37.9	41.2	39.55	41.03	51.98	4.19	0.00	0.004	60.00	2.00	45.00	0.11
85	73.85	75.4	74.63	77.55	88.63	5.08	0.00	0.003	100.00	0.00	0.00	0.12
86	68.3	68.15	68.23	70.48	82.33	5.09	0.00	0.003	100.00	0.00	45.00	0.12
87	34.55	33.9	34.23	34.83	46.83	4.30	0.00	0.003	100.00	2.00	0.00	0.12
88	32.8	34.35	33.58	34.93	46.58	4.48	0.00	0.003	100.00	2.00	45.00	0.12
89	73.5	73.05	73.28	75.58	86.38	4.55	0.00	0.003	80.00	0.00	0.00	0.09
90	64.75	61.95	63.35	66.18	77.28	5.05	0.00	0.003	80.00	0.00	45.00	0.09
91	32.2	32.25	32.23	33.03	44.55	4.14	0.00	0.003	80.00	2.00	0.00	0.09
92	32.1	28.85	30.48	32.48	43.40	4.43	0.00	0.003	80.00	2.00	45.00	0.09
93	69.6	61.7	65.65	68.60	81.45	6.75	0.00	0.003	60.00	0.00	0.00	0.06
94	65.15	62.4	63.78	66.18	77.53	4.99	0.00	0.003	60.00	0.00	45.00	0.06
95	28.35	28.2	28.28	29.15	40.95	4.31	0.00	0.003	60.00	2.00	0.00	0.06
96	26.05	28.6	27.33	29.25	40.90	4.81	0.00	0.003	60.00	2.00	45.00	0.06
97	61.35	68.8	65.08	67.93	78.90	4.95	0.00	0.002	100.00	0.00	0.00	0.08
98	56.3	56.85	56.58	61.00	73.83	8.23	0.00	0.002	100.00	0.00	45.00	0.08
99	28.8	27.8	28.30	28.98	40.63	4.14	0.00	0.002	100.00	2.00	0.00	0.08
100	32.3	31.4	31.85	32.43	44.40	4.27	0.00	0.002	100.00	2.00	45.00	0.08
101	66.65	67.8	67.23	69.18	80.98	4.92	0.00	0.002	80.00	0.00	0.00	0.06
102	56.95	59.45	58.20	61.43	72.85	5.42	0.00	0.002	80.00	0.00	45.00	0.06
103	26	25.3	25.65	26.70	38.50	4.42	0.00	0.002	80.00	2.00	0.00	0.06
104	28.3	28.6	28.45	29.35	40.45	3.98	0.00	0.002	80.00	2.00	45.00	0.06
105	62.55	63.45	63.00	64.93	76.28	4.63	0.00	0.002	60.00	0.00	0.00	0.05
106	55.7	44.25	49.98	55.05	67.40	8.34	0.00	0.002	60.00	0.00	45.00	0.05
107	22.8	22.6	22.70	23.53	35.08	4.16	0.00	0.002	60.00	2.00	0.00	0.05
108	20.45	23.45	21.95	23.70	35.28	4.66	0.00	0.002	60.00	2.00	45.00	0.05
109	55	55.65	55.33	58.20	69.00	4.86	0.00	0.001	100.00	0.00	0.00	0.07
110	47.6	49.55	48.58	51.55	62.43	5.10	0.00	0.001	100.00	0.00	45.00	0.07
111	15.75	15.7	15.73	16.50	28.25	4.25	0.00	0.001	100.00	2.00	0.00	0.07
112	17.9	17.3	17.60	18.48	30.00	4.19	0.00	0.001	100.00	2.00	45.00	0.07
113	51.8	52.65	52.23	54.88	65.98	4.94	0.00	0.001	80.00	0.00	0.00	0.06
114	47.5	45.95	46.73	48.95	61.05	5.29	0.00	0.001	80.00	0.00	45.00	0.06
115	12.85	12.35	12.60	13.18	25.08	4.21	0.00	0.001	80.00	2.00	0.00	0.06
116	13.8	14.55	14.18	15.60	27.98	4.97	0.00	0.001	80.00	2.00	45.00	0.06
117	48.7	49.25	48.98	50.78	62.05	4.51	0.00	0.001	60.00	0.00	0.00	0.03
118	42.2	44.45	43.33	45.75	57.18	4.95	0.00	0.001	60.00	0.00	45.00	0.03
119	8.2	7.95	8.08	8.98	20.58	4.25	0.00	0.001	60.00	2.00	0.00	0.03
120	12.15	9.6	10.88	12.10	23.88	4.48	0.00	0.001	60.00	2.00	45.00	0.03
121	81.7	83.8	82.75	84.80	95.73	4.51	-22.00	0.005	100.00	0.00	0.00	0.29
122	82.1	81	81.55	84.18	95.20	4.94	-22.00	0.005	100.00	0.00	45.00	0.29
123	43.9	44	43.95	44.65	56.60	4.30	-22.00	0.005	100.00	2.00	0.00	0.29
124	41.7	41.65	41.68	42.83	53.78	4.03	-22.00	0.005	100.00	2.00	45.00	0.29
125	82.75	81.05	81.90	83.98	95.68	4.92	-22.00	0.005	80.00	0.00	0.00	0.24
126	77.9	78.65	78.28	81.15	93.45	5.82	-22.00	0.005	80.00	0.00	45.00	0.24
127	42.35	40.7	41.53	42.43	54.35	4.41	-22.00	0.005	80.00	2.00	0.00	0.24

128	40.05	39.7	39.88	40.95	52.35	4.21	-22.00	0.005	80.00	2.00	45.00	0.24
129	74.45	76.3	75.38	77.75	89.13	4.88	-22.00	0.005	60.00	0.00	0.00	0.21
130	72.15	73.9	73.03	76.33	88.13	5.72	-22.00	0.005	60.00	0.00	45.00	0.21
131	38.55	37.6	38.08	38.75	50.80	4.34	-22.00	0.005	60.00	2.00	0.00	0.21
132	37	33.25	35.13	36.68	47.90	4.36	-22.00	0.005	60.00	2.00	45.00	0.21
133	80	82.2	81.10	84.03	96.15	5.82	-22.00	0.004	100.00	0.00	0.00	0.18
134	76.8	74.65	75.73	78.98	90.88	5.73	-22.00	0.004	100.00	0.00	45.00	0.18
135	42.6	42.6	42.60	43.55	54.83	4.10	-22.00	0.004	100.00	2.00	0.00	0.18
136	38.65	34.8	36.73	37.88	49.28	4.25	-22.00	0.004	100.00	2.00	45.00	0.18
137	76.1	77.7	76.90	79.70	91.08	5.17	-22.00	0.004	80.00	0.00	0.00	0.15
138	74.1	72.6	73.35	75.60	86.80	4.71	-22.00	0.004	80.00	0.00	45.00	0.15
139	39.15	39.85	39.50	40.23	52.15	4.32	-22.00	0.004	80.00	2.00	0.00	0.15
140	41.65	41.35	41.50	42.85	54.18	4.32	-22.00	0.004	80.00	2.00	45.00	0.15
141	74.3	74.45	74.38	76.45	87.68	4.68	-22.00	0.004	60.00	0.00	0.00	0.11
142	68.75	66.5	67.63	71.75	83.23	6.19	-22.00	0.004	60.00	0.00	45.00	0.11
143	37.45	36.95	37.20	38.23	50.08	4.41	-22.00	0.004	60.00	2.00	0.00	0.11
144	39.45	37.8	38.63	40.05	51.55	4.44	-22.00	0.004	60.00	2.00	45.00	0.11
145	78.1	71.8	74.95	77.88	89.00	5.18	-22.00	0.003	100.00	0.00	0.00	0.13
146	71	72.1	71.55	74.25	86.23	5.45	-22.00	0.003	100.00	0.00	45.00	0.13
147	37.95	38.6	38.28	39.23	51.88	4.83	-22.00	0.003	100.00	2.00	0.00	0.13
148	40.2	40.6	40.40	41.25	52.90	4.23	-22.00	0.003	100.00	2.00	45.00	0.13
149	75.4	74.2	74.80	77.30	88.18	4.69	-22.00	0.003	80.00	0.00	0.00	0.11
150	64.35	70.45	67.40	69.75	81.13	5.02	-22.00	0.003	80.00	0.00	45.00	0.11
151	35.15	36.3	35.73	37.03	45.80	3.52	-22.00	0.003	80.00	2.00	0.00	0.11
152	37.25	37.05	37.15	38.68	49.25	4.04	-22.00	0.003	80.00	2.00	45.00	0.11
153	70.25	64.15	67.20	69.68	82.28	6.27	-22.00	0.003	60.00	0.00	0.00	0.07
154	61.55	63.45	62.50	66.40	77.85	6.05	-22.00	0.003	60.00	0.00	45.00	0.07
155	32.15	32.1	32.13	33.35	45.28	4.56	-22.00	0.003	60.00	2.00	0.00	0.07
156	33.55	33.8	33.68	35.03	46.20	4.23	-22.00	0.003	60.00	2.00	45.00	0.07
157	71.9	68.25	70.08	71.35	82.50	4.21	-22.00	0.002	100.00	0.00	0.00	0.10
158	63.2	60.8	62.00	64.33	75.73	4.91	-22.00	0.002	100.00	0.00	45.00	0.10
159	32.8	33	32.90	33.43	45.18	4.13	-22.00	0.002	100.00	2.00	0.00	0.10
160	32.35	32.7	32.53	33.40	45.08	4.25	-22.00	0.002	100.00	2.00	45.00	0.10
161	65.4	66.25	65.83	68.08	78.75	4.43	-22.00	0.002	80.00	0.00	0.00	0.06
162	59.7	57.5	58.60	62.33	74.03	6.29	-22.00	0.002	80.00	0.00	45.00	0.06
163	26.2	26.6	26.40	27.33	38.88	4.21	-22.00	0.002	80.00	2.00	0.00	0.06
164	27.15	25.55	26.35	27.73	39.05	4.32	-22.00	0.002	80.00	2.00	45.00	0.06
165	58.4	58.2	58.30	61.18	72.90	5.42	-22.00	0.002	60.00	0.00	0.00	0.06
166	50.35	55.8	53.08	56.75	67.98	5.64	-22.00	0.002	60.00	0.00	45.00	0.06
167	22	21.45	21.73	22.70	34.03	4.12	-22.00	0.002	60.00	2.00	0.00	0.06
168	23.15	22.2	22.68	23.80	35.53	4.40	-22.00	0.002	60.00	2.00	45.00	0.06
169	52.05	50.65	51.35	53.95	65.53	5.17	-22.00	0.001	100.00	0.00	0.00	0.08
170	45.75	42.05	43.90	47.08	57.98	5.06	-22.00	0.001	100.00	0.00	45.00	0.08
171	16.85	15.5	16.18	16.88	28.40	4.09	-22.00	0.001	100.00	2.00	0.00	0.08
172	15.2	15.7	15.45	16.98	28.50	4.50	-22.00	0.001	100.00	2.00	45.00	0.08
173	50.4	50.45	50.43	52.48	63.68	4.66	-22.00	0.001	80.00	0.00	0.00	0.05
174	41.3	37.8	39.55	43.35	53.93	5.29	-22.00	0.001	80.00	0.00	45.00	0.05
175	10.75	10.4	10.58	11.38	22.65	4.02	-22.00	0.001	80.00	2.00	0.00	0.05
176	13.4	14.45	13.93	14.78	26.70	4.36	-22.00	0.001	80.00	2.00	45.00	0.05
177	48.7	46.35	47.53	49.23	60.85	4.66	-22.00	0.001	60.00	0.00	0.00	0.03
178	39.35	44.15	41.75	44.30	55.43	4.85	-22.00	0.001	60.00	0.00	45.00	0.03
179	9.25	9.55	9.40	9.93	21.70	4.12	-22.00	0.001	60.00	2.00	0.00	0.03
180	10.55	9.95	10.25	11.23	23.18	4.46	-22.00	0.001	60.00	2.00	45.00	0.03

APPENDIX B: SPECTRUM DATA

Effect on Kurtosis

Change in Orifice				
Orifice5	**Orifice17**	**Orifice29**	**Orifice41**	**Orifice53**
178.441	226.29	198.582	435.412	313.982
201.927	297.815	187.465	230.394	463.245
190.804	210.148	200.46	180.171	186.778
265.667	147.928	214.315	225.41	182.988
219.297	262.113	330.817	216.758	197.599
209.467	179.847	215.841	189.681	214.618
233.062	307.042	197.923	190.283	145.095
238.791	189.015	16.0211	307.819	223.669
194.505	240.169	532.858	271.688	201.863
186.763	246.17	209.805	308.362	226.292
221.171	190.445	143.322	181.16	310.295
267.771	179.606	38.3596	296.189	229.481
274.247	163.358	228.408	157.028	181.486
274.682	176.468	163.976	236.515	249.072
244.221	152.907	515.756	237.64	214.12
243.87	213.389	211.451	226.26	223.421
293.257	300.722	237.066	156.565	163.371
266.612	168.091	183.345	176.376	166.221
192.331	135.928	246.847	255.427	286.217
161.238	176.437	276.612	198.99	189.167
178.68	197.564	223.225	218.704	214.66
204.065	191.145	190.976	284.392	219.277
223.073	133.822	342.528	171.612	186.896
169.671	231.707	210.683	144.117	216.19
293.294	265.678	342.627	288.878	192.903
Change in Temperature		Change in Orientation		
Temperature45	**Temperature105**	**Temperature165**	**Orientation37**	**Orientation38**
201.639	191.052	140.645	158.694	187.539
246.262	180.162	163.662	177.11	154.896
226.596	221.141	187.589	221.338	178.763
228.862	167.156	396.753	220.689	182.094
185.083	191.301	182.209	161.233	310.563
189.062	171.017	212.396	143.971	267.105
174.755	239.873	359.465	157.784	257.7
167.775	312.837	197.105	166.904	192.899

300.179	241.364	190.103	289.247	241.176
124.61	269.711	249.483	254.923	217.694
252.812	179.716	278.744	201.916	185.923
240.381	211.379	171.231	187.109	267.284
194.202	173.37	164.588	209.808	179.724
194.241	203.911	195.808	147.981	205.309
179.275	404.397	202.843	200.531	154.538
197.701	329.376	231.74	220.472	161.799
13.874	181.922	161.923	210.281	304.595
370.9	426.443	177.878	143.897	156.69
220.338	200.879	218.286	245.216	270.622
203.635	155.553	206.684	157.947	191.323
202.333	162.933	216.652	138.264	182.957
183.377	206.053	210.124	169.05	173.559
187.589	183.672	242.626	165.624	177.612
284.186	210.711	278.558	270.222	188.509
407.522	203.931	221.952	168.98	297.494
Change in Pressure			Change in Distance	
Pressure37	**Pressure45**	**Pressure41**	**Distance105**	**Distance 107**
158.694	201.639	435.412	191.052	192.372
177.11	246.262	230.394	180.162	208.936
221.338	226.596	180.171	221.141	199.342
220.689	228.862	225.41	167.156	245.433
161.233	185.083	216.758	191.301	213.537
143.971	189.062	189.681	171.017	167.367
157.784	174.755	190.283	239.873	174.692
166.904	167.775	307.819	312.837	213.203
289.247	300.179	271.688	241.364	260.597
254.923	124.61	308.362	269.711	251.382
201.916	252.812	181.16	179.716	182.122
187.109	240.381	296.189	211.379	171.085
209.808	194.202	157.028	173.37	182.231
147.981	194.241	236.515	203.911	218.597
200.531	179.275	237.64	404.397	226.047
220.472	197.701	226.26	329.376	288.333
210.281	13.874	156.565	181.922	204.486
143.897	370.9	176.376	426.443	184.881
245.216	220.338	255.427	200.879	192.764
157.947	203.635	198.99	155.553	140.061
138.264	202.333	218.704	162.933	233.485
169.05	183.377	284.392	206.053	176.313

165.624	187.589	171.612	183.672	174.7801
270.222	284.186	144.117	210.711	231.636
168.98	407.522	288.878	203.931	410.18

Effect on Sum of PSD

Change in Orifice				
Orifice5	**Orifice17**	**Orifice29**	**Orifice41**	**Orifice53**
6640.14	135343	32268.1	9931.08	26915.8
6460.79	141860	34859.1	11232.1	31121.5
6241.26	117996	40612.8	9189.54	29176.4
6725.45	117005	33641.5	10547	34250.4
7589.23	158075	39500.5	10876.8	33971.3
8112.57	168888	34621.9	10571.2	30688.6
7853.09	163644	47850.4	11334.4	38837.5
9656.22	146873	51015.6	12110.1	37628.9
8712.16	163738	52671.4	13439.2	38591.6
8038.23	174787	57771.6	13560.6	35076.9
9140.65	170427	70315.7	13649.7	47432.8
8907.65	203359	71333.8	14318.3	46287
8071.7	250079	61305.3	13137.6	53403.2
8681.95	259745	78779.5	15668.6	54434.6
9966.38	199026	69518.1	15019	49524.4
10036.6	232215	63128.5	13893	67742.5
9455.9	270396	64691.1	18317.1	60862.6
8948.28	224728	64521	14827.8	73779.7
8845.88	271860	66142.1	17543	62046.9
9574.26	272280	51676.4	13318	61850.1
8296.72	176947	49680.3	14729.2	57700.3
6438.57	155129	35462.8	12240.8	49300.9
5556.18	99644.3	29937.5	8835.19	44633.4
3782.25	101920	21333.6	6419.59	36721.3
2888.34	53554.3	15828.4	5278.32	21307.6
Change in Pressure			Change in Orientation	
Pressure37	Pressure45	Pressure41	Orientation37	Orientation38
332259	576218	9931.08	332259	114168
374121	632391	11232.1	374121	107049
346373	613879	9189.54	346373	103466
347060	634233	10547	347060	102185
338206	641468	10876.8	338206	103301
385062	632737	10571.2	385062	126903

352274	686293	11334.4	352274	115924
358691	941556	12110.1	358691	145567
428054	860097	13439.2	428054	132804
379668	894454	13560.6	379668	148424
363938	947178	13649.7	363938	163681
407107	871244	14318.3	407107	146483
472210	1053400	13137.6	472210	157823
543248	993191	15668.6	543248	167934
506671	911267	15019	506671	195513
520867	889468	13893	520867	178520
570075	986186	18317.1	570075	197704
520502	823321	14827.8	520502	195318
655003	857353	17543	655003	180288
622952	736724	13318	622952	173572
484301	705885	14729.2	484301	139746
410856	555017	12240.8	410856	137291
323993	461848	8835.19	323993	103334
254581	347097	6419.59	254581	65761.4
169145	238346	5278.32	169145	48795.1
Change in Temperature		Change in Temperature		
Temperature45	Temperature105	Temperature165	Distance105	Distance 107
576218	2962.75	11824.2	2962.75	1947.21
632391	3121.86	17963.5	3121.86	2014.37
613879	2853.58	20003.3	2853.58	1942.68
634233	3100.86	14420	3100.86	2502.38
641468	2882.32	18763.9	2882.32	2801.12
632737	2866.8	21732.5	2866.8	2481.34
686293	3550.99	20864.1	3550.99	3958.3
941556	3288.54	29291.2	3288.54	3735.31
860097	3558.09	24031.9	3558.09	4814.02
894454	3414.24	30504	3414.24	4730.99
947178	3675.83	29310.5	3675.83	6192.64
871244	3973.26	34875.6	3973.26	6624.33
1053400	4413.63	40413.9	4413.63	7317.67
993191	5274.86	38924.4	5274.86	8014.21
911267	5166.15	49825.8	5166.15	9600.37
889468	7094.35	55883.8	7094.35	10119.2
986186	6874.52	67214.1	6874.52	15534.4
823321	7570.67	73572.4	7570.67	12704.1
857353	9468.41	67616.1	9468.41	12040.6
736724	9718.1	68765.1	9718.1	13012.8

705885	7911.73	60879.9	7911.73	10880.8
555017	7677.91	48825.6	7677.91	11330.2
461848	4514.9	44367.3	4514.9	8631.31
347097	4015.28	32752.1	4015.28	7032.75
238346	2778.25	22606.7	2778.25	4226

Effect on RMS PSD

Change in Orifice				
Orifice5	**Orifice17**	**Orifice29**	**Orifice41**	**Orifice53**
3.52206	75.0076	17.1169	5.93463	15.1278
3.43064	82.5077	18.7639	6.19607	18.4742
3.23188	64.5407	21.933	4.94917	15.7114
3.79067	59.9343	18.1555	5.70751	18.2403
3.97867	88.3317	22.3374	5.8393	18.4864
4.41687	91.8356	18.0919	5.69214	16.5572
4.28231	92.8822	25.315	5.96187	19.6685
5.27756	77.5099	28.9482	6.69426	20.528
4.63697	93.8965	30.4383	7.55994	20.5254
4.18183	94.6247	30.9865	7.79496	18.4808
4.9116	90.6006	35.3758	7.14467	27.5912
4.97077	108.028	251.008	8.11888	25.2331
4.45894	129.866	34.2809	6.81045	27.5963
4.82511	137.748	40.2117	8.51423	29.3308
5.43805	103.488	42.6429	8.47835	27.2083
5.53681	128.18	34.5321	7.71376	36.7653
5.30292	150.665	35.9818	9.47571	31.403
4.88131	119.796	34.3498	7.75225	38.1524
4.72424	134.738	37.3723	9.8965	33.678
4.84042	142.312	27.4539	6.96051	33.1371
4.42811	95.6041	27.2348	8.06456	32.1959
3.43254	81.5865	19.5915	6.74628	27.3016
3.05239	49.5863	17.6451	4.58909	22.9387
1.94946	56.3133	11.3422	3.2762	20.2439
1.6451	30.5113	9.07656	2.89067	11.6349
Change in Pressure			Change in Orientation	
Pressure37	**Pressure45**	**Pressure41**	**Orientation37**	**Orientati on38**
173.774	306.494	5.93463	173.774	61.5605
199.01	360.51	6.19607	199.01	55.3862
193.329	348.316	4.94917	193.329	54.526
189.527	351.658	5.70751	189.527	53.8135

174.381	350.038	5.8393	174.381	57.708
196.089	340.405	5.69214	196.089	69.7724
183.313	363.781	5.96187	183.313	64.2766
185.301	494.631	6.69426	185.301	78.1434
247.002	460.331	7.55994	247.002	72.7994
215.737	438.57	7.79496	215.737	81.5937
200.046	515.073	7.14467	200.046	85.144
216.913	484.752	8.11888	216.913	81.3988
263.805	570.394	6.81045	263.805	83.7315
277.805	529.202	8.51423	277.805	89.9612
275.175	481.793	8.47835	275.175	99.7942
275.532	467.389	7.71376	275.532	93.0886
301.234	526.942	9.47571	301.234	109.695
267.7	471.961	7.75225	267.7	100.413
366.816	465.835	9.8965	366.816	100.567
318.874	398.25	6.96051	318.874	90.2341
244.607	390.145	8.06456	244.607	74.4815
214.731	297.309	6.74628	214.731	73.8291
170.159	243.796	4.58909	170.159	54.144
137.382	197.008	3.2762	137.382	35.0702
89.2331	145.235	2.89067	89.2331	28.192
Change in Temperature			Change in Distance	
Temperature45	**Temperature105**	**Temperature165**	**Distance105**	**Distance 107**
306.494	1.55834	6.02253	1.55834	1.05169
360.51	1.66108	9.1022	1.66108	1.10415
348.316	1.52988	10.6022	1.52988	1.01066
351.658	1.61885	7.83328	1.61885	1.38832
350.038	1.55218	10.1178	1.55218	1.4998
340.405	1.51438	11.3096	1.51438	1.27636
363.781	1.98633	11.4694	1.98633	2.11207
494.631	1.85513	15.4393	1.85513	1.99477
460.331	1.98496	12.5493	1.98496	2.74612
438.57	1.81321	16.8931	1.81321	2.59074
515.073	1.91225	16.4988	1.91225	3.27789
484.752	2.11719	18.2099	2.11719	3.55663
570.394	2.3574	21.1417	2.3574	3.87277
529.202	2.84568	20.7643	2.84568	4.34063
481.793	2.93128	26.3578	2.93128	5.09453
467.389	4.09142	32.0192	4.09142	5.61861
526.942	3.63729	34.8769	3.63729	8.31812
471.961	4.53953	38.7623	4.53953	6.68066

465.835	4.90131	36.8295	4.90131	6.49812
398.25	5.01789	36.8489	5.01789	6.5488
390.145	4.20875	32.2252	4.20875	5.88742
297.309	4.09914	26.6938	4.09914	5.95417
243.796	2.44185	24.912	2.44185	4.58187
197.008	2.13389	18.3402	2.13389	3.88981
145.235	1.494	12.0531	1.494	2.3286

Effect on Maximum PSD

Change in Orifice				
Orifice5	**Orifice17**	**Orifice29**	**Orifice41**	**Orifice53**
92.4109	1914.3	442.752	201.64	493.483
89.5941	2796.28	505.404	167.227	774.726
91.9435	1550.27	583.527	118.592	385.823
115.964	1239.81	517.781	176.811	487.291
120.669	3002.81	786.675	184.166	439.84
133.867	2305.71	550.523	129.528	418.889
139.517	3137.86	742.187	149.672	427.986
164.017	1806.83	962.785	244.413	575.714
117.342	2446.13	1448.5	229.669	545.321
104.646	2647.25	878.824	277.27	587.832
137.62	2519.1	784.155	191.363	922.819
143.498	2582.38	1189.01	249.114	669.356
157.956	3122.4	936.197	140.381	791.49
161.826	3154.1	1021.6	246.922	990.701
170.811	2315.92	1789.33	219.97	795.522
163.902	3196.69	882.449	222.235	1052.09
180.784	5073.83	1037.79	216.184	669.246
176.868	2405.7	846.28	199.902	898.543
124.368	3002.98	1053.96	274.067	1217.05
125.284	3053.96	1058.59	191.772	818.123
108.449	2373.81	711.127	232.334	853.938
95.4621	2017.66	412.429	239.024	717.32
86.7962	1093.26	643.512	106.726	605.791
49.5641	1514.64	318.649	79.9338	514.571
51.0759	928.958	322.908	91.6132	302.972
Change in Pressure			Change in Orientation	
Pressure37	**Pressure45**	**Pressure41**	**Orientation37**	**Orientation38**
3930.79	9039.21	201.64	3930.79	1574.19

4560.98	10601.3	167.227	4560.98	1424.73
4991.46	10847.5	118.592	4991.46	1356.06
4894.16	9878.44	176.811	4894.16	1335.34
3878.01	8192.99	184.166	3878.01	2093.11
4639.95	8668.93	129.528	4639.95	2130.71
4175.9	9236.49	149.672	4175.9	2172.98
4849.98	12261.7	244.413	4849.98	2047.35
7691.69	17316.4	229.669	7691.69	2053.86
6378.7	9543.84	277.27	6378.7	947.267
5360.87	16232.2	191.363	5360.87	238.31
5016.52	13912.2	249.114	5016.52	2879.88
6986.44	15104.8	140.381	6986.44	2185
5571.76	14487.4	246.922	5571.76	2444.25
7671.01	12313.3	219.97	7671.01	2243.74
8514.25	12890.3	222.235	8514.25	2151.63
9197.39	18890.2	216.184	9197.39	3841.18
5453.02	17757	199.902	5453.02	2303.31
10458.1	14160	274.067	10458.1	3196.59
7344.17	10579.6	191.772	7344.17	2263.29
5870.82	10351.2	232.334	5870.82	1876.8
4822.75	7222.24	239.024	4822.75	1743.06
4160.65	6057.25	106.726	4160.65	1549.86
4844.53	6046.97	79.9338	4844.53	936.037
2136.54	5461.17	91.6132	2136.54	971.89
Change in Temperature			Change in Distance	
Temperature45	**Temperature105**	**Temperature165**	**Distance105**	**Distance 107**
9039.21	43.6734	122.475	43.6734	27.4562
10601.3	37.6823	260.888	37.6823	29.8577
10847.5	41.2463	248.076	41.2463	25.8157
9878.44	38.0378	305.967	38.0378	41.6498
8192.99	38.8731	254.197	38.8731	40.521
8668.93	39.5703	341.691	39.5703	30.1514
9236.49	55.9234	454.971	55.9234	52.1531
12261.7	61.5422	417.198	61.5422	58.9127
17316.4	58.6708	325.7	58.6708	97.6803
9543.84	66.923	495.721	66.923	80.6891
16232.2	52.7852	523.425	52.7852	89.4173
13912.2	54.729	493.65	54.729	76.8955
15104.8	62.8399	463.545	62.8399	103.749
14487.4	75.3747	579.722	75.3747	114.603
12313.3	115.599	835.483	115.599	167.285

12890.3	161.592	860.807	161.592	177.096
18890.2	93.9727	800.768	93.9727	232.169
17757	185.132	898.454	185.132	188.655
14160	145.453	1100.98	145.453	177.925
10579.6	119.34	1001.29	119.34	138.152
10351.2	91.2931	910.87	91.2931	174.112
7222.24	108.57	786.2	108.57	146.186
6057.25	62.0835	749.724	62.0835	115.66
6046.97	65.9813	608.093	65.9813	112.433
5461.17	41.0764	351.267	41.0764	99.3804

Effect on Frequency at Maximum PSD

Change in Orifice				
Orifice5	**Orifice17**	**Orifice29**	**Orifice41**	**Orifice53**
17.334	76.416	63.7207	54.6875	33.6914
185.059	192.627	178.467	136.475	103.516
274.902	278.809	275.879	260.01	296.631
359.619	378.418	329.59	328.857	352.051
475.586	412.842	429.199	458.74	438.477
550.537	547.119	563.965	597.412	558.105
621.338	623.047	654.785	633.301	622.559
755.371	720.947	708.984	734.619	770.02
810.547	847.9	843.75	867.676	897.217
953.125	915.771	910.889	989.746	943.604
1034.18	1013.18	1026.86	1091.31	1090.82
1179.2	1126.46	1136.47	1168.95	1135.5
1223.63	1269.04	1282.96	1218.26	1291.75
1369.14	1333.74	1371.58	1380.62	1371.83
1473.14	1405.76	1435.06	1414.31	1416.26
1593.26	1582.76	1523.19	1545.41	1515.38
1673.58	1686.04	1660.4	1667.97	1688.72
1763.18	1710.21	1769.78	1780.76	1744.38
1843.26	1863.53	1837.65	1838.62	1856.45
1972.41	1953.86	1927.25	1956.79	1903.08
2090.58	2009.28	2043.21	2022.46	2028.08
2165.28	2167.72	2104.49	2103.52	2122.56
2292.97	2236.08	2219.97	2259.28	2208.74
2354.25	2320.07	2389.16	2332.03	2305.42
2412.6	2418.21	2463.13	2448	2437.01

Change in Pressure			Change in Orientation	
Pressure37	**Pressure45**	**Pressure41**	**Orientation37**	**Orientation38**
84.9609	78.8574	54.6875	84.9609	10.9863
126.709	143.555	136.475	126.709	105.469
216.064	263.672	260.01	216.064	299.072
300.537	320.313	328.857	300.537	393.311
448.242	466.553	458.74	448.242	417.236
569.58	579.834	597.412	569.58	561.279
689.453	667.236	633.301	689.453	622.559
758.057	769.043	734.619	758.057	751.221
884.521	883.301	867.676	884.521	820.801
976.563	923.34	989.746	976.563	2266.19
1098.14	1079.1	1091.31	1098.14	1069.34
1140.38	1135.5	1168.95	1140.38	1100.59
1291.75	1237.3	1218.26	1291.75	1208.5
1377.44	1342.29	1380.62	1377.44	1305.18
1489.75	1410.16	1414.31	1489.75	1414.79
1505.62	1561.28	1545.41	1505.62	1594.97
1616.7	1607.67	1667.97	1616.7	1664.55
1707.03	1774.41	1780.76	1707.03	1785.4
1817.14	1853.27	1838.62	1817.14	1841.06
1972.9	1971.68	1956.79	1972.9	1925.54
2051.27	2047.12	2022.46	2051.27	2081.3
2140.38	2140.63	2103.52	2140.38	2118.65
2250.24	2236.57	2259.28	2250.24	2214.11
2360.11	2309.57	2332.03	2360.11	2302.25
2434.81	2414.06	2448	2434.81	2402.59
Change in Temperature			Change in Distance	
Temperature45	**Temperature105**	**Temperature165**	**Distance105**	**Distance 107**
78.8574	52.2461	48.584	52.2461	87.1582
143.555	190.918	171.387	190.918	163.086
263.672	253.174	214.844	253.174	207.52
320.313	312.012	315.186	312.012	362.549
466.553	451.66	484.863	451.66	428.711
579.834	584.473	591.309	584.473	598.633
667.236	688.965	609.375	688.965	647.705
769.043	794.189	770.996	794.189	791.504
883.301	894.775	876.465	894.775	886.963
923.34	936.279	909.18	936.279	947.51
1079.1	1044.92	1040.77	1044.92	1053.96
1135.5	1174.32	1170.17	1174.32	1109.86

1237.3	1211.18	1284.91	1211.18	1215.09
1342.29	1374.51	1335.45	1374.51	1327.15
1410.16	1428.47	1482.67	1428.47	1463.62
1561.28	1584.96	1511.23	1584.96	1584.23
1607.67	1675.54	1668.21	1675.54	1693.6
1774.41	1746.83	1783.94	1746.83	1739.75
1853.27	1807.86	1871.83	1807.86	1853.03
1971.68	1971.44	1964.84	1971.44	1986.33
2047.12	2079.35	2067.14	2079.35	2093.75
2140.63	2117.19	2112.3	2117.19	2188.96
2236.57	2237.06	2278.32	2237.06	2289.06
2309.57	2313.48	2354.25	2313.48	2302.25
2414.06	2471.44	2459.23	2471.44	2470.21

APPENDIX C: SDT 270

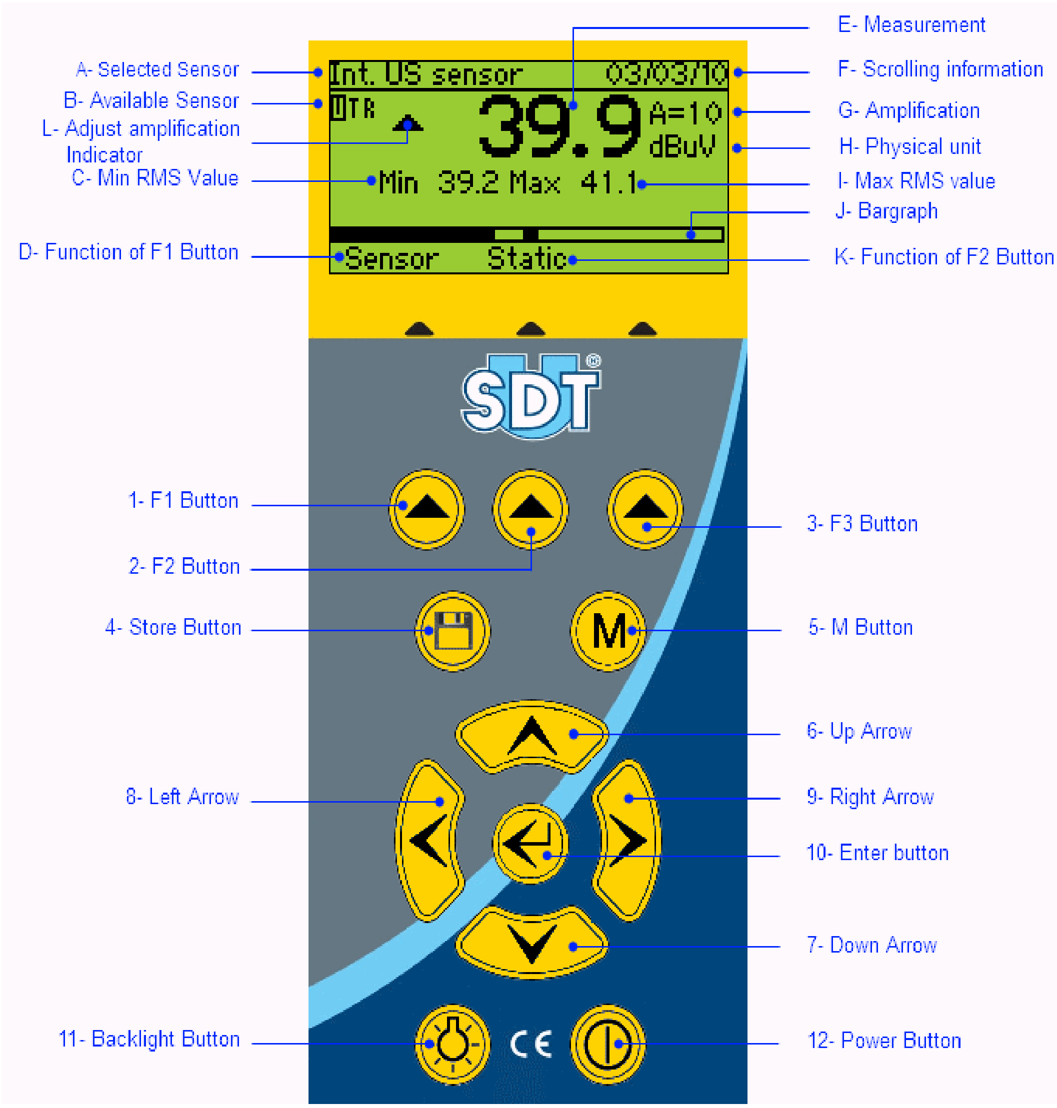

Screen information

A- Selected Sensor:

 Indicates the name of the sensor currently in use.

B- Available Sensors:

 indicates which sensors are available

 U is for Internal US Sensor

 T is for built-in Thermometer

 R is for Built-in Tachometer

 B is for the sensor connected to the black connector

 R is for the sensor connected to the red connector

 Depends on the SDT270 Version.

C- Min RMS value:

 Indicates the lowest RMS value measured

 This value is refreshed when the amplification is changed.
I- Max RMS value:
 Indicates the highest RMS value measured
 The value is refreshed when amplification is changed.
E- Measurement:
 Displays the Measurement
 The Measurement freezes when the M Button is pressed.
F- Scrolling information:
 Remaining battery power.
 Date.
 Hour.
G- Amplification
 Indicates the currently selected amplification
 Used for ultrasonic sensors
 Minimum is 0 dB
 Maximum is 90 dB.
H- Physical unit:
 Indicates the physical unit of the Measurement.
J- Barograph:
 Reacts continuously to the ultrasonic signal.
 The vertical bar will latch for 5 seconds to show the Max RMS attained
D- Function of F1 Button:
 Indicates the function of the F1 Button for this mode.
 Changes dynamically according to the used Measurement mode.
 In this example, the F1 Button switches from available Sensors which are U (Internal Sensor) T (built-in Thermometer) or R (built-in Tachometer).
K- Function of F2 Button:
 Indicates the function of the F2 Button for this mode.
 Change dynamically according to the used Measurement mode.
 In this example, the F2 Button switches from Static Mode to Dynamic Mode.
Function of F3 Button:
 For this particular screen, the F3 Button has no function.
Keyboard functions
1- F1 Button:
 The function of the F1 Button is displayed on the bottom of the screen as mentioned in paragraph D- Function of F1 Button.
 The F1 Button function changes in a dynamic way.
2- F2 Button:
 The function of the F2 Button is displayed on the bottom of the screen as mentioned in paragraph K- Function of F2 Button
 The F2 key function changes in a dynamic way.
3- F3 Button
 The function of the F3 Button is displayed on the bottom of the screen. In this particular example, F3 had no function.
 The F3 key function changes in a dynamic way.
4- Store Button

 Stores the measurements inside the Database.
5- M key
 Freezes and unfreezes a Static Measurement in Static Mode
 Start a Dynamic Measurement in Dynamic Mode.
6- Up Arrow
 Increases the Amplification.
7- Down Arrow
 Decreases the Amplification.
8- Left Arrow
 Reduces the headphone volume.
9- Right arrow
 Increases the headphone volume.
10- Enter Button
 Opens the Menus.
11- Backlight Button
 3-way toggle button between off, on at low intensity and on at high intensity.
12- Power Button
 Use to turn the SDT270 on and off.

APPENDIX D: VALIDATION DATA

Analysis No.	1	2	3	4	5	6	7	8	9	10	11	12
PCA-1ds	41.9	13.8	6.1	11.0	2.3	13.9	2.3	2.5	0.7	5.9	0.8	1.3
PCA-1dr	11.3	9.9	10.1	3.4	3.6	0.5	1.2	3.4	4.6	2.5	0.0	0.1
PCA-1dm	41.9	13.8	6.1	11.0	2.3	13.9	2.3	2.5	0.7	5.9	0.8	1.3
PCA-1ps	3.1	7.3	2.3	1.2	1.9	2.7	6.8	5.2	4.6	1.8	2.7	0.5
PCA-1pr	4.5	5.9	1.6	1.9	1.8	2.0	9.7	24.9	2.4	3.7	1.1	2.1
PCA-1pm	12.7	0.5	4.8	10.7	4.7	9.5	1.9	41.0	1.5	12.2	1.6	0.2
PCA-1ts	0.3	5.2	2.1	0.1	0.7	2.4	57.1	2.6	4.6	0.9	0.9	0.3
PCA-1tr	0.4	2.1	1.0	0.1	1.2	1.3	67.7	2.5	2.4	0.8	1.1	0.4
PCA-1tm	17.7	1.3	1.1	3.8	0.5	3.7	60.5	1.2	3.4	1.4	0.2	1.1
PCA-2ds	4.3	1.1	1.7	9.6	4.6	3.3	5.6	1.2	0.3	0.2	0.8	2.1
PCA-2dr	3.9	1.5	1.4	8.8	4.8	3.2	8.3	1.4	0.6	0.1	0.4	1.7
PCA-2dm	6.9	1.8	9.5	0.6	10.9	5.0	15.9	0.5	19.6	0.8	4.6	0.5
PCA-2ps	2.7	20.1	6.1	0.1	3.3	0.1	2.0	2.2	0.1	0.9	15.2	1.3
PCA-2pr	2.7	18.6	5.0	0.3	4.4	0.2	4.5	1.3	0.9	0.7	12.3	0.8
PCA-2pm	2.2	3.9	7.0	2.1	42.2	3.3	6.0	1.8	3.6	3.3	2.5	1.5
PCA-2ts	3.3	6.6	6.8	1.2	0.3	0.3	0.5	4.3	2.6	1.2	16.1	5.7
PCA-2tr	4.0	6.1	4.5	0.8	0.2	0.2	4.5	4.1	2.7	0.5	16.2	4.9
PCA-2tm	1.1	0.2	9.2	0.7	0.0	2.5	80.5	2.5	1.3	0.4	4.4	0.5
PCA-3ds	23.3	7.1	7.0	4.1	5.3	2.1	8.5	10.1	3.7	0.5	0.7	0.6
PCA-3dr	18.3	5.9	4.7	4.9	5.5	1.8	7.8	10.0	3.6	0.9	4.5	0.5
PCA-3dm	1.0	3.0	6.3	1.5	54.1	0.0	2.5	15.6	3.7	3.3	1.9	2.0
PCA-3ps	5.7	5.1	7.1	5.0	4.3	4.0	4.4	2.8	3.9	2.9	1.5	0.9
PCA-3pr	5.3	5.6	6.8	5.6	4.7	4.4	4.8	2.5	3.9	2.8	1.5	0.8
PCA-3pm	3.9	6.5	7.7	1.8	4.2	6.3	5.4	3.5	4.0	3.8	2.7	0.5
PCA-3ts	7.0	3.7	3.0	4.3	4.3	4.1	4.0	3.8	2.8	3.5	1.8	0.4
PCA-3tr	6.9	4.2	3.1	4.9	4.7	4.3	2.3	4.0	3.2	3.5	1.8	0.5
PCA-3tm	3.4	3.9	2.2	3.4	2.5	2.1	75.1	7.2	5.5	2.6	3.1	2.6
PCA-4ds	3.4	6.9	11.2	4.5	7.3	3.0	3.2	10.8	1.6	1.1	0.7	1.0
PCA-4dr	3.3	5.3	12.7	5.3	6.5	3.3	3.2	11.8	1.7	1.5	0.7	0.5
PCA-4dm	5.7	14.6	1.1	4.3	7.9	7.0	4.4	6.5	4.6	1.6	5.6	8.1
PCA-4ps	4.5	5.0	5.2	4.2	3.9	3.4	4.8	3.2	3.1	2.2	6.0	1.4
PCA-4pr	4.6	5.0	5.1	4.2	4.0	3.4	4.5	3.3	3.1	2.0	6.3	1.8
PCA-4pm	5.2	6.3	6.3	3.9	5.0	1.8	4.6	5.6	5.4	3.1	1.5	0.5
PCA-4ts	5.8	4.0	3.4	4.0	2.8	3.0	4.3	3.7	2.1	4.7	1.9	1.2
PCA-4tr	6.3	4.1	3.7	3.9	2.9	3.0	4.5	3.8	2.2	5.1	1.5	1.3
PCA-4tm	12.1	7.5	5.0	13.2	5.5	1.1	4.5	9.4	6.0	7.4	2.5	7.3
PCA-5ds	6.3	7.7	5.0	5.0	5.6	4.1	4.7	3.8	4.0	3.7	3.5	0.7
PCA-5dr	7.1	4.9	5.0	5.8	5.6	4.0	4.9	4.4	4.7	3.9	1.5	2.3
PCA-5dt	9.8	43.0	3.9	7.9	13.1	4.7	6.7	8.7	15.5	2.2	5.4	2.2
PCA-5ps	9.5	8.4	9.3	8.8	7.2	7.0	5.5	4.2	10.8	18.8	18.0	8.7
PCA-5pr	10.1	5.7	8.9	9.9	7.3	7.1	5.6	5.1	10.3	17.9	17.0	10.0

PCA-5pm	9.2	35.3	3.5	16.3	0.1	0.1	0.2	9.8	12.5	4.3	10.7	11.6
PCA-5ts	5.9	3.7	5.1	5.4	4.2	4.3	13.2	3.6	4.0	3.9	1.6	0.8
PCA-5tr	5.6	1.9	3.4	4.8	3.3	3.6	31.8	4.1	3.4	3.9	1.5	0.8
PCA-5tm	7.4	11.8	2.4	11.5	0.1	0.0	87.5	1.9	10.9	0.6	5.0	2.8
PCA-6ds	12.4	12.8	18.5	11.7	3.4	3.5	11.0	7.0	1.0	3.4	3.3	5.4
PCA-6dr	14.1	9.7	23.7	13.6	3.8	6.3	13.6	6.6	0.9	1.8	2.9	4.3
PCA-6dm	10.9	38.6	4.1	22.8	7.0	0.1	2.0	5.1	0.1	0.7	0.3	1.5
PCA-6ps	12.3	10.3	11.7	15.7	7.7	14.4	3.5	4.0	1.4	3.4	13.9	5.2
PCA-6pr	13.5	7.1	11.9	18.8	7.2	15.0	4.1	4.3	1.5	3.0	12.3	5.6
PCA-6pm	10.4	40.4	0.0	15.7	3.8	17.2	7.3	0.8	5.0	1.0	0.8	0.5
PCA-6ts	14.6	10.4	11.6	12.7	3.2	2.1	46.9	1.6	2.2	0.8	5.3	2.8
PCA-6tr	12.4	5.6	10.2	12.5	2.6	1.4	61.7	1.1	2.4	0.6	5.0	3.1
PCA-6tm	14.3	8.9	1.0	13.1	21.2	0.1	86.6	1.3	1.8	1.3	1.1	1.0

Analysis No.	**13**	**14**	**15**	**16**	**17**	**18**	**19**	**20**	**21**	**22**	**23**	**24**	**25**
PCA-1ds	0.8	4.9	0.7	3.6	9.0	4.2	7.9	3.6	33.0	4.8	11.3	2.6	10.9
PCA-1dr	1.4	0.0	0.0	1.2	5.6	4.7	22.2	27.1	47.6	7.4	8.1	1.2	23.0
PCA-1dm	0.8	4.9	0.7	3.6	9.0	4.2	7.9	3.6	33.0	4.8	11.3	2.6	10.9
PCA-1ps	3.5	12.4	3.0	0.8	9.2	3.0	16.0	31.0	14.1	10.4	0.7	30.5	25.5
PCA-1pr	8.1	5.7	4.5	1.4	13.4	0.7	15.8	24.4	16.3	7.1	2.8	20.4	17.9
PCA-1pm	0.9	0.0	3.2	0.1	18.3	1.0	11.1	19.1	7.5	3.1	9.2	1.7	23.6
PCA-1ts	1.1	4.1	2.0	1.3	3.3	2.6	10.0	23.1	6.3	1.3	11.2	22.6	33.8
PCA-1tr	2.9	3.7	1.7	1.2	4.6	2.0	8.5	16.4	4.7	1.3	13.3	23.4	35.2
PCA-1tm	1.3	2.0	2.1	1.6	18.7	4.3	10.7	1.8	4.0	0.3	12.7	17.4	27.1
PCA-2ds	2.7	2.1	2.9	1.4	2.8	3.4	8.2	10.7	14.3	21.4	20.8	23.5	51.0
PCA-2dr	2.8	1.9	2.0	2.3	3.1	3.1	7.9	12.5	15.1	20.8	17.5	25.5	49.5
PCA-2dm	0.7	0.1	4.3	0.7	9.2	2.8	6.6	6.8	5.4	4.2	12.6	22.7	47.3
PCA-2ps	1.7	3.4	2.3	2.3	2.6	9.6	8.9	17.4	11.0	1.6	7.9	28.4	48.6
PCA-2pr	1.6	4.3	1.6	2.4	3.9	10.2	10.3	17.8	8.6	2.1	8.9	30.0	46.6
PCA-2pm	13.6	5.0	6.7	1.3	4.4	2.9	4.7	11.9	23.5	4.6	6.0	11.5	24.7
PCA-2ts	1.7	1.9	1.6	3.4	1.4	7.2	14.7	18.6	9.9	8.3	12.0	23.4	46.9
PCA-2tr	1.7	1.7	1.2	3.0	1.7	6.7	15.3	18.9	11.0	7.4	12.1	24.4	46.1
PCA-2tm	0.5	2.0	2.6	0.0	10.5	1.0	5.4	8.3	3.5	3.6	7.3	12.3	39.6
PCA-3ds	19.1	4.1	2.7	2.0	7.0	1.1	1.5	2.2	2.6	1.0	12.5	27.4	43.5
PCA-3dr	16.6	4.1	3.8	0.5	5.4	1.8	2.4	6.2	2.8	4.2	11.9	29.2	42.6
PCA-3dm	1.6	5.0	9.3	0.7	1.5	4.6	0.4	4.7	3.9	5.9	5.5	26.7	35.7
PCA-3ps	2.0	2.5	1.9	1.0	13.0	2.8	8.9	4.8	15.1	10.9	13.0	24.9	51.6
PCA-3pr	1.3	2.4	1.7	1.7	12.7	3.5	8.6	5.2	15.7	10.6	11.3	25.2	51.3
PCA-3pm	2.8	4.2	0.0	3.6	3.9	12.4	7.1	9.2	25.2	9.3	10.1	16.3	45.4
PCA-3ts	1.7	3.7	1.0	0.4	9.4	3.0	9.2	9.7	13.9	17.2	13.1	25.0	50.3
PCA-3tr	1.5	3.4	0.8	0.4	8.6	3.1	9.7	10.1	15.0	16.0	13.6	25.4	49.1
PCA-3tm	0.4	4.5	0.6	0.3	0.1	1.8	0.6	2.4	10.9	3.8	6.0	21.7	33.5

PCA-4ds	0.7	0.2	0.2	2.0	1.2	1.7	0.1	6.7	9.8	13.5	34.3	21.3	53.7
PCA-4dr	1.8	0.2	0.6	1.8	1.3	1.6	1.2	4.9	11.3	13.8	34.0	22.4	49.7
PCA-4dm	8.0	2.0	3.1	3.9	3.2	1.0	8.3	7.5	0.6	9.4	28.7	18.2	34.6
PCA-4ps	5.6	0.3	2.4	10.4	7.7	10.1	19.6	6.9	12.8	12.8	35.7	16.3	12.7
PCA-4pr	5.2	0.2	2.4	10.0	8.1	9.4	20.3	7.3	11.9	13.0	35.4	15.4	14.0
PCA-4pm	1.9	1.1	1.3	2.7	4.9	14.4	22.3	5.0	14.4	13.6	31.6	15.3	22.0
PCA-4ts	0.6	0.3	1.8	2.0	0.6	3.9	10.7	16.7	16.1	17.2	16.8	19.1	53.3
PCA-4tr	0.5	0.2	1.7	2.3	1.1	4.0	9.7	16.5	15.8	16.7	17.3	18.2	53.6
PCA-4tm	7.3	0.9	1.2	7.0	0.3	0.6	1.2	13.6	10.4	17.9	19.7	8.6	29.9
PCA-5ds	12.5	8.8	31.2	25.1	15.0	11.5	11.7	1.9	0.3	10.0	2.4	13.4	2.3
PCA-5dr	1.3	10.8	34.1	18.8	17.0	12.4	17.9	2.5	0.2	15.2	3.4	8.6	3.5
PCA-5dt	6.4	1.9	4.7	1.7	10.3	5.1	26.2	0.1	1.3	11.0	3.7	1.3	3.0
PCA-5ps	2.4	7.4	9.5	11.0	19.6	10.3	6.0	1.6	5.8	4.5	0.5	4.2	1.0
PCA-5pr	2.0	8.2	11.2	9.9	19.7	11.2	5.5	1.8	6.3	3.2	0.7	4.3	0.8
PCA-5pm	0.4	3.2	15.8	12.3	14.0	8.7	14.6	0.2	2.5	3.1	4.0	6.8	0.7
PCA-5ts	1.6	8.4	7.6	14.3	9.7	12.2	9.8	1.6	0.8	4.6	11.2	21.8	40.6
PCA-5tr	1.4	9.4	7.1	12.9	9.1	13.0	9.7	1.5	0.8	4.5	9.5	18.3	34.9
PCA-5tm	1.2	1.6	0.2	7.4	3.3	5.1	3.9	0.4	6.5	1.8	10.0	4.8	11.9
PCA-6ds	1.1	5.2	1.3	6.7	25.4	11.8	4.1	6.1	3.6	10.1	2.5	16.8	11.8
PCA-6dr	0.5	2.4	2.6	5.2	17.9	14.6	4.8	5.3	3.4	6.4	1.3	21.7	12.6
PCA-6dm	2.1	6.8	0.2	0.8	0.7	9.1	2.2	13.3	6.6	25.6	33.5	5.2	0.8
PCA-6ps	10.6	1.1	2.1	6.7	9.8	10.8	4.2	4.6	7.1	5.2	8.9	10.3	14.9
PCA-6pr	10.4	0.5	2.5	7.2	11.2	9.5	4.1	4.3	6.3	4.4	9.7	10.5	14.9
PCA-6pm	11.9	3.3	3.4	41.3	10.1	5.7	0.7	2.6	0.1	6.6	0.9	7.6	2.8
PCA-6ts	1.8	0.8	2.1	0.4	3.8	5.3	3.9	5.4	4.8	5.5	5.1	16.4	30.6
PCA-6tr	1.4	0.7	2.7	0.4	3.9	7.0	4.3	4.8	4.2	4.4	4.4	16.7	26.6
PCA-6tm	3.7	1.7	1.7	0.0	0.4	3.6	0.3	4.3	0.8	12.3	5.0	6.8	7.6